VISVESVARAYA TECHNOLOGICAL UNIVERSITY

Jnana Sangama, Belagavi – 590 018

A PROJECT REPORT ON

"PREDICTION OF EVAPORATION USING SOFT COMPUTING TECHNIQUES"

Submitted in Partial Fulfilment for the Award of Degree of

Bachelor of Engineering

In

Civil Engineering

(18CVP85: PROJECT WORK)

Submitted by

Name	USN
MEGHANA H P	1RN19CV023

Under the Guidance of

Mr. MAHADEVA M

Assistant Professor

ISRO-IIRS Institute

Coordinator Dept. of Civil Engineering, RNSIT

RNS INSTITUTE OF TECHNOLOGY

Department of Civil Engineering

Bengaluru – 560 098

2022-2023

RNS INSTITUTE OF TECHNOLOGY

Dr.Vishnuvardhan Road, Channasandra, Bengaluru – 560 098

Department of Civil Engineering

CERTIFICATE

Certified that the Project work entitled **"PREDICTION OF EVAPORATION USING SOFT COMPUTING TECHNIQUES"** is carried out by **MEGHANA H P-1RN19CV023** in partial fulfilment for the award of Bachelor of Engineering in **Civil Engineering**, Visvesvaraya Technological University, Belagavi, during the year 2022-2023.It is certified that all corrections /suggestions indicated for internal assessment have been incorporated in the report. The project report has been approved as it satisfies the academic requirements in respect of project work prescribed for the award of the degree of **Bachelor of Engineering (18CVP85: PROJECT WORK).**

24/5

Signature of Guide	Signature of HOD	Signature of Principal
Mr. Mahadeva M	**Dr. Abhijith C C**	**Dr. Ramesh Babu H S**
Assistant Professor	Head of the Department	Principal

External - Viva

Name of the examiners	Signature with date
1. CHETHAN CHANDRU	26/5/23
2. ABHILASH NR	26/5/23

DECLARATION

We hereby declare that the entire work embodied in this project report titled, **"PREDICTION OF EVAPORATION USING SOFT COMPUTING TECHNIQUES"** submitted to Visvesvaraya Technological University, Belagavi, is carried out by usat Department of **Civil Engineering,** RNS Institute of Technology, Bengaluru, under the guidance of **Mr. MAHADEVA M**, Assistant Professor. This report has not been submitted in part or full for the award of any diploma or degree of this or any other University.

STUDENT NAME	USN	Signature
MEGHANA H P	**1RN19CV023**	

ACKNOWLEDGEMENT

It is my privilege and duty to acknowledge the kind of help and guidance from several people in preparation of this report. It would not have been possible to prepare this report in this form without their valuable help, cooperation and guidance.

My sincere thanks to guide **Mr Mahadeva M, Assistant Professor, RNSIT** for his valuable suggestions and guidance throughout the period of this report.

I express gratitude to **Dr. Abhijith C C, Professor and Head, Department of Civil Engineering, RNSIT** for his valuable suggestions and guidance throughout the period of this report.

I like to express my sincere gratitude to **Dr. Ramesh Babu H S, Principal, RNSIT** for his encouragement for the conduction of this project work.

I would like to express gratitude to our beloved Founder Late **Dr. R N Shetty** and Management of RNSIT for providing state of art facilities in the Institute.

I would like to express gratitude to our beloved Chairman **Mr Satish Shetty** and Management of RNSIT for providing state of art facilities in the Institute,

The Project work on **"PREDICTION OF EVAPORATION USING SOFT COMPUTING TECHNIQUES"** was very helpful in giving the necessary background information and inspiration in choosing this topic for the project.

Last but not the least, I wish to thank our parents for their continuous support for my studies as well as for constantly encouraging to learn engineering. Their personal sacrifice in providing this opportunity to learn engineering is gratefully acknowledged.

Place: Bengaluru **MEGHANA H P (1RN19CV023)**

ABSTRACT

Evaporation is a vital process in hydrology and environmental sciences, influencing water resource management, agriculture, and climate modelling. Accurate prediction of evaporation rates is crucial for effective planning and decision-making in various domains. This report presents a comprehensive analysis of utilizing soft computing techniques for the prediction of evaporation rates.

Soft computing techniques, such as artificial neural networks (ANNs) have shown promising capabilities in modeling complex and nonlinear systems. In this study, historical meteorological data, including temperature, humidity, wind speed, and solar radiation, are used as inputs to the soft computing models.

Additionally, the report discusses the challenges encountered during the model development process, such as overfitting, selection of appropriate input variables, and optimization of model parameters. Strategies for mitigating these challenges are proposed and discussed in detail.

Overall, this report contributes to the advancement of evaporation prediction using soft computing techniques, highlighting their potential as reliable tools for addressing the challenges associated with accurate estimation of evaporation rates. The findings presented herein have significant implications for researchers, practitioners, and policymakers involved in hydrology, environmental sciences, and related fields.

CONTENT

CONTENTS

CHAPTER-1

INTRODUCTION

Evaporation is **the process whereby liquid water is converted to water vapour (vaporization) and removed from the evaporating surface (vapour removal)**. Water evaporates from a variety of surfaces, such as lakes, rivers, pavements, soils and wet vegetation.

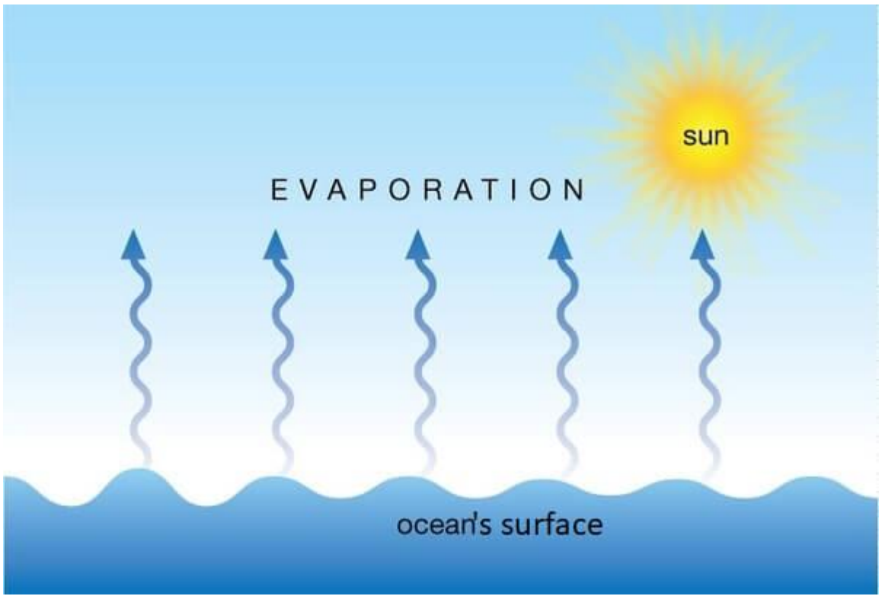

Fig. 1: Evaporation

Fig. 2: Evaporation is the process by which a liquid turns into a gas

Energy is required to change the state of the molecules of water from liquid to vapour. Direct solar radiation and, to a lesser extent, the ambient temperature of the air provide this energy. The driving force to removing water vapour from the evaporating surface is the difference between the water vapour pressure at the evaporating surface and that of the surrounding atmosphere. As evaporation proceeds, the surrounding air becomes gradually saturated and the process will slow down and might stop if the wet air is not transferred to the atmosphere. The replacement of the saturated air with drier air depends greatly on wind speed. Hence, solar radiation, air temperature, air humidity and wind speed are climatological parameters to consider when assessing the evaporation process.

Where the evaporating surface is the soil surface, the degree of shading of the crop canopy and the amount of water available at the evaporating surface are other factors that affect the evaporation process. Frequent rains, irrigation and water transported upwards in a soil from a shallow water table wet the soil surface. Where the soil is able to supply water fast enough to satisfy the evaporation demand, the evaporation from the soil is determined only by the meteorological conditions.

However, where the interval between rains and irrigation becomes large and the ability of the soil to conduct moisture to near the surface is small, the water content in the topsoil drops and the soil surface dries out. Under these circumstances the limited availability of water exerts a controlling influence on soil evaporation. In the absence of any supply of water to the soil surface, evaporation decreases rapidly and may cease almost completely within a few days.

In a liquid, certain particles always have greater kinetic energy than others. When a liquid is well below its boiling point, some of its particles have enough energy to overcome the forces of attraction between them and escape from the surface of the liquid as vapour (or gas). As a result, a liquid’s fast-moving particles (or molecules) continually escape from the liquid to form vapour (or gas).

1.1 Importance

Evaporation from the oceans is vital to the production of fresh water. Because more than 70 percent of the Earth’s surface is covered by oceans, they are the major source of water in the atmosphere. When that water evaporates, the salt is left behind. The fresh-water vapour then condenses into clouds, many of which drift over land. Precipitation from those clouds fills lakes, rivers, and streams with fresh water.

These changes between states (melting, freezing, and evaporating) happen because as the temperature either increases or decreases, the molecules in a substance begin to speed up or slow down. In a solid, the molecule are tightly packed and only vibrate against each other. In a liquid, the molecules move freely, but stay close together. In a gas, they move around wildly and have a great deal of space between them.

Evaporation from the oceans is vital to the production of fresh water. Because more than 70 percent of the Earth’s surface is covered by oceans, they are the major source of water in the atmosphere. When that water

evaporates, the salt is left behind. The fresh-water vapour then condenses into clouds, many of which drift over land.

Precipitation from those clouds fills lakes, rivers, and streams with fresh water. Evaporation is a major and important process that plays a critical role in both the water balance evaporation components and the land surface energy balance. Worldwide 60-80% of the rainfall evaporates, making it the largest outgoing flux in the water balance and therefore of highest importance for hydrologic modelling, flood and drought risk assessments, climate change studies, and water resources management and planning. However, the technical challenges and costs of producing high resolution, accurate, and reliable data sets over various spatial scales implies that evaporation is not widely measured. Instead, actual evaporation is commonly estimated by hydrological modelling and remote sensing. Hydrological modelling, however, is not a very reliable way to estimate evaporation because hydrological rainfall-runoff models are relatively insensitive to the parameterization of evaporation when the model is calibrated on runoff only. When looking at other internal model states such as soil moisture, or groundwater, it is shown that rainfall runoff models are sensitive to evaporation inputs. Knowledge on evaporation is thus of utmost importance for model realism ('getting the right answer for the right reason'). This becomes especially critical for hydrological systems in a changing world with a variety of anthropogenic influences.

1.2 Factors affecting of evapotranspiration:

Weather parameters, crop characteristics, management and environmental aspects are factors affecting evaporation and transpiration.

- **Weather parameters:** The principal weather parameters affecting evapotranspiration are radiation, air temperature, humidity and wind speed. Several procedures have been developed to assess the evaporation rate from these parameters. The evaporation power of the atmosphere is expressed by the reference crop evapotranspiration (ETo). The reference crop evapotranspiration represents the evapotranspiration from a standardized vegetated surface.
- **Crop factors:** The crop type, variety and development stage should be considered when assessing the evapotranspiration from crops grown in large, well-managed fields. Differences in resistance to transpiration, crop height, crop roughness, reflection, ground cover and crop rooting characteristics result in different ET levels in different types of crops under identical environmental conditions. Crop evapotranspiration under standard conditions (ETo) refers to the evaporating demand from crops that are grown in large fields under optimum soil water, excellent management and environmental conditions, and achieve full production under the given climatic conditions.

- **Management and environmental conditions:** Factors such as soil salinity, poor land fertility, limited application of fertilizers, the presence of hard or impenetrable soil horizons, the absence of control of diseases and pests and poor soil management may limit the crop development and reduce the evapotranspiration. Other factors to be considered when assessing ET are ground cover, plant density and the soil water content. The effect of soil water content on ET is conditioned primarily by the magnitude of the water deficit and the type of soil. On the other hand, too much water will result in water logging which might damage the root and limit root water uptake by inhibiting respiration
- **Temperature:** Temperature is one of the most important factors affecting evaporation. Higher temperatures increase the kinetic energy of the liquid molecules, causing them to move faster and escape from the surface more quickly. Therefore, higher temperatures lead to faster evaporation rates.
- **Wind Speed:** Wind speed affects evaporation by increasing the rate at which water vapor is carried away from the surface. Wind blows away the saturated air from the surface of the liquid, allowing more air to come into contact with the liquid and increasing the rate of evaporation.
- **Surface Area:** The surface area of the liquid also affects the rate of evaporation. The larger the surface area, the more liquid molecules are exposed to the air, leading to a higher rate of evaporation.
- **Humidity:** Humidity is the amount of water vapour in the air. When the air is already saturated with water vapour, the rate of evaporation decreases since there is less room for more water vapour in the air. In contrast, when the air is dry, the rate of evaporation is faster since there is more room for additional water vapour in the air

1.3 Causes of evaporation:

- We know that liquids like water are made up of a number of molecules.
- All these molecules at surface have higher level of kinetic energy move away from other molecules.
- This energy is more than force of attraction binding different molecules.
- This causes water to get converted into water vapour and causes evaporation.

1.4 Scope:

- Evaporation is one of the largest water losses from most of the dams, lakes and water bodies in India.
- Estimating the evaporation rate enables us to apply the proper evaporation mitigation technologies.
- In this study, the feasibility of different evaporation estimation methods was studied to find an optimum method with a fair trade off between cost and accuracy.
- The optimum method may vary depending on the climate.
- Evapotranspiration from the land surface plays a key role in maintaining the balance of land surface water-lakes-reservoirs and the energy balance of the earth’s surface.

CHAPTER-2

LITERATURE REVIEW

***Snyder et. al, (2005),*"Simplified Estimation of Reference Evapotranspiration from Pan Evaporation Data in California"**

The paper "Simplified Estimation of Reference Evapotranspiration from Pan Evaporation Data in California" proposes a method to estimate reference evapotranspiration (ET_0) using pan evaporation data in California, where the availability of weather data is limited.

The paper provides a clear description of the methodology used to estimate ET0 from pan evaporation data. The authors use a simplified version of the Penman-Monteith equation, which requires fewer weather variables and is therefore more suitable for areas with limited weather data. They also provide a comprehensive analysis of the accuracy of their method, comparing their estimates to those obtained using the full Penman-Monteith equation and to actual ET_0 measurements obtained from weather stations.

The results of the study show that the simplified method provides reasonably accurate estimates of ET_0, with errors of less than 10% in most cases. The authors also provide recommendations for the use of the method in different regions of California, based on the correlation between pan evaporation and ET_0 in each region.

Overall, the paper provides a valuable contribution to the field of water resources management, particularly for areas where weather data is limited. The method proposed in the paper could be useful for irrigation scheduling and water management in California and other similar regions. The analysis and validation of the method also provide insights into the limitations and uncertainties of using pan evaporation data to estimate ET_0.

***Özlem Terzi, M. ErolKeskin and E. Dilek Taylan (2006)* "Estimating Evaporation Using ANFIS"**

The paper proposes using an Adaptive Neuro-Fuzzy Inference System (ANFIS) to estimate evaporation from a water surface. The ANFIS model is trained using input data such as temperature, relative humidity, wind speed, and solar radiation. The study evaluates the performance of the ANFIS model against actual measurements of evaporation and compares it to other commonly used evaporation estimation methods. The results suggest that the ANFIS model is a reliable and accurate method for estimating evaporation. The study highlights the potential of using ANFIS models for water resource management applications

Joel E. Cahoon a, Thomas A. Costello b and Jim A. Ferguson (1990) **“Estimating pan evaporation using limited meteorological observations”**

The paper presents a method for estimating pan evaporation using limited meteorological observations, specifically mean daily temperature, mean daily wind speed, and daily sunshine hours. The method involves using a regression analysis to develop equations that relate pan evaporation to the meteorological variables. The study evaluates the performance of the equations using data from multiple locations and compares the results to pan evaporation estimated using more complex methods. The results suggest that the method presented in the paper is a useful tool for estimating pan evaporation using limited meteorological observations. However, the study also highlights the limitations of the method and suggests further research to improve the accuracy of the estimates.

I. J. VERMAE et,al,(2006-2008) **“Recent variations and trends in pan evaporation over India”**

The paper titled "Recent variations and trends in pan evaporation over India" examines changes and trends in pan evaporation over India during the period from 1961 to 2010. The authors use innovative trend analysis methods such as Mann-Kendall test, Sen's slope estimator, and wavelet analysis to investigate the temporal variations and trends in pan evaporation over the study period.

The study finds that pan evaporation over India has been decreasing since the 1990s, with an average annual decrease of 0.33 mm per year. The authors attribute this decrease to various factors such as changes in surface solar radiation, wind speed, and atmospheric humidity.

One of the strengths of the paper is its use of innovative trend analysis methods that allow for a more comprehensive examination of the changes and trends in pan evaporation over India. The study also provides insights into the potential impacts of climate change on water resources in India and highlights the need for effective water management strategies.

However, one limitation of the study is its reliance on data from a limited number of stations across India, which may not be representative of the entire country. Additionally, the study does not consider the potential impact of land use changes on pan evaporation.

Overall, the paper makes a valuable contribution to the understanding of pan evaporation trends and variations in India and provides useful insights for water resource management and planning.

Hossein Tabard et,al(2010) **“Changes of Pan Evaporation in the West of Iran”**

Pan evaporation is a measure of the amount of water that evaporates from a surface in a specific location over a given time period. It is affected by various factors such as temperature, humidity, wind speed, and solar radiation. Changes in pan evaporation can provide insights into the local climate and weather patterns.

In the west of Iran, changes in pan evaporation have been observed over the years. According to studies, there has been a decreasing trend in pan evaporation in this region since the 1970s. This is in contrast to the global trend of increasing pan evaporation observed in many other parts of the world.

Several factors have been suggested as possible causes of this decreasing trend in pan evaporation in the west of Iran. One of the main factors is the decrease in solar radiation due to an increase in air pollution, which reduces the amount of sunlight reaching the surface. Other factors that may contribute to this trend include changes in atmospheric moisture content, wind speed, and temperature.

The decreasing trend in pan evaporation in the west of Iran has important implications for water resources management and agricultural practices in the region. It suggests that there may be a decrease in water loss due to evaporation, which could potentially benefit agricultural activities by increasing the amount of available water for irrigation. However, it is important to note that this trend should be studied in conjunction with other climatic factors to better understand its implications for the region.

Anurag Malik et al. (2018) **"Daily Pan Evaporation Estimation using Heuristic Methods with Gamma test"**

The combination of significant input variables for radial basis neural network (RBNN), self-organising map neural network (SOMNN) and multiple linear regression (MLR) were done and the results obtained from these were compared with climate based empirical models such as Penman, Stephens-Stewart, Griffiths, Christiansen, Priestly-Taylor and Jensen-Burman-Allen models.

Using these models, it was found that the Penman model and Stephan's-Stewart models gave relatively accurate values when compared with the Pan Evaporation on the basis of root-mean squared (RMSE) and correlation coefficient (r) for conventional methods.

Gicy M et al. (2018) **"Sensitivity Analysis of FAO-56 Penman– Monteith Reference Evapotranspiration Estimates Using Monte Carlo Simulations"**

Sensitivity analysis was performed using the FAO-56 Penman–Monteith reference evapotranspiration (ET0) model and Monte Carlo (MC) simulations on four stations: Jodhpur, Hyderabad, Bangalore, Pattambi. Sensitivity indices representing the sensitivity of ET0 values to the various input variables were obtained as output from the analysis.

It was found that temperature played a major role in the evapotranspiration in all the stations. However, this study also identifies net radiation as being most critical in a humid location, whereas wind speed appears to be more important in arid, semiarid, and sub-humid climates. Also there is a need of precise measurements of each climate variable in order to get accurate values of Evapotranspiration.

Debnath et al. (2015) **"Sensitivity Analysis of FAO-56 Penman-Monteith Method for Different Agro-ecological Regions of India"**

The paper uses FAO-56 Penman–Monteith reference evapotranspiration (ET0) model to perform sensitivity analysis in the following regions of India Kovilpatti and Parbhani (semi-arid), Mohanpur(humid), and Ludhiana and Ranichauri (sub-humid). Sensitivity analysis is performed by increasing and decreasing the climate variables such as maximum temperature (Tmax), minimum temperature (Tmin), Solar radiation (Rs) , and relative humidity (RHavg)

It was found that net radiation as being most critical in a humid location whereas wind speed appears to be more important in arid , semiarid, and sub-humid climates. Results of sensitivity analysis also provide crucial information on critical climate variables that need to be considered in evaluating the impact of future climate changes on irrigation water requirements of agricultural crops.

Benzaghta et al. (2012) **"Prediction of evaporation in tropical climate using artificial neural network climate based models"**

The purpose of this study was to investigate the ability of ANN technique to accurately estimate the daily evaporation from humid environments using Batu Dam reservoir, Sekangor, Malaysia as a case study. Also to compare ANN models. Meteorological and pan evaporation data were used to develop the ANN models and the output from the ANN models was compared to the output of the selected climate based models.

The ANN-4 model which has inputs of air temperature, wind speed, humidity and solar radiation performed the best among all the models (i.e., ANN-1, ANN-2, ANN-3, ANN-4) climate based models the tests indicate that, the Priestly-Taylor model gave more accurate output when it was applied to predict evaporation from reservoirs in tropical climate.

Pankaj Kumar et al, (2012) **"Evaporation estimation using artificial neural network"**

The purpose of this study was to investigate the potential of using ANN model to predict evaporation as affected by climatic factors in Pantnagar. The input combinations used in this application to estimate evaporation for Pantnagar station were Air temperature (°C), Relative humidity (%), Wind velocity (m/s) and Sunshine hours (hour) of a month and and Evaporation (mm) of that month t was considered as output of the models.

Higher the values of correlation coefficients and lower values of root mean square error suggests the applicability of ANN model for evaporation estimation. The present study discusses the application and usefulness of artificial neural network based modeling approach in predicating the evaporation losses over a region. The results are quite encouraging and suggest the usefulness of neural network based modeling techniques in accurate prediction of the evaporation.

Surinder Deswal et al, (2008) **"Artificial neural network based modeling of evaporation losses in reservoirs"**

The purpose of this study is to develop a suitable ANN model by considering the feed-forward back propagation learning algorithm in the estimation of daily pan evaporation from meteorological parameters and its performance comparison with simple and multiple linear regression approaches.

The results are quite encouraging and suggest the usefulness of neural network based modeling technique in accurate prediction of the evaporation as an alternative to the simple linear regression approach and multiple linear regression approach as well. This study also concludes that a combination of mean air temperature, wind speed, sunshine hour and mean relative humidity provides better performance in predicting the evaporation losses.

Milan Gocic and SlavisaTrajkovic (2013) **"Analysis of changes in meteorological variables using Mann-Kendall and Sen's slope estimator statistical tests in Serbia"**

The paper analyses changes in meteorological variables in Serbia using two statistical tests: the Mann-Kendall test and Sen's slope estimator. The study examines trends in temperature, precipitation, and wind speed data over a 50-year period. The Mann-Kendall test is used to detect the presence of trends, while Sen's slope estimator is used to estimate the magnitude of the trend. The results show significant trends in temperature and precipitation variables, with increasing temperatures and decreasing precipitation observed in many regions. The study concludes that the Mann-Kendall and Sen's slope estimator tests are useful tools for analysing trends in meteorological variables and can provide valuable information for climate change studies and water resource management. However, the study also notes the need for caution when interpreting the results of trend analysis and emphasizes the importance of considering other factors that may influence the observed trends.

2.1 Appraisal of review literature

*Snyder et. al [1],*The paper proposes a simplified method to estimate reference evapotranspiration in California using pan evaporation data. The method involves multiplying the pan evaporation data by a conversion factor derived from empirical data. The study found that the simplified method was a reliable alternative for estimating reference evapotranspiration in California.

*Özlem Terzi et. al.[2],*The paper proposes using an ANFIS model to estimate evaporation from a water surface. The study evaluates the performance of the ANFIS model against actual measurements of evaporation and compares it to other commonly used evaporation estimation methods. The results suggest that the ANFIS model is a reliable and accurate method for estimating evaporation.

*Joel E. Cahoonet,al[3],*The paper presents a method for estimating pan evaporation using limited meteorological observations and evaluates the performance of the method using regression analysis. The results suggest that the method is a useful tool for estimating pan evaporation with limited data.

*I. J. VERMAE et,al,[4],*The paper investigates changes and trends in pan evaporation over India between 1961 and 2010 using innovative trend analysis methods such as Mann-Kendall test, Sen's slope estimator, and wavelet analysis. The study finds a decreasing trend in pan evaporation since the 1990s, which could have implications for water resource management and planning in India. The paper provides valuable insights into the potential impacts of climate change on regional hydrology and highlights the need for effective water management strategies

*Hossein Tabard et,al[5],*The paper "Changes of Pan Evaporation in the West of Iran" by Hossein Tabari et al. (2010) provides an insightful analysis of the decreasing trend in pan evaporation in the west of Iran. The authors highlight the possible causes and implications of this trend for water resources management and agriculture in the region.

*Anurag Malik et al.[6],*The paper proposes using heuristic methods and the Gamma test to estimate daily pan evaporation. The study evaluates the performance of the method using data from multiple locations and compares the results to other commonly used methods. The results suggest that the heuristic method with the Gamma test is a reliable and accurate method for estimating daily pan evaporation

*Gicy M et al.[7],*The paper conducts a sensitivity analysis of FAO-56 Penman-Monteith reference evapotranspiration estimates using Monte Carlo simulations. The study evaluates the impact of input parameters, such as temperature, humidity, and wind speed, on the accuracy of the estimates. The results suggest that the accuracy of the estimates is highly sensitive to changes in some of the input parameters, and the sensitivity varies by location and time of year. The study highlights the importance of considering the uncertainty associated with input parameters when using the FAO-56 Penman-Monteith equation for reference evapotranspiration estimation.

*Debnathet al.[8],*The paper conducts a sensitivity analysis of the FAO-56 Penman-Monteith method for different agro-ecological regions of India. The study evaluates the impact of variations in input parameters, such as temperature, humidity, and wind speed, on the accuracy of the estimates. The results suggest that the sensitivity of the estimates to changes in input parameters varies by agro-ecological region, and some regions are more sensitive than others. The study emphasizes the need for regional calibration of the FAO-56 Penman-Monteith method for accurate reference evapotranspiration estimation in India.

Benzaghta et al [9], The paper presents the use of artificial neural network (ANN) climate-based models for predicting evaporation in tropical climates. The study evaluates the performance of the ANN models using data from multiple locations and compares the results to other commonly used methods. The results suggest that the ANN climate-based models are a reliable and accurate method for predicting evaporation in tropical climates. The study highlights the potential of ANN models for improving water resource management in regions with limited data

Pankaj Kumar et al [10], The paper presents the use of an artificial neural network (ANN) for estimating evaporation from a water surface. The study evaluates the performance of the ANN model using data from multiple locations and compares the results to other commonly used methods. The results suggest that the ANN model is a reliable and accurate method for estimating evaporation. The study highlights the potential of ANN models for improving water resource management and irrigation scheduling.

SurinderDeswal et al,[11] The paper presents the use of an artificial neural network (ANN) model for modeling evaporation losses in reservoirs. The study evaluates the performance of the ANN model using data from multiple reservoirs and compares the results to other commonly used methods. The results suggest that the ANN model is a reliable and accurate method for modelling evaporation losses in reservoirs. The study highlights the potential of ANN models for improving water resource management and reservoir operations.

*Milan Gocic et al,[12]*The paper analyses changes in meteorological variables in Serbia using the Mann-Kendall and Sen's slope estimator statistical tests. The study evaluates the trends and magnitude of changes in variables such as temperature, precipitation, and wind speed over a period of time. The results suggest that there have been significant changes in meteorological variables in Serbia, including increasing temperature and decreasing precipitation, and the magnitude of the changes varies by location and time period. The study highlights the importance of monitoring and analysing changes in meteorological variables for effective climate change adaptation and mitigation strategies.

2.2 RESEARCH GAP:

- One potential research gap in the study by Snyder et al. (2005) is that it does not address the impact of vegetation on evapotranspiration. Vegetation can affect evapotranspiration rates through factors such as leaf area index, root density, and soil moisture availability. Further research could investigate the influence of vegetation on reference evapotranspiration estimation using the proposed method. Another potential research gap is that the paper focuses solely on using pan evaporation data to estimate reference evapotranspiration. It is unclear whether the proposed method would perform as well when using other meteorological variables, such as temperature, humidity, and wind speed. Further research could investigate the accuracy and applicability of the proposed method compared to other commonly used methods for estimating reference evapotranspiration using various meteorological data.
- One potential research gap in the study by Terzi et al. (2006) is that it focuses solely on using the adaptive neuro-fuzzy inference system (ANFIS) to estimate evaporation without comparing its performance to other commonly used methods. Further research could investigate the accuracy and applicability of the ANFIS approach compared to other commonly used methods for estimating evaporation. Another potential research gap is that the study was conducted using data from a single meteorological station in Turkey. It is unclear whether the ANFIS approach would perform as well with data from other regions or under different climatic conditions. Further research could investigate the generalization of the ANFIS approach for evaporation estimation in different regions.
- One potential research gap in the study by Cahoon et al. (1990) is that it focuses solely on using limited meteorological observations to estimate pan evaporation without comparing its performance to other commonly used methods. Further research could investigate the accuracy and applicability of the proposed method compared to other commonly used methods for estimating pan evaporation. Another potential research gap is that the study was conducted using data from a single location in Mississippi, USA. It is unclear whether the proposed method would perform as well with data from other regions or under different climatic conditions. Further research could investigate the generalization of the method for pan evaporation estimation in different regions.
- This paper by Verme shows the research gap that Assessing the implications of pan evaporation trends for water resource management: The declining trends in pan evaporation over India have important implications for water resource management and agricultural planning. More research is needed to understand how these trends may impact water availability, crop yields, and other factors that are important for food security and economic development in India.

there is a need for more research on the recent variations and trends in pan evaporation over India. By better understanding these trends and their underlying drivers, researchers and policymakers can develop more effective strategies for managing water resources and promoting sustainable development in India.

- Lack of recent and comprehensive studies: Despite the importance of Pan evaporation changes in the west of Iran, there may be a lack of recent and comprehensive studies that provide a detailed analysis of the changes and their underlying causes. Therefore, a research gap could be to conduct a study that covers the recent period and provides an in-depth analysis of the factors affecting Pan evaporation changes. Comparative studies that compare Pan evaporation changes in the west of Iran with other regions or countries can provide a valuable perspective on the changes and their underlying causes. Therefore, a research gap could be to conduct a comparative study that compares Pan evaporation changes in the west of Iran with other regions or countries.
- A potential research gap could be the lack of comparative studies between different heuristic methods and their effectiveness in estimating daily pan evaporation. While heuristic methods have been widely used in hydrological modeling, their performance in estimating daily pan evaporation has not been extensively evaluated. Therefore, a research gap could exist in investigating the suitability and reliability of different heuristic methods, such as genetic algorithms, particle swarm optimization, ant colony optimization, etc., for daily pan evaporation estimation. It could exist in exploring the transferability of heuristic methods for daily pan evaporation estimation across different regions with varying climatic conditions. While heuristic methods have been shown to be effective in hydrological modeling, their transferability to different regions and climatic conditions has not been extensively evaluated. Therefore, a research gap could exist in investigating the suitability and reliability of different heuristic methods for daily pan evaporation estimation across different regions with varying climatic conditions.
- The FAO-56 Penman-Monteith method is widely used for estimating reference evapotranspiration, particularly in agriculture and water management applications. However, the method relies on a number of input parameters, which can introduce uncertainty and affect the accuracy of the estimates. Thus, the paper could address this issue by identifying the most sensitive input parameters and assessing their impact on the estimates. This study aims to fill this research gap by conducting a Monte Carlo sensitivity analysis of the FAO-56 Penman-Monteith method, which can help improve the accuracy of reference evapotranspiration estimates and inform better water management decisions.
- A potential research gap for the paper could be to conduct a comprehensive analysis of the sensitivity of the FAO-56 Penman-Monteith method for estimating crop water requirements in different agro-ecological regions of India. This study could involve collecting and analyzing data on meteorological parameters, soil characteristics, and crop types from various locations across India to assess the accuracy and reliability of the FAO-56 Penman-Monteith method in different agro-ecological regions. The

findings of this study could have significant implications for water management practices and agricultural productivity in India.

- Based on the title of your proposed research paper, one possible research gap could be the lack of studies specifically focused on predicting evaporation in tropical climates using artificial neural network (ANN) climate-based models.While there have been several studies on predicting evaporation using artificial neural network (ANN) models, there is a gap in research when it comes to predicting evaporation in tropical climates using climate-based models. Tropical climates have unique environmental conditions such as high temperature, high humidity, and high precipitation, which can significantly influence the evaporation rate. Therefore, there is a need to develop an ANN model that takes into account the climatic variables specific to tropical regions to predict evaporation accurately.
- There are several potential research gaps that could be explored for a paper on evaporation estimation using artificial neural networks. Comparison with other estimation methods: While artificial neural networks have been used to estimate evaporation in some studies, it would be valuable to compare their performance with other methods, such as empirical equations or physical models. This could help to identify situations where one method is more appropriate than others. Sensitivity analysis: Artificial neural networks typically have many input parameters, and it would be interesting to explore how sensitive the evaporation estimates are to changes in these parameters. This could help to identify which input parameters are most important for accurate evaporation estimation.
- There are several potential research gaps that could be explored in the context of artificial neural network (ANN) based modeling of evaporation losses in reservoirs. Here are a few possibilities Lack of real-world data: One potential research gap is the lack of real-world data on evaporation losses in reservoirs. While there is a significant body of literature on the subject, much of it is based on theoretical or laboratory data. Therefore, it may be challenging to develop ANN models that accurately reflect the complexities of real-world reservoirs without access to robust and reliable data. Limited scope of previous studies: Another research gap is the limited scope of previous studies on ANN-based modeling of evaporation losses in reservoirs. Many studies have focused on the development and validation of models, but there has been less exploration of the practical applications of these models or the potential limitations of using ANNs for this purpose.
- Based on the title of the paper, it appears that the research aims to analyze changes in meteorological variables in Serbia using Mann-Kendall and Sen slope estimator statistical tests.Lack of use of statistical tests for trend analysis: If previous studies in Serbia have not utilized Mann-Kendall and Sen slope estimator statistical tests, then the study could be the first to apply these tests in the region and provide insights into their usefulness for trend analysis. Limited research on specific meteorological variables: If previous research in Serbia has focused on only a few meteorological variables, then the study could

expand the scope of research to include other variables and provide a more comprehensive understanding of how meteorological conditions are changing in the region. Lack of studies on the impacts of changing meteorological variables: If previous studies in Serbia have only analyzed changes in meteorological variables without exploring their impacts on the environment, economy, or society, then the study could provide a more holistic understanding of the implications of changing meteorological conditions.

OBJECTIVES OF THE PROPOSED WORK:

- To Estimate the reference evaporation(ET) by using the PM method (FAO 56).
- To evaluate how much each meteorological variables contributed to the trend of ET.
- To calculate each climate variable to the variations in ET.
- To estimate ET using ANN “Artificial Neural Network”.

CHAPTER-3

STUDY AREA

The Gandhi KrishiVignana Kendra (GKVK) station in Bangalore is a weather observatory under the India Meteorological Department (IMD). The station provides weather data for Bangalore and its surrounding areas.

SI.NO	Station	State	Latitude	Longitude	Altitude	Climate
1.	GKVK	Karnataka	13.0801°N	77.5785°E	927m	Sub-Humid

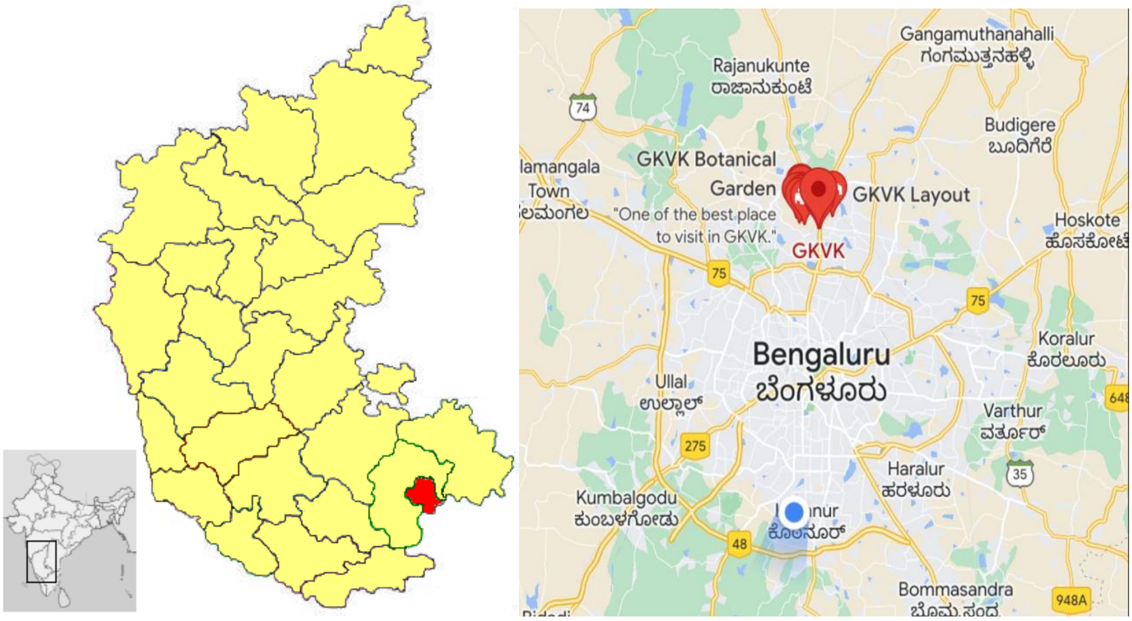

Fig .3: Gandhi KrishiVignana Kendra (GKVK) station in Bangalore

3.1 DATA TO BE USED:

The details of the study area for the various parameters requested are as follows:

- ✓ Maximum temperature (Tmax)°C
- ✓ Minimum temperature (Tmax) °C
- ✓ Altitude(z) m
- ✓ Wind speed (u_2)m/s
- ✓ Relative humidity (RH)%
- ✓ Sunshine hours (ws) kmph

Maximum Temperature (Tmax)°C:

The maximum temperature at the GKVK station in Bangalore is recorded using a maximum thermometer. The study area for maximum temperature is the area within a radius of approximately 5 km around the GKVK station. The maximum temperature is typically recorded during the day when the sun is at its peak, between 1 pm to 4 pm.

Minimum Temperature (Tmax) °C:

The minimum temperature at the GKVK station in Bangalore is recorded using a minimum thermometer. The study area for minimum temperature is the area within a radius of approximately 5 km around the GKVK station. The minimum temperature is typically recorded during the night when the temperature drops to its lowest point, between 2 am to 6 am.

Altitude(z) m:

The GKVK station in Bangalore is located at an altitude of approximately 920 meters above sea level. The study area for altitude is the surrounding area within a radius of approximately 5 km around the GKVK station.

Wind Speed (u2) m/s:

The wind speed at the GKVK station in Bangalore is measured using an anemometer. The study area for wind speed is the area within a radius of approximately 5 km around the GKVK station. The wind speed is typically recorded at a height of 10 meters above ground level.

Relative Humidity (RH) %:

The relative humidity at the GKVK station in Bangalore is measured using a hygrometer. The study area for relative humidity is the area within a radius of approximately 5 km around the GKVK station. The relative humidity is typically recorded twice a day, at 8:30 am and 5:30 pm

Sunshine Hours (ws) kmph:

The sunshine hours at the GKVK station in Bangalore are calculated using a sunshine recorder. The study area for sunshine hours is the area within a radius of approximately 5 km around the GKVK station. The sunshine hours are typically recorded between 6 am to 6 pm.

CHAPTER-4

METHODOLOGY

4.1 CONVENTIONAL METHOD TO FIND OUT REFERENCE EVAPOTRANSPIRATION:

Microsoft excel software is used to compute the reference evapotranspiration using various empirical formulas; out of which Penman-Montecito and Stefan's-Steward models showed relatively closer values to the actual evaporation.

4.1.1 To calculate ET using the Penman-Monteith equation:

$$ET_o = \frac{0.408\,\Delta(R_n - G) + \gamma \frac{900}{T+273} u_2 (e_s - e_a)}{\Delta + \gamma(1+0.34\,u_2)}$$ ……………………..….(1)

where ETo= reference evapotranspiration [mm day^{-1}]

Rn= net radiation at the crop surface [MJ m^{-2} day^{-1}]

G= soil heat flux density [MJ m^{-2} day^{-1}]

T= mean daily air temperature at 2 m height [°C]

u2= wind speed at 2 m height [m s^{-1}]

es= saturation vapour pressure [kPa]

ea= actual vapour pressure [kPa]

es-ea=saturation vapour pressure deficit [kPa]

Δ= slope vapour pressure curve [kPa °C^{-1}]

γ= psychometric constant [kPa °C^{-1}]

4.1.2 To calculate ET using the Stephan-Stewart equation:

The sensitivity coefficients for each climatic variable (i.e., Tmax, Tmin, Rs, RHavg, and Ws) were derived from the ratio of change in ETo to the unit of change (either increase or decrease) in each climatic variable on a daily basis.

$$E_P = R_S(a + bT_m)$$ ....(2)

where Ep= reference evapotranspiration [mm day^{-1}]

Rs= daily shortwave radiation [MJ m^{-2} day^{-1}]

a and b= fitting constants

Tmean= Mean temperature [°C]

4.2 SENSITIVITY ANALYSIS

Sensitivity analysis is used to identify how much variations in the input values for a given variable impact the results for a mathematical model. Here, the input refers to the climate variables and the output is the evaporation. The input variables are maximum temperature, minimum temperature, net radiation, relative humidity and wind speed. For this, the sensitivity coefficient for each climatic variable) were derived from the ratio of change in ET_o to the unit of change in each climatic variable on a daily basis. It is represented as follows:

$$\mathbf{C_s = CH_{ETo}/CH_{CV}} \ldots\ldots\ldots\ldots\ldots\ldots\ldots\ldots\ldots\ldots\ldots\ldots..(3)$$

where C_s = sensitivity coefficient
CH_{ETo} = change in ETo with respect to change in climate variables
CH_{CV} = change in climate variable

4.3 TREND ANALYSIS

Trend analysis of evapotranspiration involves studying the changes in the rate of evapotranspiration over a period of time. This can be done using various techniques, including statistical analysis, remote sensing, modeling, and field observations. Statistical analysis involves analyzing historical data to identify trends and patterns in evapotranspiration rates over time. This can be done using techniques such as linear regression or time-series analysis, which can help to detect trends and estimate the rate of change in evapotranspiration over time. For example, a linear regression analysis can be used to determine whether the rate of evapotranspiration is increasing or decreasing over a given period of time. Remote sensing techniques can also be used to detect changes in evapotranspiration rates over time. For example, satellite-based remote sensing can be used to measure surface temperature and vegetation indices, which can provide information on the rate of evapotranspiration. This information can then be used to estimate changes in evapotranspiration rates over time. Modeling techniques can also be used to simulate the process of evapotranspiration and predict how it will change over time. These models can take into account various factors that affect evapotranspiration, such as temperature, humidity, and soil moisture. The models can be used to forecast future evapotranspiration rates under different scenarios, such as changes in climate or land use. Finally, field observations of evapotranspiration rates can be made using instruments such as lysimeters or eddy covariance systems. These instruments can provide direct measurements of evapotranspiration rates, which can be used to validate and calibrate models and remote sensing data.

Trend analysis of evapotranspiration is important for understanding how water resources are being affected by climate change and human activities such as land use change and irrigation. It can help to identify regions that are becoming drier or wetter and to develop strategies for managing water resources in these regions. It can also be used to monitor the effectiveness of water management practices and to improve our understanding of the complex interactions between the land surface and the atmosphere.

Analysis of trends in monthly evaporation and solar radiation in the face of climate change gives useful information for better planning and management of water resources. This paper examines the monthly evaporation and solar radiation trend using the recently developed innovative trend analysis method (ITAM). The monthly evaporation trend result shows that 75% of the months indicated decreasing trend with the month of February, March, August and April decreased significantly at 0.1%, 10%, 10% and 5% significance level respectively. As regards solar radiation all the months indicated decreasing trend with January, July and October shown a decreasing trend at 5% significant level. By comparing the Mann-Kendall method with the ITAM the reliability of ITAM was ascertained. Hence, ITAM can be effectively utilized in climate change scenarios where useful information is needed for accurate management and planning of water resources.

Tests for the detection of significant trends in climatologist time series can be classified as parametric and non-parametric methods. Parametric trend tests require data to be independent and normally distributed, while non-parametric trend tests require only that the data be independent. In this study, two non-parametric methods (Mann-Kendall and Sen's slope estimator) were used to detect the meteorological variables' trends.

4.3.1 Methodology for Mann-Kendall test:

The Mann-Kendall test is a statistical test used to detect trends in time-series data. It is a non-parametric test, which means that it does not make assumptions about the distribution of the data. The test is widely used in hydrology, climatology, and environmental science to analyze time-series data of hydro logical and climatological variables.

The methodology of the Mann-Kendall test involves the following steps:

- Calculation of the test statistic, S: The test statistic, S, is calculated by comparing the number of pairs of data points that have a positive difference with the number of pairs that have a negative difference. The formula for the test statistic is.

$$S = \sum_{i-1}^{n-1} \sum_{i+1}^{n} sign(X_j - X_i) \quad \ldots\ldots\ldots\ldots\ldots\ldots \text{(1)}$$

Where:

n: numbers of data points.

Xj and Xi are annual values in years j and I,j> 1 and Sign (Xj-Xi) calculated using the equation:

$$Sign(Xj - Xi) = \begin{cases} -1\, for(X_j - X_i) < 0 \\ 0\, for(X_j - X_i) = 0 \\ +1\, fir(X_j - X_i) > 0 \end{cases} \quad \ldots\ldots\ldots\ldots\ldots\ (2)$$

- Calculation of the variance of S:

The variance of S is calculated using the following formula:

$$Var(S) = \frac{1}{18}\left[n(n-1)(2n+5)\right] \ldots\ldots\ldots\ldots\ (3)$$

Where:

n is the data points number.

- Calculation of the standardized test statistic, Z:

The standardized test statistic, Z, is calculated using the following formula:

$$Z = \begin{cases} \dfrac{S-1}{\sqrt{\mathrm{var}(S)}}, ifS < 0 \\ 0 ifS = 0 \\ \dfrac{S+1}{\sqrt{\mathrm{var}(S), ifS > 0}} \end{cases} \quad \ldots\ldots\ldots\ldots\ldots\ldots\ldots\ (4)$$

- The Mann-Kendall test can also be extended to detect trends in seasonal or spatial data by using modified versions of the test statistic and variance.

4.3.2 Methodology for Sen's slope test:

- developed the non-parametric procedure for estimating the slope of trend in the sample of K pairs of data:

$$Q = Median\left(\frac{x_j - x_k}{j-k}\right) j > k \ \ldots\ldots\ldots\ldots\ (1)$$

Where:

Q is a slope estimate.

X_j are X_k the values at times j and k,

K grade y data

CHAPTER-5

SOFTWARE USED

1. Ms office Excel.
2. XLSTAT
3. R STUDIO

5.1 To calculate ET using the Penman-Monteith by Ms office Excel.

Step 1: The daily average of the climate variables i.e., maximum temperature and minimum temperature are computed and are pasted as per the Julian days.

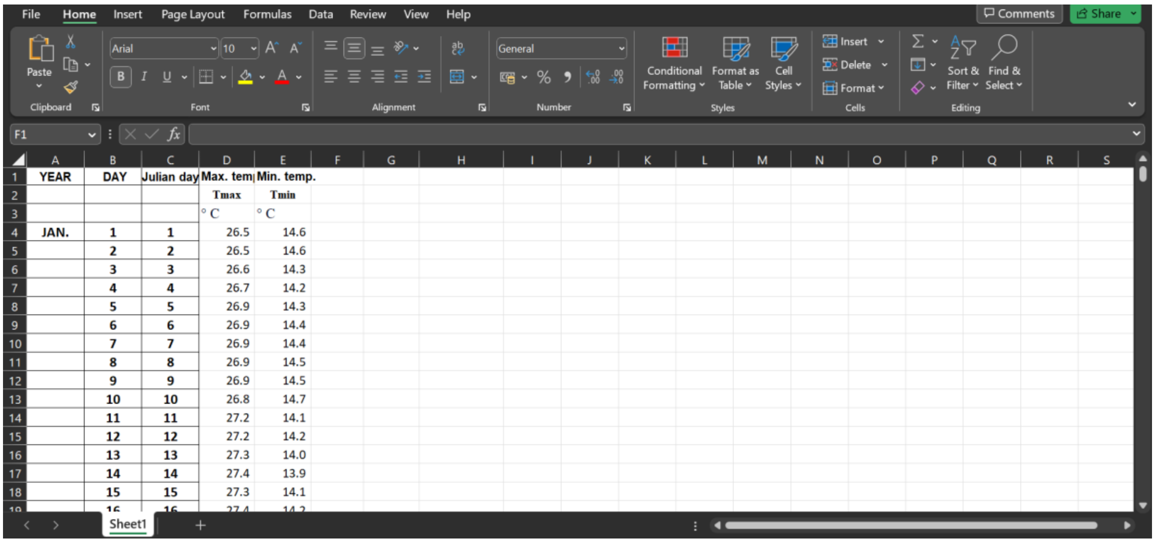

YEAR	DAY	Julian day	Max. temp. Tmax °C	Min. temp. Tmin °C
JAN.	1	1	26.5	14.6
	2	2	26.5	14.6
	3	3	26.6	14.3
	4	4	26.7	14.2
	5	5	26.9	14.3
	6	6	26.9	14.4
	7	7	26.9	14.4
	8	8	26.9	14.5
	9	9	26.9	14.5
	10	10	26.8	14.7
	11	11	27.2	14.1
	12	12	27.2	14.2
	13	13	27.3	14.0
	14	14	27.4	13.9
	15	15	27.3	14.1

Fig.4: Daily average of maximum temperature and minimum temperature

Step 2: The mean temperature is computed, which is (maximum temperature + minimum temperature)/2

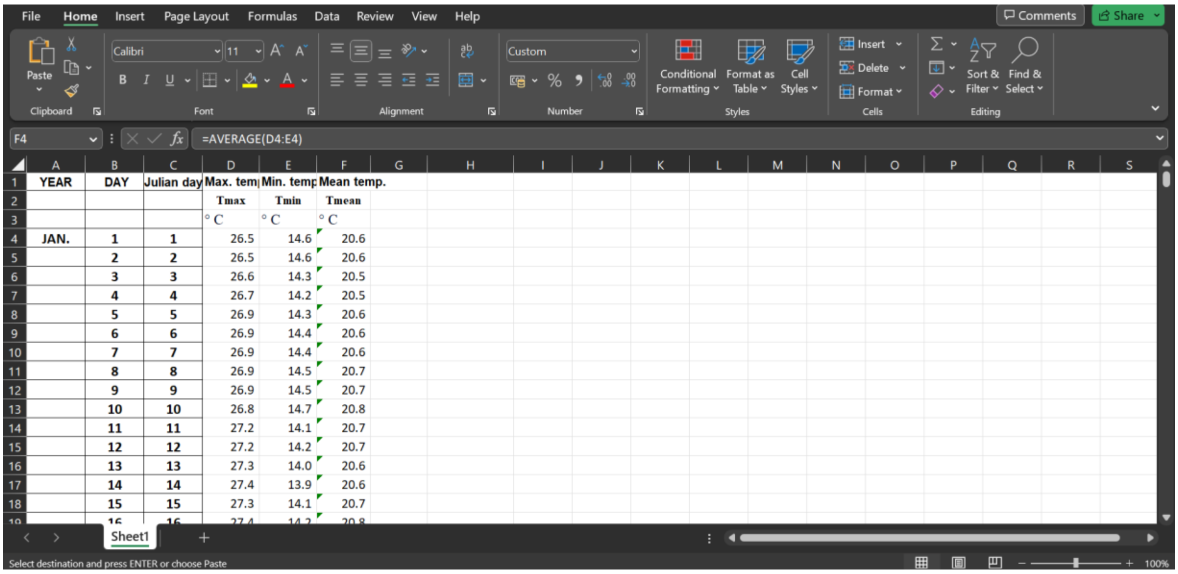

=AVERAGE(D4:E4)

YEAR	DAY	Julian day	Max. temp. Tmax °C	Min. temp. Tmin °C	Mean temp. Tmean °C
JAN.	1	1	26.5	14.6	20.6
	2	2	26.5	14.6	20.6
	3	3	26.6	14.3	20.5
	4	4	26.7	14.2	20.5
	5	5	26.9	14.3	20.6
	6	6	26.9	14.4	20.6
	7	7	26.9	14.4	20.6
	8	8	26.9	14.5	20.7
	9	9	26.9	14.5	20.7
	10	10	26.8	14.7	20.8
	11	11	27.2	14.1	20.7
	12	12	27.2	14.2	20.7
	13	13	27.3	14.0	20.6
	14	14	27.4	13.9	20.6
	15	15	27.3	14.1	20.7

Fig.5: Mean of maximum temperature and minimum temperature

Step 3: Sunshine hours and wind speed(kmph) data's daily average is computed and copied. Wind speed is converted into m/s. (ws*(1000/60*60))

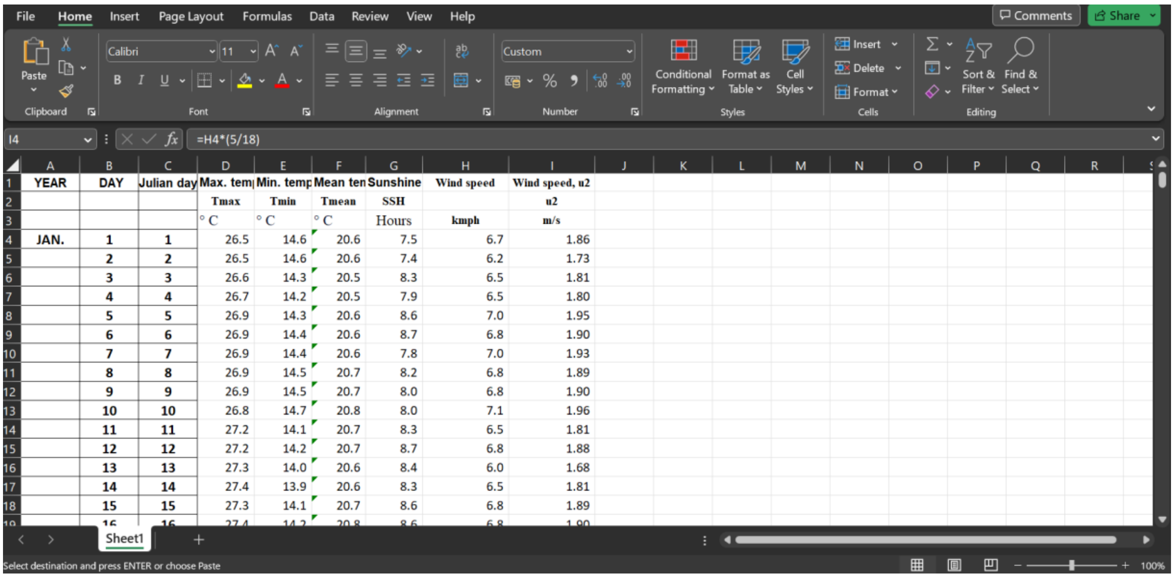

YEAR	DAY	Julian day	Max. tem	Min. temp	Mean ten	Sunshine	Wind speed	Wind speed, u2
			Tmax	Tmin	Tmean	SSH		u2
			°C	°C	°C	Hours	kmph	m/s
JAN.	1	1	26.5	14.6	20.6	7.5	6.7	1.86
	2	2	26.5	14.6	20.6	7.4	6.2	1.73
	3	3	26.6	14.3	20.5	8.3	6.5	1.81
	4	4	26.7	14.2	20.5	7.9	6.5	1.80
	5	5	26.9	14.3	20.6	8.6	7.0	1.95
	6	6	26.9	14.4	20.6	8.7	6.8	1.90
	7	7	26.9	14.4	20.6	7.8	7.0	1.93
	8	8	26.9	14.5	20.7	8.2	6.8	1.89
	9	9	26.9	14.5	20.7	8.0	6.8	1.90
	10	10	26.8	14.7	20.8	8.0	7.1	1.96
	11	11	27.2	14.1	20.7	8.3	6.5	1.81
	12	12	27.2	14.2	20.7	8.7	6.8	1.88
	13	13	27.3	14.0	20.6	8.4	6.0	1.68
	14	14	27.4	13.9	20.6	8.3	6.5	1.81
	15	15	27.3	14.1	20.7	8.6	6.8	1.89

Fig. 6: Daily average of Sunshine hours and wind speed

Step 4: Altitude of the given place is entered.

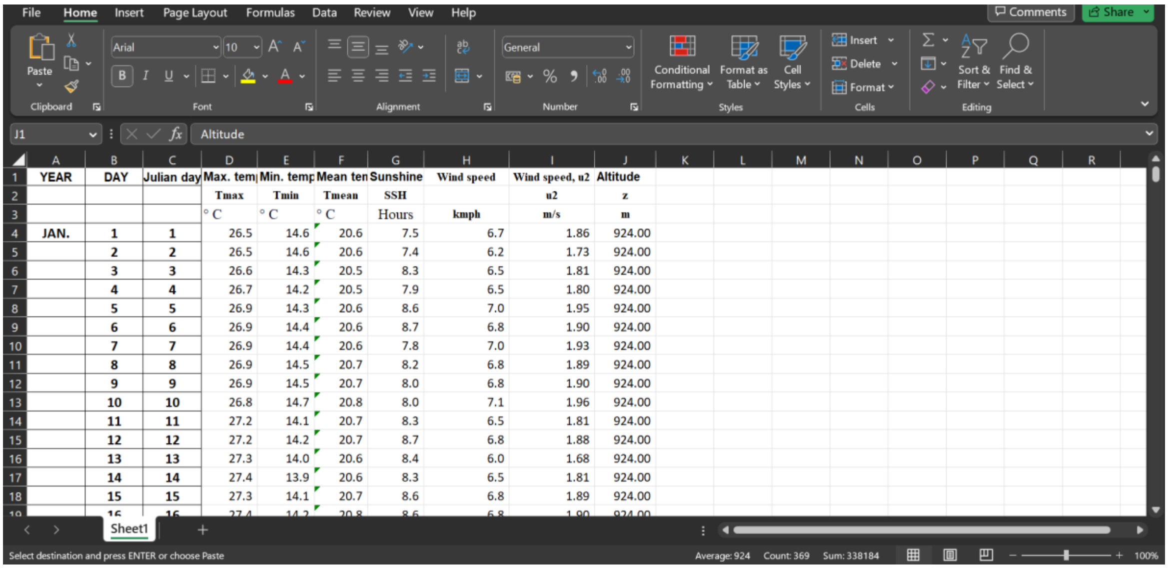

YEAR	DAY	Julian day	Max. tem	Min. temp	Mean ten	Sunshine	Wind speed	Wind speed, u2	Altitude
			Tmax	Tmin	Tmean	SSH		u2	z
			°C	°C	°C	Hours	kmph	m/s	m
JAN.	1	1	26.5	14.6	20.6	7.5	6.7	1.86	924.00
	2	2	26.5	14.6	20.6	7.4	6.2	1.73	924.00
	3	3	26.6	14.3	20.5	8.3	6.5	1.81	924.00
	4	4	26.7	14.2	20.5	7.9	6.5	1.80	924.00
	5	5	26.9	14.3	20.6	8.6	7.0	1.95	924.00
	6	6	26.9	14.4	20.6	8.7	6.8	1.90	924.00
	7	7	26.9	14.4	20.6	7.8	7.0	1.93	924.00
	8	8	26.9	14.5	20.7	8.2	6.8	1.89	924.00
	9	9	26.9	14.5	20.7	8.0	6.8	1.90	924.00
	10	10	26.8	14.7	20.8	8.0	7.1	1.96	924.00
	11	11	27.2	14.1	20.7	8.3	6.5	1.81	924.00
	12	12	27.2	14.2	20.7	8.7	6.8	1.88	924.00
	13	13	27.3	14.0	20.6	8.4	6.0	1.68	924.00
	14	14	27.4	13.9	20.6	8.3	6.5	1.81	924.00
	15	15	27.3	14.1	20.7	8.6	6.8	1.89	924.00

Fig.7: Altitude of the given place

Step 5: Maximum vapour pressure and minimum vapour pressure are computed using maximum temperature, minimum temperature respectively using table 2.3 from FAO-56.

Saturation vapour pressure is computed by using the mean of the above mentioned two.

Actual vapour pressure is computed in the same method using the mean temperature.

Vapour pressure deficit is calculated by taking the difference of actual vapour pressure and saturation vapour pressure.

$$e^{o}(T) = 0.6108 \exp\left[\frac{17.27\,T}{T + 237.3}\right] \qquad \ldots\ldots\ldots\ldots\ldots\ldots\ldots\ (2)$$

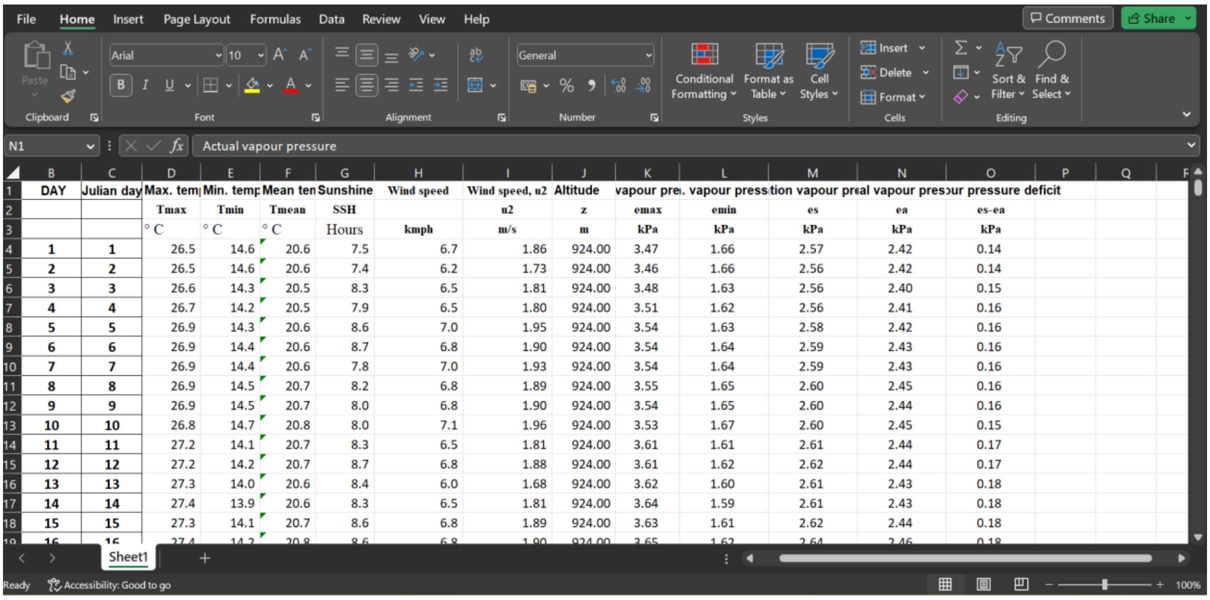

DAY	Julian day	Max. tem	Min. temp	Mean ten	Sunshine	Wind speed	Wind speed, u2	Altitude	vapour pre	. vapour press	tion vapour pr	al vapour pres	ur pressure deficit
		Tmax	Tmin	Tmean	SSH		u2	z	emax	emin	es	ea	es-ea
		°C	°C	°C	Hours	kmph	m/s	m	kPa	kPa	kPa	kPa	kPa
1	1	26.5	14.6	20.6	7.5	6.7	1.86	924.00	3.47	1.66	2.57	2.42	0.14
2	2	26.5	14.6	20.6	7.4	6.2	1.73	924.00	3.46	1.66	2.56	2.42	0.14
3	3	26.6	14.3	20.5	8.3	6.5	1.81	924.00	3.48	1.63	2.56	2.40	0.15
4	4	26.7	14.2	20.5	7.9	6.5	1.80	924.00	3.51	1.62	2.56	2.41	0.16
5	5	26.9	14.3	20.6	8.6	7.0	1.95	924.00	3.54	1.63	2.58	2.42	0.16
6	6	26.9	14.4	20.6	8.7	6.8	1.90	924.00	3.54	1.64	2.59	2.43	0.16
7	7	26.9	14.4	20.6	7.8	7.0	1.93	924.00	3.54	1.64	2.59	2.43	0.16
8	8	26.9	14.5	20.7	8.2	6.8	1.89	924.00	3.55	1.65	2.60	2.45	0.16
9	9	26.9	14.5	20.7	8.0	6.8	1.90	924.00	3.54	1.65	2.60	2.44	0.16
10	10	26.8	14.7	20.8	8.0	7.1	1.96	924.00	3.53	1.67	2.60	2.45	0.15
11	11	27.2	14.1	20.7	8.3	6.5	1.81	924.00	3.61	1.61	2.61	2.44	0.17
12	12	27.2	14.2	20.7	8.7	6.8	1.88	924.00	3.61	1.62	2.62	2.44	0.17
13	13	27.3	14.0	20.6	8.4	6.0	1.68	924.00	3.62	1.60	2.61	2.43	0.18
14	14	27.4	13.9	20.6	8.3	6.5	1.81	924.00	3.64	1.59	2.61	2.43	0.18
15	15	27.3	14.1	20.7	8.6	6.8	1.89	924.00	3.63	1.61	2.62	2.44	0.18

Fig. 8: Maximum temperature, minimum temperature respectively using table 2.3 from FAO-56.

Step 6: Relative humidity's daily average is computed and pasted.

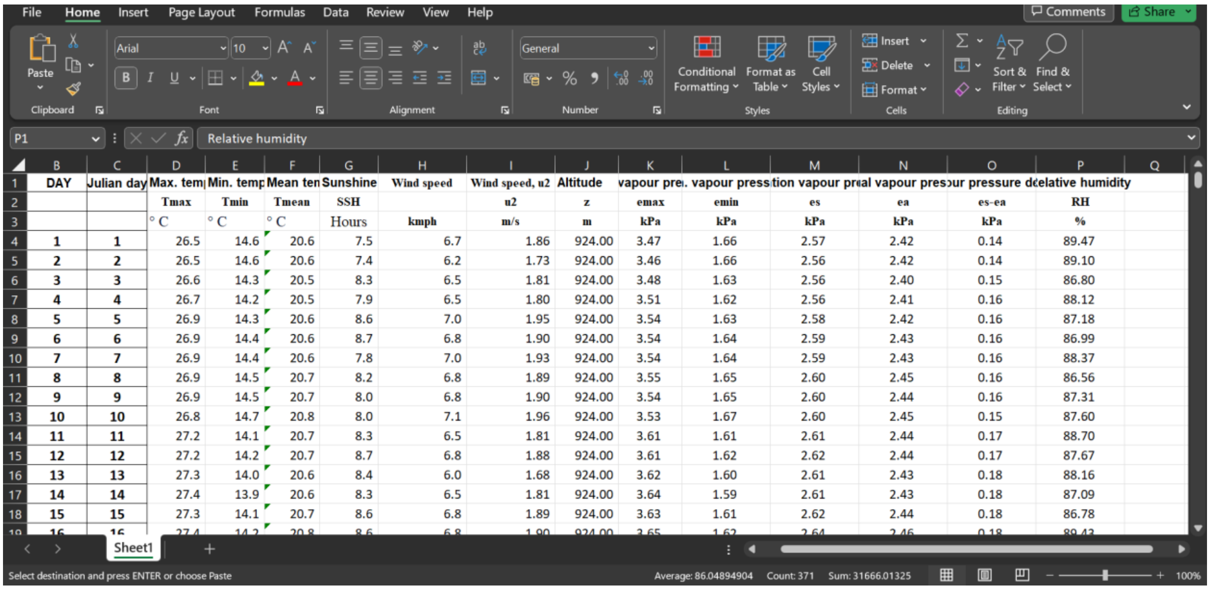

DAY	Julian day	Max. tem	Min. temp	Mean ten	Sunshine	Wind speed	Wind speed, u2	Altitude	vapour pre	. vapour press	tion vapour pr	al vapour pres	ur pressure d	elative humidity
		Tmax	Tmin	Tmean	SSH		u2	z	emax	emin	es	ea	es-ea	RH
		°C	°C	°C	Hours	kmph	m/s	m	kPa	kPa	kPa	kPa	kPa	%
1	1	26.5	14.6	20.6	7.5	6.7	1.86	924.00	3.47	1.66	2.57	2.42	0.14	89.47
2	2	26.5	14.6	20.6	7.4	6.2	1.73	924.00	3.46	1.66	2.56	2.42	0.14	89.10
3	3	26.6	14.3	20.5	8.3	6.5	1.81	924.00	3.48	1.63	2.56	2.40	0.15	86.80
4	4	26.7	14.2	20.5	7.9	6.5	1.80	924.00	3.51	1.62	2.56	2.41	0.16	88.12
5	5	26.9	14.3	20.6	8.6	7.0	1.95	924.00	3.54	1.63	2.58	2.42	0.16	87.18
6	6	26.9	14.4	20.6	8.7	6.8	1.90	924.00	3.54	1.64	2.59	2.43	0.16	86.99
7	7	26.9	14.4	20.6	7.8	7.0	1.93	924.00	3.54	1.64	2.59	2.43	0.16	88.37
8	8	26.9	14.5	20.7	8.2	6.8	1.89	924.00	3.55	1.65	2.60	2.45	0.16	86.56
9	9	26.9	14.5	20.7	8.0	6.8	1.90	924.00	3.54	1.65	2.60	2.44	0.16	87.31
10	10	26.8	14.7	20.8	8.0	7.1	1.96	924.00	3.53	1.67	2.60	2.45	0.15	87.60
11	11	27.2	14.1	20.7	8.3	6.5	1.81	924.00	3.61	1.61	2.61	2.44	0.17	88.70
12	12	27.2	14.2	20.7	8.7	6.8	1.88	924.00	3.61	1.62	2.62	2.44	0.17	87.67
13	13	27.3	14.0	20.6	8.4	6.0	1.68	924.00	3.62	1.60	2.61	2.43	0.18	88.16
14	14	27.4	13.9	20.6	8.3	6.5	1.81	924.00	3.64	1.59	2.61	2.43	0.18	87.09
15	15	27.3	14.1	20.7	8.6	6.8	1.89	924.00	3.63	1.61	2.62	2.44	0.18	86.78

Fig .9: Relative humidity's daily average is computed

Step 7: Slope of saturation vapour pressure curve, Δ is calculated using table 2.4 from FAO-56

$$\Delta = \frac{4098\left[0.6108\exp\left(\frac{17.27\,T}{T+237.3}\right)\right]}{(T+237.3)^2} \quad \ldots\ldots\ldots\ldots\ldots\ldots\ldots\ldots\ (3)$$

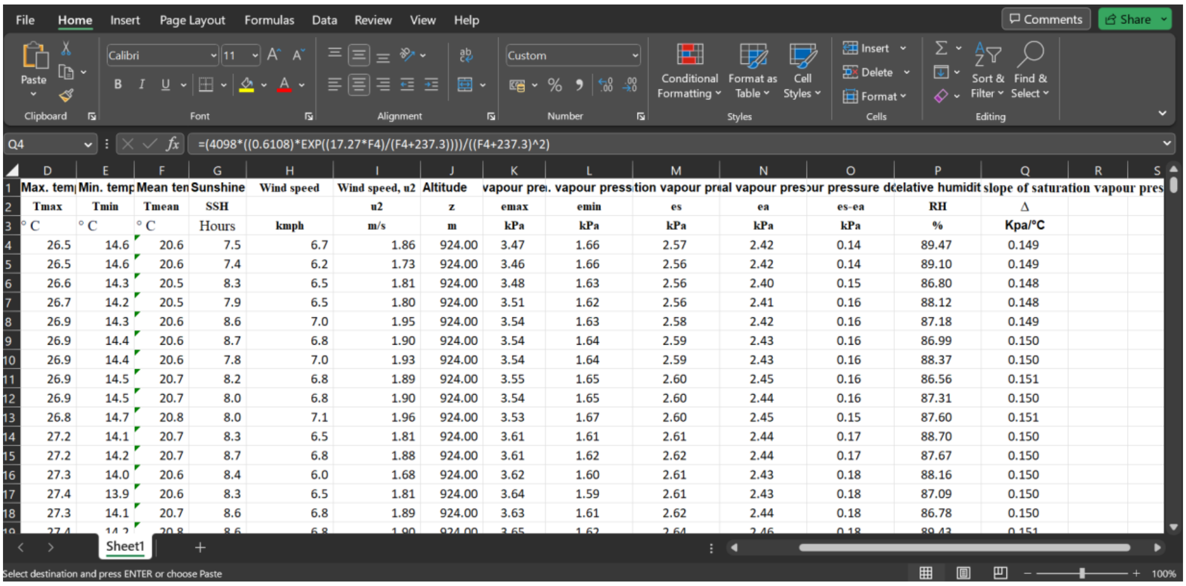

	D	E	F	G	H	I	J	K	L	M	N	O	P	Q
1	Max. tem	Min. temp	Mean ten	Sunshine	Wind speed	Wind speed, u2	Altitude	vapour pre	. vapour press	tion vapour pr	al vapour pres	ur pressure d	elative humidit	slope of saturation vapour pres
2	Tmax	Tmin	Tmean	SSH		u2	z	emax	emin	es	ea	es-ea	RH	Δ
3	° C	° C	° C	Hours	kmph	m/s	m	kPa	kPa	kPa	kPa	kPa	%	Kpa/°C
4	26.5	14.6	20.6	7.5	6.7	1.86	924.00	3.47	1.66	2.57	2.42	0.14	89.47	0.149
5	26.5	14.6	20.6	7.4	6.2	1.73	924.00	3.46	1.66	2.56	2.42	0.14	89.10	0.149
6	26.6	14.3	20.5	8.3	6.5	1.81	924.00	3.48	1.63	2.56	2.40	0.15	86.80	0.148
7	26.7	14.2	20.5	7.9	6.5	1.80	924.00	3.51	1.62	2.56	2.41	0.16	88.12	0.148
8	26.9	14.3	20.6	8.6	7.0	1.95	924.00	3.54	1.63	2.58	2.42	0.16	87.18	0.149
9	26.9	14.4	20.6	8.7	6.8	1.90	924.00	3.54	1.64	2.59	2.43	0.16	86.99	0.150
10	26.9	14.4	20.6	7.8	7.0	1.93	924.00	3.54	1.64	2.59	2.43	0.16	88.37	0.150
11	26.9	14.5	20.7	8.2	6.8	1.89	924.00	3.55	1.65	2.60	2.45	0.16	86.56	0.151
12	26.9	14.5	20.7	8.0	6.8	1.90	924.00	3.54	1.65	2.60	2.44	0.16	87.31	0.150
13	26.8	14.7	20.8	8.0	7.1	1.96	924.00	3.53	1.67	2.60	2.45	0.15	87.60	0.151
14	27.2	14.1	20.7	8.3	6.5	1.81	924.00	3.61	1.61	2.61	2.44	0.17	88.70	0.150
15	27.2	14.2	20.7	8.7	6.8	1.88	924.00	3.61	1.62	2.62	2.44	0.17	87.67	0.150
16	27.3	14.0	20.6	8.4	6.0	1.68	924.00	3.62	1.60	2.61	2.43	0.18	88.16	0.150
17	27.4	13.9	20.6	8.3	6.5	1.81	924.00	3.64	1.59	2.61	2.43	0.18	87.09	0.150
18	27.3	14.1	20.7	8.6	6.8	1.89	924.00	3.63	1.61	2.62	2.44	0.18	86.78	0.150

Fig .10: Slope of saturation vapour pressure curve.

Step 8: Psychometrics constant is calculated using table 2.2 from FAO-56

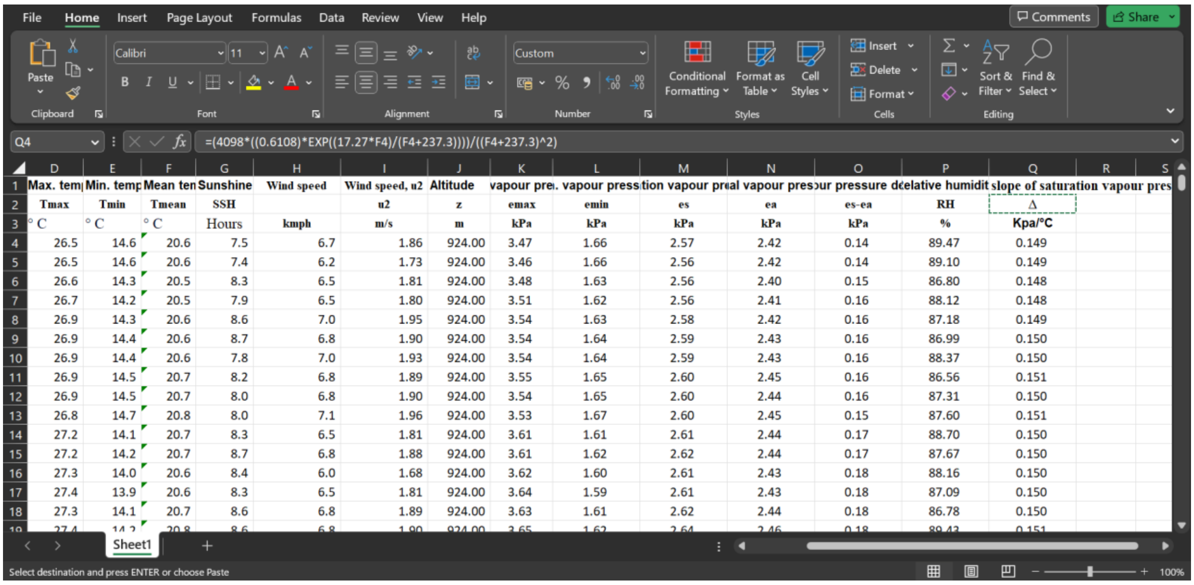

	D	E	F	G	H	I	J	K	L	M	N	O	P	Q
1	Max. tem	Min. temp	Mean ten	Sunshine	Wind speed	Wind speed, u2	Altitude	vapour pre	. vapour press	tion vapour pr	al vapour pres	ur pressure d	elative humidit	slope of saturation vapour pres
2	Tmax	Tmin	Tmean	SSH		u2	z	emax	emin	es	ea	es-ea	RH	Δ
3	° C	° C	° C	Hours	kmph	m/s	m	kPa	kPa	kPa	kPa	kPa	%	Kpa/°C
4	26.5	14.6	20.6	7.5	6.7	1.86	924.00	3.47	1.66	2.57	2.42	0.14	89.47	0.149
5	26.5	14.6	20.6	7.4	6.2	1.73	924.00	3.46	1.66	2.56	2.42	0.14	89.10	0.149
6	26.6	14.3	20.5	8.3	6.5	1.81	924.00	3.48	1.63	2.56	2.40	0.15	86.80	0.148
7	26.7	14.2	20.5	7.9	6.5	1.80	924.00	3.51	1.62	2.56	2.41	0.16	88.12	0.148
8	26.9	14.3	20.6	8.6	7.0	1.95	924.00	3.54	1.63	2.58	2.42	0.16	87.18	0.149
9	26.9	14.4	20.6	8.7	6.8	1.90	924.00	3.54	1.64	2.59	2.43	0.16	86.99	0.150
10	26.9	14.4	20.6	7.8	7.0	1.93	924.00	3.54	1.64	2.59	2.43	0.16	88.37	0.150
11	26.9	14.5	20.7	8.2	6.8	1.89	924.00	3.55	1.65	2.60	2.45	0.16	86.56	0.151
12	26.9	14.5	20.7	8.0	6.8	1.90	924.00	3.54	1.65	2.60	2.44	0.16	87.31	0.150
13	26.8	14.7	20.8	8.0	7.1	1.96	924.00	3.53	1.67	2.60	2.45	0.15	87.60	0.151
14	27.2	14.1	20.7	8.3	6.5	1.81	924.00	3.61	1.61	2.61	2.44	0.17	88.70	0.150
15	27.2	14.2	20.7	8.7	6.8	1.88	924.00	3.61	1.62	2.62	2.44	0.17	87.67	0.150
16	27.3	14.0	20.6	8.4	6.0	1.68	924.00	3.62	1.60	2.61	2.43	0.18	88.16	0.150
17	27.4	13.9	20.6	8.3	6.5	1.81	924.00	3.64	1.59	2.61	2.43	0.18	87.09	0.150
18	27.3	14.1	20.7	8.6	6.8	1.89	924.00	3.63	1.61	2.62	2.44	0.18	86.78	0.150

Fig .11: Psychometric constant γ is calculated.

Step 9: Soil heat flux is assumed to be zero according to FAO-56

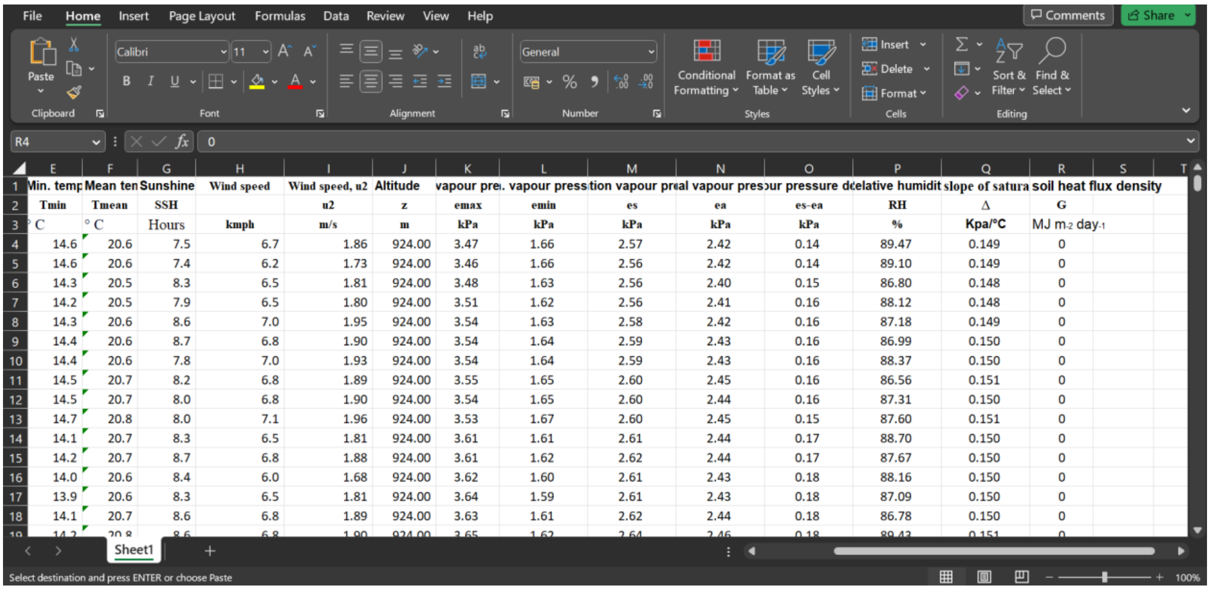

	E	F	G	H	I	J	K	L	M	N	O	P	Q	R
1	Min. temp	Mean ten	Sunshine	Wind speed	Wind speed, u2	Altitude	vapour pre	. vapour press	tion vapour pr	al vapour pres	ur pressure de	elative humidit	slope of satura	soil heat flux density
2	Tmin	Tmean	SSH		u2	z	emax	emin	es	ea	es-ea	RH	Δ	G
3	°C	°C	Hours	kmph	m/s	m	kPa	kPa	kPa	kPa	kPa	%	Kpa/°C	MJ m-2 day-1
4	14.6	20.6	7.5	6.7	1.86	924.00	3.47	1.66	2.57	2.42	0.14	89.47	0.149	0
5	14.6	20.6	7.4	6.2	1.73	924.00	3.46	1.66	2.56	2.42	0.14	89.10	0.149	0
6	14.3	20.5	8.3	6.5	1.81	924.00	3.48	1.63	2.56	2.40	0.15	86.80	0.148	0
7	14.2	20.5	7.9	6.5	1.80	924.00	3.51	1.62	2.56	2.41	0.16	88.12	0.148	0
8	14.3	20.6	8.6	7.0	1.95	924.00	3.54	1.63	2.58	2.42	0.16	87.18	0.149	0
9	14.4	20.6	8.7	6.8	1.90	924.00	3.54	1.64	2.59	2.43	0.16	86.99	0.150	0
10	14.4	20.6	7.8	7.0	1.93	924.00	3.54	1.64	2.59	2.43	0.16	88.37	0.150	0
11	14.5	20.7	8.2	6.8	1.89	924.00	3.55	1.65	2.60	2.45	0.16	86.56	0.151	0
12	14.5	20.7	8.0	6.8	1.90	924.00	3.54	1.65	2.60	2.44	0.16	87.31	0.150	0
13	14.7	20.8	8.0	7.1	1.96	924.00	3.53	1.67	2.60	2.45	0.15	87.60	0.151	0
14	14.1	20.7	8.3	6.5	1.81	924.00	3.61	1.61	2.61	2.44	0.17	88.70	0.150	0
15	14.2	20.7	8.7	6.8	1.88	924.00	3.61	1.62	2.62	2.44	0.17	87.67	0.150	0
16	14.0	20.6	8.4	6.0	1.68	924.00	3.62	1.60	2.61	2.43	0.18	88.16	0.150	0
17	13.9	20.6	8.3	6.5	1.81	924.00	3.64	1.59	2.61	2.43	0.18	87.09	0.150	0
18	14.1	20.7	8.6	6.8	1.89	924.00	3.63	1.61	2.62	2.44	0.18	86.78	0.150	0

Fig. 12: Soil heat flux

Step 10: Latitude in decimal degrees is noted and the same is converted to radians

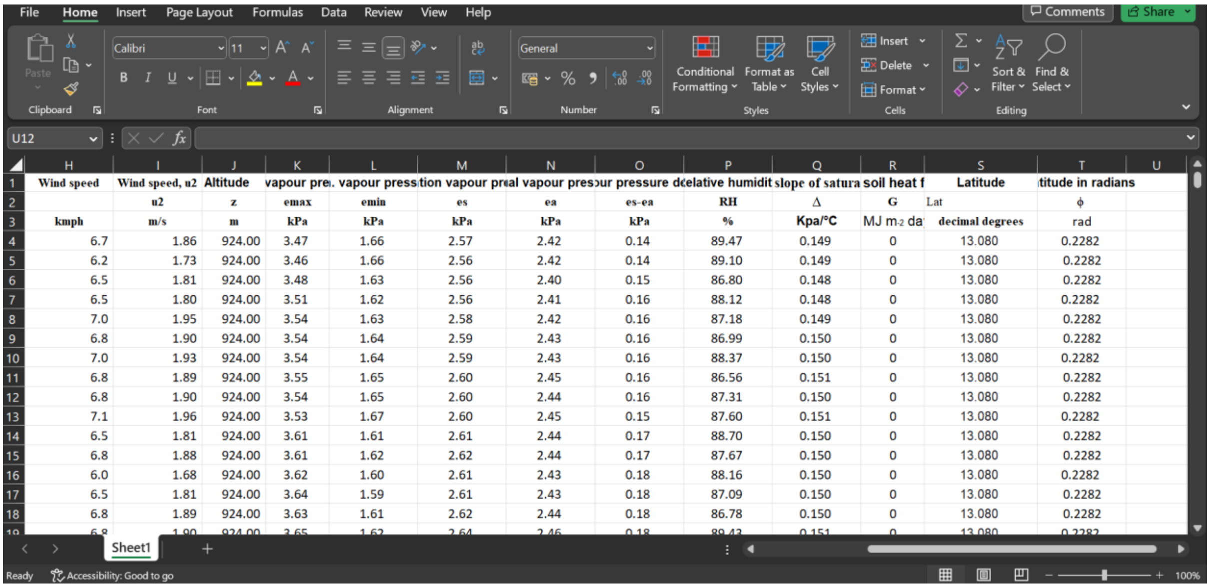

	H	I	J	K	L	M	N	O	P	Q	R	S	T
1	Wind speed	Wind speed, u2	Altitude	vapour pre	. vapour press	tion vapour pr	al vapour pres	ur pressure de	elative humidit	slope of satura	soil heat f	Latitude	titude in radians
2		u2	z	emax	emin	es	ea	es-ea	RH	Δ	G	Lat	ϕ
3	kmph	m/s	m	kPa	kPa	kPa	kPa	kPa	%	Kpa/°C	MJ m-2 da	decimal degrees	rad
4	6.7	1.86	924.00	3.47	1.66	2.57	2.42	0.14	89.47	0.149	0	13.080	0.2282
5	6.2	1.73	924.00	3.46	1.66	2.56	2.42	0.14	89.10	0.149	0	13.080	0.2282
6	6.5	1.81	924.00	3.48	1.63	2.56	2.40	0.15	86.80	0.148	0	13.080	0.2282
7	6.5	1.80	924.00	3.51	1.62	2.56	2.41	0.16	88.12	0.148	0	13.080	0.2282
8	7.0	1.95	924.00	3.54	1.63	2.58	2.42	0.16	87.18	0.149	0	13.080	0.2282
9	6.8	1.90	924.00	3.54	1.64	2.59	2.43	0.16	86.99	0.150	0	13.080	0.2282
10	7.0	1.93	924.00	3.54	1.64	2.59	2.43	0.16	88.37	0.150	0	13.080	0.2282
11	6.8	1.89	924.00	3.55	1.65	2.60	2.45	0.16	86.56	0.151	0	13.080	0.2282
12	6.8	1.90	924.00	3.54	1.65	2.60	2.44	0.16	87.31	0.150	0	13.080	0.2282
13	7.1	1.96	924.00	3.53	1.67	2.60	2.45	0.15	87.60	0.151	0	13.080	0.2282
14	6.5	1.81	924.00	3.61	1.61	2.61	2.44	0.17	88.70	0.150	0	13.080	0.2282
15	6.8	1.88	924.00	3.61	1.62	2.62	2.44	0.17	87.67	0.150	0	13.080	0.2282
16	6.0	1.68	924.00	3.62	1.60	2.61	2.43	0.18	88.16	0.150	0	13.080	0.2282
17	6.5	1.81	924.00	3.64	1.59	2.61	2.43	0.18	87.09	0.150	0	13.080	0.2282
18	6.8	1.89	924.00	3.63	1.61	2.62	2.44	0.18	86.78	0.150	0	13.080	0.2282

Fig. 13: Latitude in decimal degrees is noted

Step 11: Inverse relative distance Earth-Sun, dr is calculated from Eq. 23, page 49 of FAO-56

$$d_r = 1+0.033 \cos(2\pi J/365) \quad \ldots\ldots\ldots\ldots\ldots\ldots\ldots (4)$$

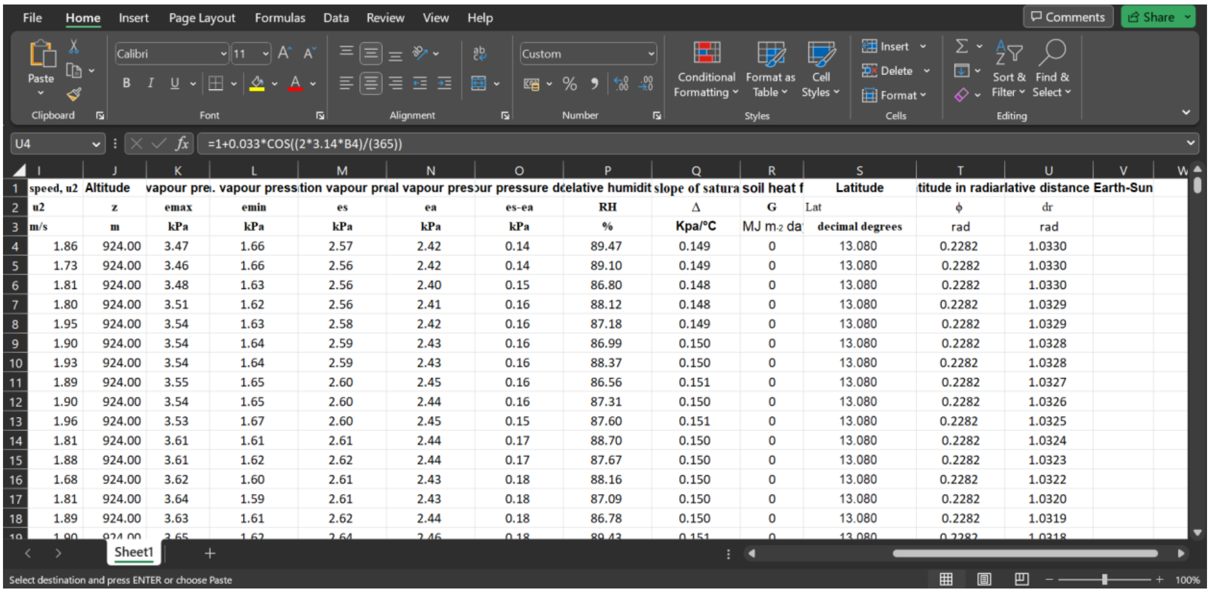

U4 =1+0.033*COS((2*3.14*B4)/(365))

	speed, u2	Altitude	vapour pre	vapour press	tion vapour pre	al vapour pres	ur pressure de	elative humidit	slope of satura	soil heat f	Latitude	titude in radia	lative distance Earth-Sun
2	u2	z	emax	emin	es	ea	es-ea	RH	Δ	G	Lat	φ	dr
3	m/s	m	kPa	kPa	kPa	kPa	kPa	%	Kpa/°C	MJ m-2 da	decimal degrees	rad	rad
4	1.86	924.00	3.47	1.66	2.57	2.42	0.14	89.47	0.149	0	13.080	0.2282	1.0330
5	1.73	924.00	3.46	1.66	2.56	2.42	0.14	89.10	0.149	0	13.080	0.2282	1.0330
6	1.81	924.00	3.48	1.63	2.56	2.40	0.15	86.80	0.148	0	13.080	0.2282	1.0330
7	1.80	924.00	3.51	1.62	2.56	2.41	0.16	88.12	0.148	0	13.080	0.2282	1.0329
8	1.95	924.00	3.54	1.63	2.58	2.42	0.16	87.18	0.149	0	13.080	0.2282	1.0329
9	1.90	924.00	3.54	1.64	2.59	2.43	0.16	86.99	0.150	0	13.080	0.2282	1.0328
10	1.93	924.00	3.54	1.64	2.59	2.43	0.16	88.37	0.150	0	13.080	0.2282	1.0328
11	1.89	924.00	3.55	1.65	2.60	2.45	0.16	86.56	0.151	0	13.080	0.2282	1.0327
12	1.90	924.00	3.54	1.65	2.60	2.44	0.16	87.31	0.150	0	13.080	0.2282	1.0326
13	1.96	924.00	3.53	1.67	2.60	2.45	0.15	87.60	0.151	0	13.080	0.2282	1.0325
14	1.81	924.00	3.61	1.61	2.61	2.44	0.17	88.70	0.150	0	13.080	0.2282	1.0324
15	1.88	924.00	3.61	1.62	2.62	2.44	0.17	87.67	0.150	0	13.080	0.2282	1.0323
16	1.68	924.00	3.62	1.60	2.61	2.43	0.18	88.16	0.150	0	13.080	0.2282	1.0322
17	1.81	924.00	3.64	1.59	2.61	2.43	0.18	87.09	0.150	0	13.080	0.2282	1.0320
18	1.89	924.00	3.63	1.61	2.62	2.44	0.18	86.78	0.150	0	13.080	0.2282	1.0319

Fig. 14: Calculation Inverse relative distance Earth-Sun

Step 12: Solar declination, δ is calculated using Eq. 24, page 49 of FAO- 56

$$\delta = 0.409 \sin(2\pi J/365 - 1.39) \ldots\ldots\ldots\ldots\ldots\ldots\ldots \quad (5)$$

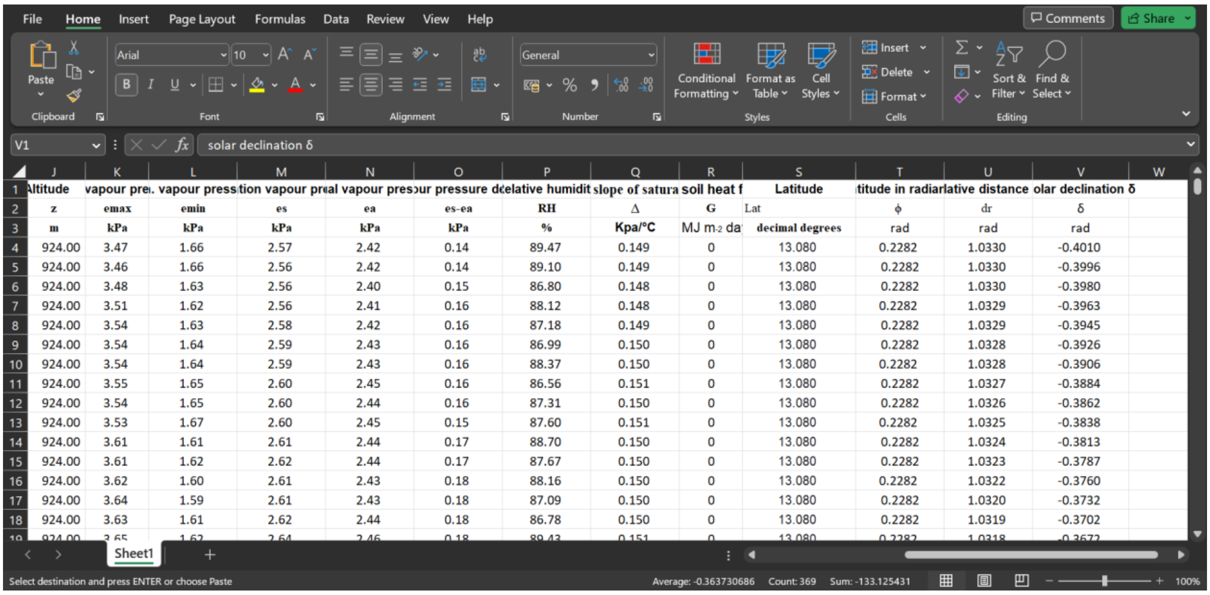

V1 solar declination δ

	Altitude	vapour pre	vapour press	tion vapour pre	al vapour pres	ur pressure de	elative humidit	slope of satura	soil heat f	Latitude	titude in radia	lative distance	olar declination δ
2	z	emax	emin	es	ea	es-ea	RH	Δ	G	Lat	φ	dr	δ
3	m	kPa	kPa	kPa	kPa	kPa	%	Kpa/°C	MJ m-2 da	decimal degrees	rad	rad	rad
4	924.00	3.47	1.66	2.57	2.42	0.14	89.47	0.149	0	13.080	0.2282	1.0330	-0.4010
5	924.00	3.46	1.66	2.56	2.42	0.14	89.10	0.149	0	13.080	0.2282	1.0330	-0.3996
6	924.00	3.48	1.63	2.56	2.40	0.15	86.80	0.148	0	13.080	0.2282	1.0330	-0.3980
7	924.00	3.51	1.62	2.56	2.41	0.16	88.12	0.148	0	13.080	0.2282	1.0329	-0.3963
8	924.00	3.54	1.63	2.58	2.42	0.16	87.18	0.149	0	13.080	0.2282	1.0329	-0.3945
9	924.00	3.54	1.64	2.59	2.43	0.16	86.99	0.150	0	13.080	0.2282	1.0328	-0.3926
10	924.00	3.54	1.64	2.59	2.43	0.16	88.37	0.150	0	13.080	0.2282	1.0328	-0.3906
11	924.00	3.55	1.65	2.60	2.45	0.16	86.56	0.151	0	13.080	0.2282	1.0327	-0.3884
12	924.00	3.54	1.65	2.60	2.44	0.16	87.31	0.150	0	13.080	0.2282	1.0326	-0.3862
13	924.00	3.53	1.67	2.60	2.45	0.15	87.60	0.151	0	13.080	0.2282	1.0325	-0.3838
14	924.00	3.61	1.61	2.61	2.44	0.17	88.70	0.150	0	13.080	0.2282	1.0324	-0.3813
15	924.00	3.61	1.62	2.62	2.44	0.17	87.67	0.150	0	13.080	0.2282	1.0323	-0.3787
16	924.00	3.62	1.60	2.61	2.43	0.18	88.16	0.150	0	13.080	0.2282	1.0322	-0.3760
17	924.00	3.64	1.59	2.61	2.43	0.18	87.09	0.150	0	13.080	0.2282	1.0320	-0.3732
18	924.00	3.63	1.61	2.62	2.44	0.18	86.78	0.150	0	13.080	0.2282	1.0319	-0.3702

Average: -0.363730686 Count: 369 Sum: -133.125431

Fig .15: Solar declination calculation

Step 13: Sunset hour angle, ωs is calculated using Eq. 25, page 49 of FAO-56

$$\omega_s = \arccos[-\tan(\varphi)\tan(\delta)] \ldots\ldots\ldots\ldots\ldots\ldots \quad (6)$$

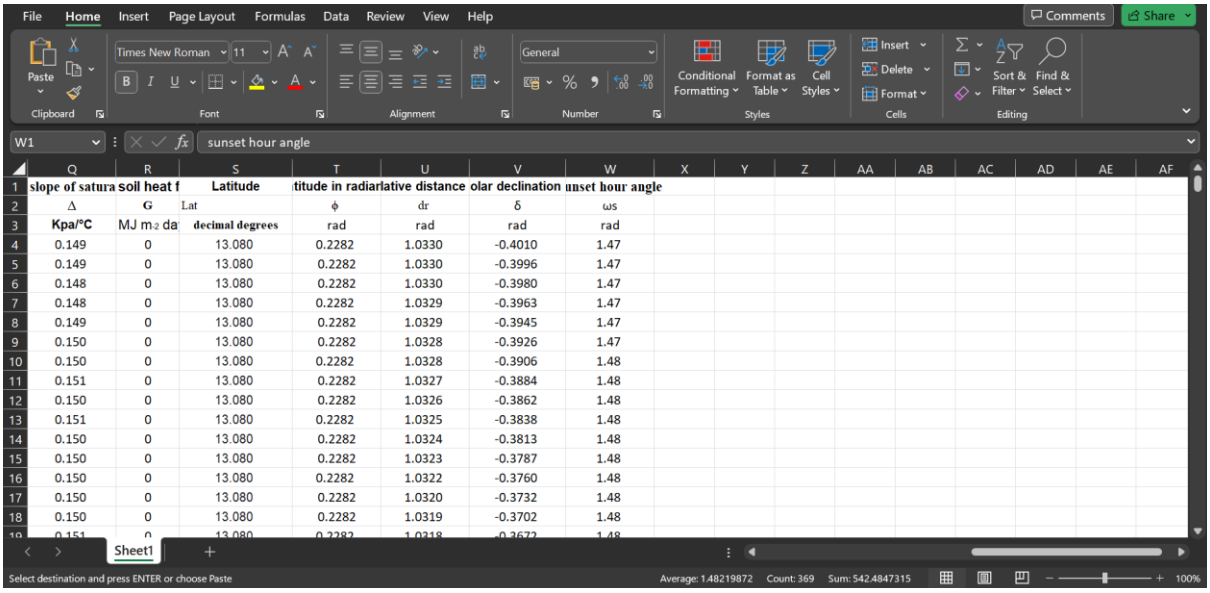

	Q	R	S	T	U	V	W
1	slope of satura	soil heat f	Latitude	titude in radiar	lative distance	olar declination	unset hour angle
2	Δ	G	Lat	ϕ	dr	δ	ωs
3	Kpa/°C	MJ m-2 da	decimal degrees	rad	rad	rad	rad
4	0.149	0	13.080	0.2282	1.0330	-0.4010	1.47
5	0.149	0	13.080	0.2282	1.0330	-0.3996	1.47
6	0.148	0	13.080	0.2282	1.0330	-0.3980	1.47
7	0.148	0	13.080	0.2282	1.0329	-0.3963	1.47
8	0.149	0	13.080	0.2282	1.0329	-0.3945	1.47
9	0.150	0	13.080	0.2282	1.0328	-0.3926	1.47
10	0.150	0	13.080	0.2282	1.0328	-0.3906	1.48
11	0.151	0	13.080	0.2282	1.0327	-0.3884	1.48
12	0.150	0	13.080	0.2282	1.0326	-0.3862	1.48
13	0.151	0	13.080	0.2282	1.0325	-0.3838	1.48
14	0.150	0	13.080	0.2282	1.0324	-0.3813	1.48
15	0.150	0	13.080	0.2282	1.0323	-0.3787	1.48
16	0.150	0	13.080	0.2282	1.0322	-0.3760	1.48
17	0.150	0	13.080	0.2282	1.0320	-0.3732	1.48
18	0.150	0	13.080	0.2282	1.0319	-0.3702	1.48

Fig .16: Sunset hour angle calculation.

Step 14: Solar constant Gsc is assumed to be 0.082

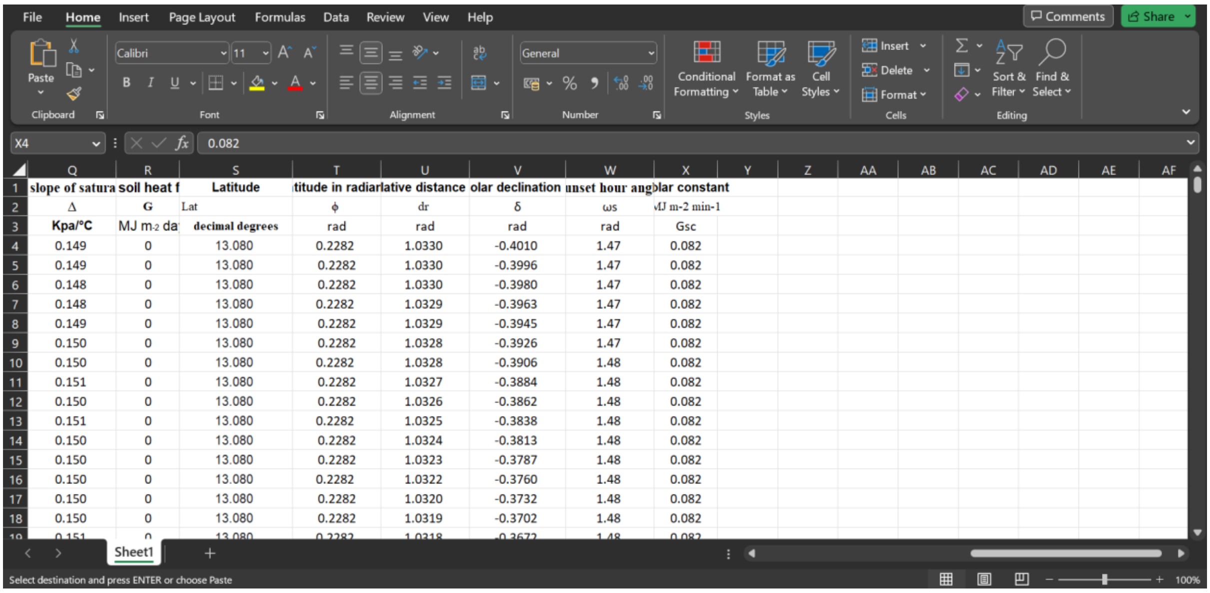

	Q	R	S	T	U	V	W	X
1	slope of satura	soil heat f	Latitude	titude in radiar	lative distance	olar declination	unset hour ang	lar constant
2	Δ	G	Lat	ϕ	dr	δ	ωs	MJ m-2 min-1
3	Kpa/°C	MJ m-2 da	decimal degrees	rad	rad	rad	rad	Gsc
4	0.149	0	13.080	0.2282	1.0330	-0.4010	1.47	0.082
5	0.149	0	13.080	0.2282	1.0330	-0.3996	1.47	0.082
6	0.148	0	13.080	0.2282	1.0330	-0.3980	1.47	0.082
7	0.148	0	13.080	0.2282	1.0329	-0.3963	1.47	0.082
8	0.149	0	13.080	0.2282	1.0329	-0.3945	1.47	0.082
9	0.150	0	13.080	0.2282	1.0328	-0.3926	1.47	0.082
10	0.150	0	13.080	0.2282	1.0328	-0.3906	1.48	0.082
11	0.151	0	13.080	0.2282	1.0327	-0.3884	1.48	0.082
12	0.150	0	13.080	0.2282	1.0326	-0.3862	1.48	0.082
13	0.151	0	13.080	0.2282	1.0325	-0.3838	1.48	0.082
14	0.150	0	13.080	0.2282	1.0324	-0.3813	1.48	0.082
15	0.150	0	13.080	0.2282	1.0323	-0.3787	1.48	0.082
16	0.150	0	13.080	0.2282	1.0322	-0.3760	1.48	0.082
17	0.150	0	13.080	0.2282	1.0320	-0.3732	1.48	0.082
18	0.150	0	13.080	0.2282	1.0319	-0.3702	1.48	0.082

Fig .17: Solar constant.

Step 15: From eq. 21 of page 47, extra-terrestrial radiation, R_a is calculated.

$$R_a = \frac{12\,(60)}{\pi} G_{sc}\, d_r \left[(\omega_2 - \omega_1)\sin(\varphi)\sin(\delta) + \cos(\varphi)\cos(\delta)(\sin(\omega_2) - \sin(\omega_1))\right] \quad \ldots\ldots\ldots\ldots (7)$$

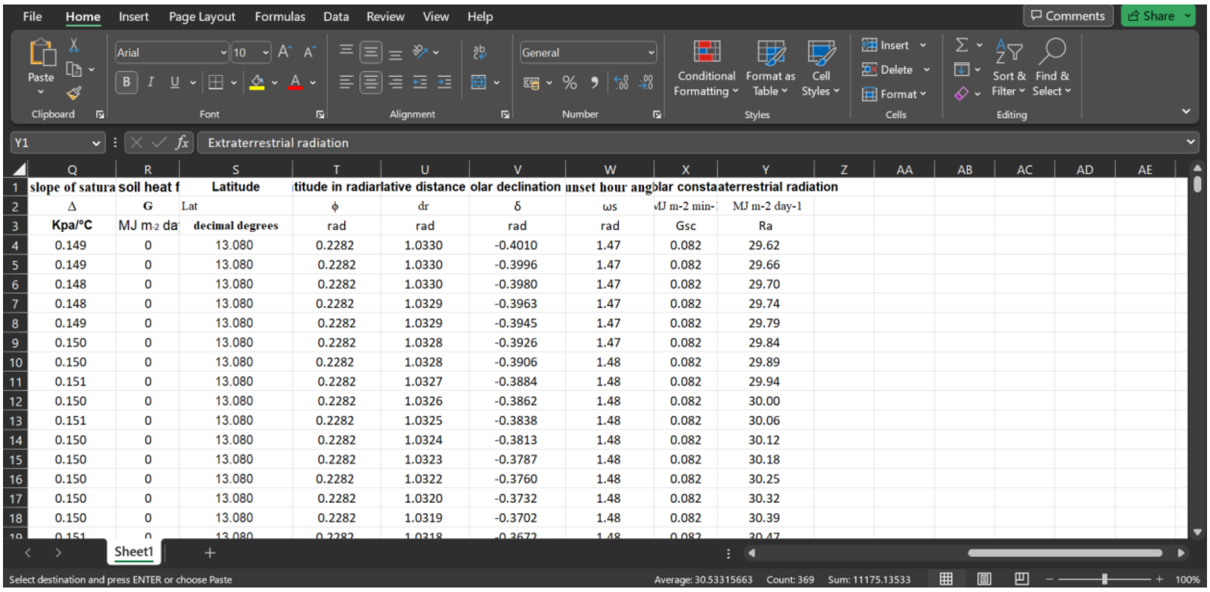

	Q	R	S	T	U	V	W	X	Y
1	slope of satura	soil heat f	Latitude	titude in radia	lative distance	olar declination	unset hour ang	olar consta	aterrestrial radiation
2	Δ	G	Lat	ϕ	dr	δ	ωs	MJ m-2 min-1	MJ m-2 day-1
3	Kpa/°C	MJ m-2 da	decimal degrees	rad	rad	rad	rad	Gsc	Ra
4	0.149	0	13.080	0.2282	1.0330	-0.4010	1.47	0.082	29.62
5	0.149	0	13.080	0.2282	1.0330	-0.3996	1.47	0.082	29.66
6	0.148	0	13.080	0.2282	1.0330	-0.3980	1.47	0.082	29.70
7	0.148	0	13.080	0.2282	1.0329	-0.3963	1.47	0.082	29.74
8	0.149	0	13.080	0.2282	1.0329	-0.3945	1.47	0.082	29.79
9	0.150	0	13.080	0.2282	1.0328	-0.3926	1.47	0.082	29.84
10	0.150	0	13.080	0.2282	1.0328	-0.3906	1.48	0.082	29.89
11	0.151	0	13.080	0.2282	1.0327	-0.3884	1.48	0.082	29.94
12	0.150	0	13.080	0.2282	1.0326	-0.3862	1.48	0.082	30.00
13	0.151	0	13.080	0.2282	1.0325	-0.3838	1.48	0.082	30.06
14	0.150	0	13.080	0.2282	1.0324	-0.3813	1.48	0.082	30.12
15	0.150	0	13.080	0.2282	1.0323	-0.3787	1.48	0.082	30.18
16	0.150	0	13.080	0.2282	1.0322	-0.3760	1.48	0.082	30.25
17	0.150	0	13.080	0.2282	1.0320	-0.3732	1.48	0.082	30.32
18	0.150	0	13.080	0.2282	1.0319	-0.3702	1.48	0.082	30.39

Fig .18. Extra-terrestrial radiation, R_a is calculated

Step 16: Daylight hours, N is calculated using eq.34, page 48 of FAO-56

$$N = \frac{24}{\pi}\,\omega_s \qquad \dots\dots\dots\dots\dots\dots \ (8)$$

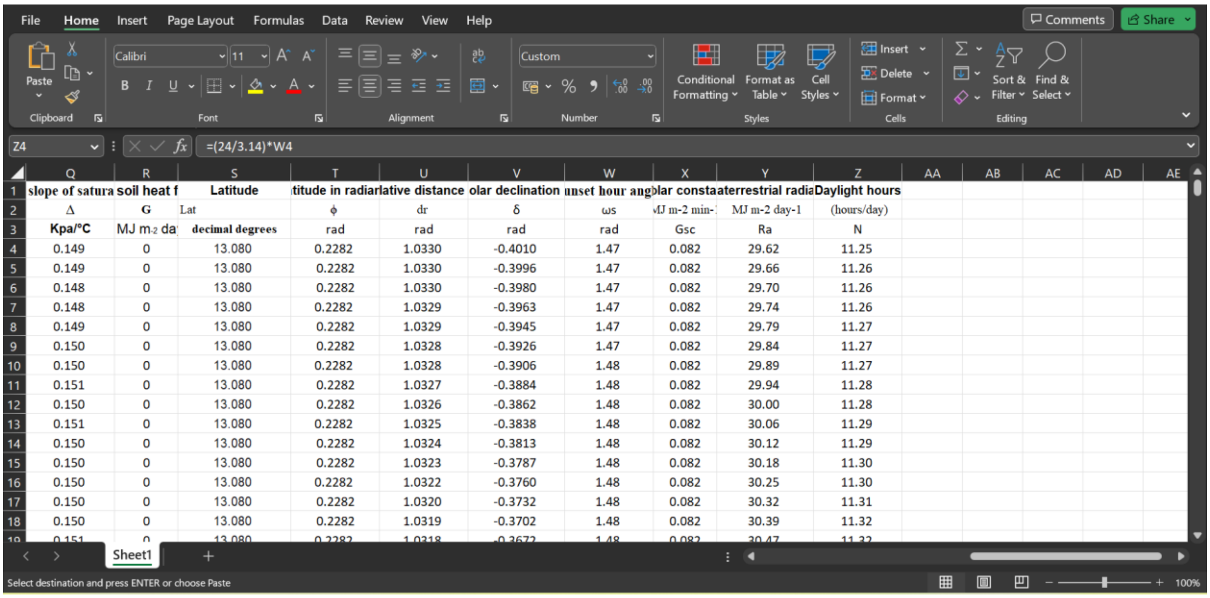

	Q	R	S	T	U	V	W	X	Y	Z
1	slope of satura	soil heat f	Latitude	titude in radia	lative distance	olar declination	unset hour ang	olar consta	aterrestrial radia	Daylight hours
2	Δ	G	Lat	ϕ	dr	δ	ωs	MJ m-2 min-1	MJ m-2 day-1	(hours/day)
3	Kpa/°C	MJ m-2 da	decimal degrees	rad	rad	rad	rad	Gsc	Ra	N
4	0.149	0	13.080	0.2282	1.0330	-0.4010	1.47	0.082	29.62	11.25
5	0.149	0	13.080	0.2282	1.0330	-0.3996	1.47	0.082	29.66	11.26
6	0.148	0	13.080	0.2282	1.0330	-0.3980	1.47	0.082	29.70	11.26
7	0.148	0	13.080	0.2282	1.0329	-0.3963	1.47	0.082	29.74	11.26
8	0.149	0	13.080	0.2282	1.0329	-0.3945	1.47	0.082	29.79	11.27
9	0.150	0	13.080	0.2282	1.0328	-0.3926	1.47	0.082	29.84	11.27
10	0.150	0	13.080	0.2282	1.0328	-0.3906	1.48	0.082	29.89	11.27
11	0.151	0	13.080	0.2282	1.0327	-0.3884	1.48	0.082	29.94	11.28
12	0.150	0	13.080	0.2282	1.0326	-0.3862	1.48	0.082	30.00	11.28
13	0.151	0	13.080	0.2282	1.0325	-0.3838	1.48	0.082	30.06	11.29
14	0.150	0	13.080	0.2282	1.0324	-0.3813	1.48	0.082	30.12	11.29
15	0.150	0	13.080	0.2282	1.0323	-0.3787	1.48	0.082	30.18	11.30
16	0.150	0	13.080	0.2282	1.0322	-0.3760	1.48	0.082	30.25	11.30
17	0.150	0	13.080	0.2282	1.0320	-0.3732	1.48	0.082	30.32	11.31
18	0.150	0	13.080	0.2282	1.0319	-0.3702	1.48	0.082	30.39	11.32

Fig .19: Daylight hours

Step 17: Solar radiation, R_s is calculated using eq. 35, page 50 of FAO-56

$$R_s = \left(a_s + b_s \frac{n}{N}\right) R_a \qquad \dots\dots\dots\dots\dots\dots\dots\dots \ (9)$$

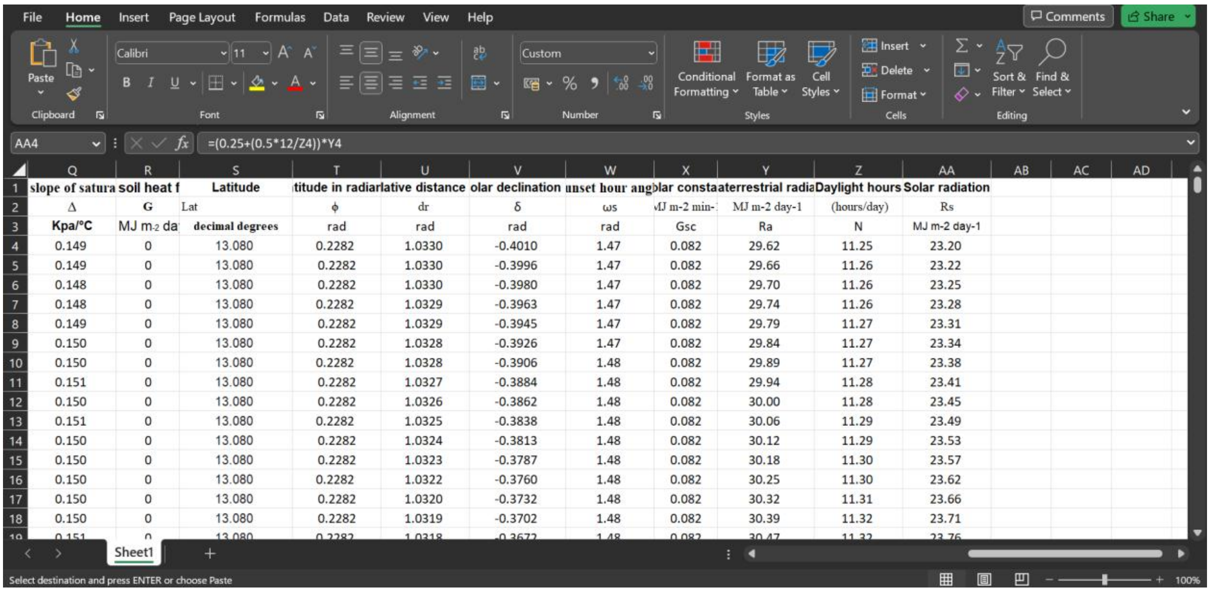

Q	R	S	T	U	V	W	X	Y	Z	AA
slope of satura	soil heat f	Latitude	titude in radiar	lative distance	olar declination	unset hour ang	olar consta	aterrestrial radia	Daylight hours	Solar radiation
Δ	G	Lat	φ	dr	δ	ωs	MJ m-2 min-	MJ m-2 day-1	(hours/day)	Rs
Kpa/°C	MJ m-2 da	decimal degrees	rad	rad	rad	rad	Gsc	Ra	N	MJ m-2 day-1
0.149	0	13.080	0.2282	1.0330	-0.4010	1.47	0.082	29.62	11.25	23.20
0.149	0	13.080	0.2282	1.0330	-0.3996	1.47	0.082	29.66	11.26	23.22
0.148	0	13.080	0.2282	1.0330	-0.3980	1.47	0.082	29.70	11.26	23.25
0.148	0	13.080	0.2282	1.0329	-0.3963	1.47	0.082	29.74	11.26	23.28
0.149	0	13.080	0.2282	1.0329	-0.3945	1.47	0.082	29.79	11.27	23.31
0.150	0	13.080	0.2282	1.0328	-0.3926	1.47	0.082	29.84	11.27	23.34
0.150	0	13.080	0.2282	1.0328	-0.3906	1.48	0.082	29.89	11.27	23.38
0.151	0	13.080	0.2282	1.0327	-0.3884	1.48	0.082	29.94	11.28	23.41
0.150	0	13.080	0.2282	1.0326	-0.3862	1.48	0.082	30.00	11.28	23.45
0.151	0	13.080	0.2282	1.0325	-0.3838	1.48	0.082	30.06	11.29	23.49
0.150	0	13.080	0.2282	1.0324	-0.3813	1.48	0.082	30.12	11.29	23.53
0.150	0	13.080	0.2282	1.0323	-0.3787	1.48	0.082	30.18	11.30	23.57
0.150	0	13.080	0.2282	1.0322	-0.3760	1.48	0.082	30.25	11.30	23.62
0.150	0	13.080	0.2282	1.0320	-0.3732	1.48	0.082	30.32	11.31	23.66
0.150	0	13.080	0.2282	1.0319	-0.3702	1.48	0.082	30.39	11.32	23.71

Fig. 20: Solar radiation.

Step 18: Clear sky solar radiation, R_{so} is calculated using eq. 36, page 51 of FAO-56 and Net solar radiation, R_{ns}=0.77*R_s

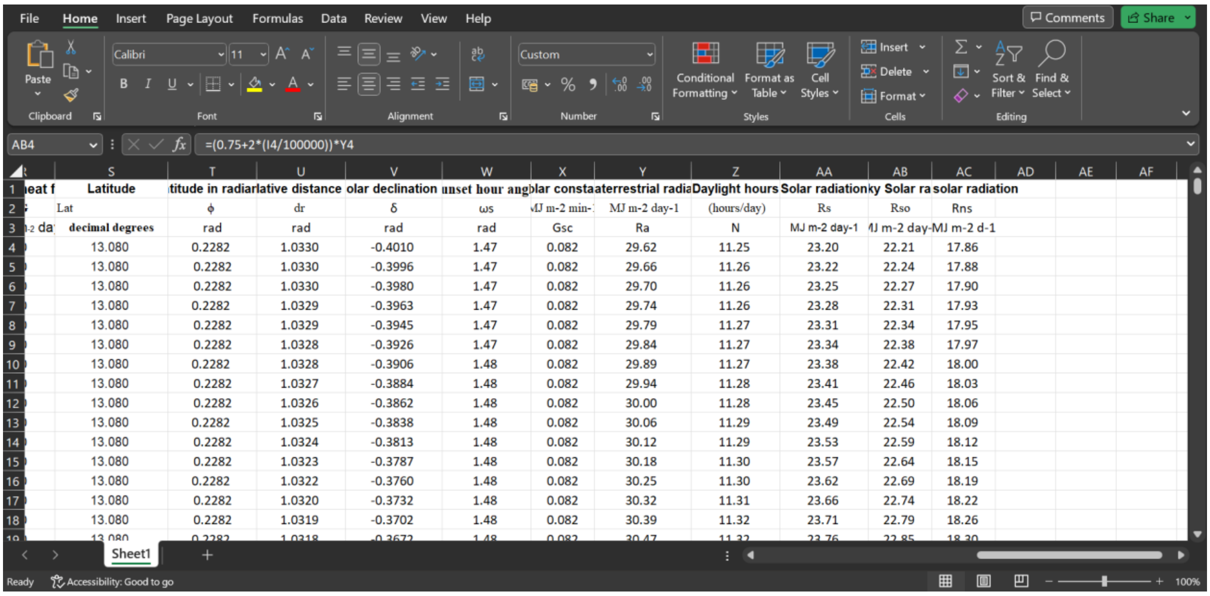

S	T	U	V	W	X	Y	Z	AA	AB	AC
Latitude	titude in radiar	lative distance	olar declination	unset hour ang	olar consta	aterrestrial radia	Daylight hours	Solar radiation	ky Solar ra	solar radiation
Lat	φ	dr	δ	ωs	MJ m-2 min-	MJ m-2 day-1	(hours/day)	Rs	Rso	Rns
decimal degrees	rad	rad	rad	rad	Gsc	Ra	N	MJ m-2 day-1	MJ m-2 day-	MJ m-2 d-1
13.080	0.2282	1.0330	-0.4010	1.47	0.082	29.62	11.25	23.20	22.21	17.86
13.080	0.2282	1.0330	-0.3996	1.47	0.082	29.66	11.26	23.22	22.24	17.88
13.080	0.2282	1.0330	-0.3980	1.47	0.082	29.70	11.26	23.25	22.27	17.90
13.080	0.2282	1.0329	-0.3963	1.47	0.082	29.74	11.26	23.28	22.31	17.93
13.080	0.2282	1.0329	-0.3945	1.47	0.082	29.79	11.27	23.31	22.34	17.95
13.080	0.2282	1.0328	-0.3926	1.47	0.082	29.84	11.27	23.34	22.38	17.97
13.080	0.2282	1.0328	-0.3906	1.48	0.082	29.89	11.27	23.38	22.42	18.00
13.080	0.2282	1.0327	-0.3884	1.48	0.082	29.94	11.28	23.41	22.46	18.03
13.080	0.2282	1.0326	-0.3862	1.48	0.082	30.00	11.28	23.45	22.50	18.06
13.080	0.2282	1.0325	-0.3838	1.48	0.082	30.06	11.29	23.49	22.54	18.09
13.080	0.2282	1.0324	-0.3813	1.48	0.082	30.12	11.29	23.53	22.59	18.12
13.080	0.2282	1.0323	-0.3787	1.48	0.082	30.18	11.30	23.57	22.64	18.15
13.080	0.2282	1.0322	-0.3760	1.48	0.082	30.25	11.30	23.62	22.69	18.19
13.080	0.2282	1.0320	-0.3732	1.48	0.082	30.32	11.31	23.66	22.74	18.22
13.080	0.2282	1.0319	-0.3702	1.48	0.082	30.39	11.32	23.71	22.79	18.26

Fig. 21: Solar radiation

Step 19: Stefan-Boltzmann constant, σTK4 is calculated using table 2.8 of FAO-56

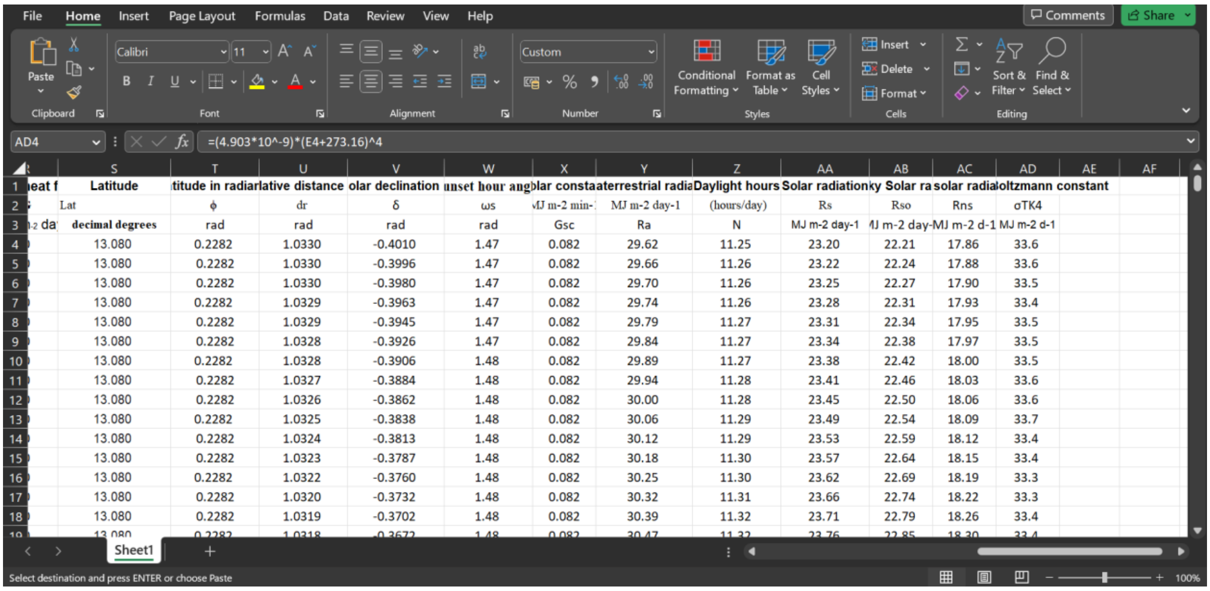

	S	T	U	V	W	X	Y	Z	AA	AB	AC	AD
1	Latitude	titude in radiar	lative distance	olar declination	unset hour ang	lar consta	aterrestrial radia	Daylight hours	Solar radiation	ky Solar ra	solar radia	oltzmann constant
2	Lat	ϕ	dr	δ	ωs	MJ m-2 min-	MJ m-2 day-1	(hours/day)	Rs	Rso	Rns	σTK4
3	decimal degrees	rad	rad	rad	rad	Gsc	Ra	N	MJ m-2 day-1	MJ m-2 day-	MJ m-2 d-1	MJ m-2 d-1
4	13.080	0.2282	1.0330	-0.4010	1.47	0.082	29.62	11.25	23.20	22.21	17.86	33.6
5	13.080	0.2282	1.0330	-0.3996	1.47	0.082	29.66	11.26	23.22	22.24	17.88	33.6
6	13.080	0.2282	1.0330	-0.3980	1.47	0.082	29.70	11.26	23.25	22.27	17.90	33.5
7	13.080	0.2282	1.0329	-0.3963	1.47	0.082	29.74	11.26	23.28	22.31	17.93	33.4
8	13.080	0.2282	1.0329	-0.3945	1.47	0.082	29.79	11.27	23.31	22.34	17.95	33.5
9	13.080	0.2282	1.0328	-0.3926	1.47	0.082	29.84	11.27	23.34	22.38	17.97	33.5
10	13.080	0.2282	1.0328	-0.3906	1.48	0.082	29.89	11.27	23.38	22.42	18.00	33.5
11	13.080	0.2282	1.0327	-0.3884	1.48	0.082	29.94	11.28	23.41	22.46	18.03	33.6
12	13.080	0.2282	1.0326	-0.3862	1.48	0.082	30.00	11.28	23.45	22.50	18.06	33.6
13	13.080	0.2282	1.0325	-0.3838	1.48	0.082	30.06	11.29	23.49	22.54	18.09	33.7
14	13.080	0.2282	1.0324	-0.3813	1.48	0.082	30.12	11.29	23.53	22.59	18.12	33.4
15	13.080	0.2282	1.0323	-0.3787	1.48	0.082	30.18	11.30	23.57	22.64	18.15	33.4
16	13.080	0.2282	1.0322	-0.3760	1.48	0.082	30.25	11.30	23.62	22.69	18.19	33.3
17	13.080	0.2282	1.0320	-0.3732	1.48	0.082	30.32	11.31	23.66	22.74	18.22	33.3
18	13.080	0.2282	1.0319	-0.3702	1.48	0.082	30.39	11.32	23.71	22.79	18.26	33.4

Fig .22: Stefan-Boltzmann constant

Step 20: Using eq.39 from page 52, net outgoing longwave radiation R_{nl} is calculated.

Net radiation Rn is calculated by taking the difference of R_{ns} and R_{nl}.

$$R_{nl} = \sigma\left[\frac{T_{max,K}^{\;4} + T_{min,K}^{\;4}}{2}\right]\left(0.34 - 0.14\sqrt{e_a}\right)\left(1.35\frac{R_s}{R_{so}} - 0.35\right) \qquad \text{………… (10)}$$

$$R_n = R_{ns} - R_{nl} \qquad \text{…………………… (11)}$$

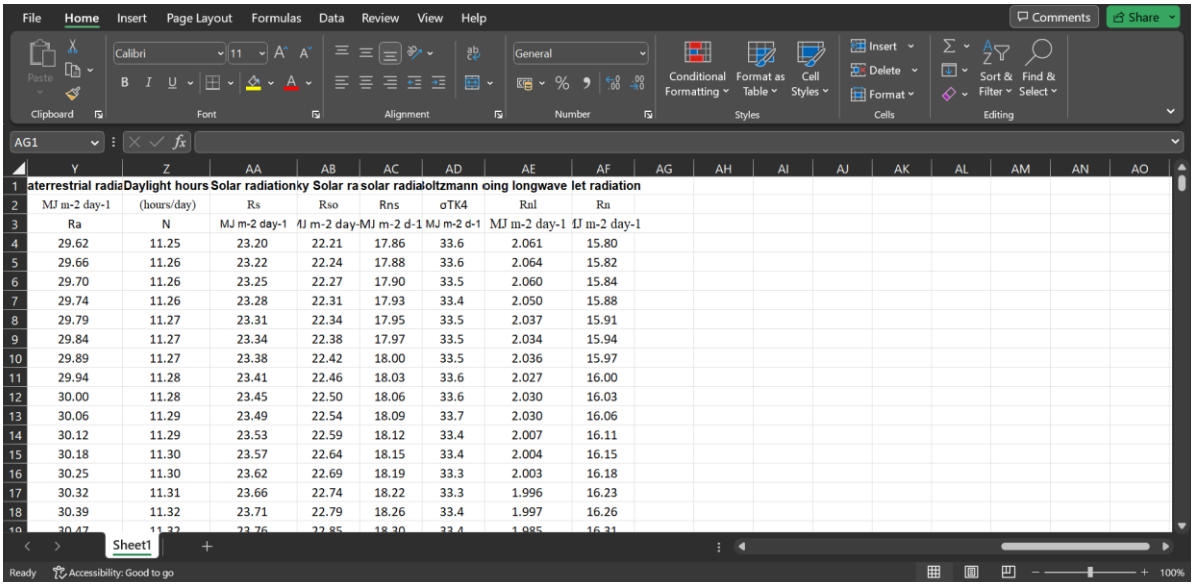

	Y	Z	AA	AB	AC	AD	AE	AF
1	aterrestrial radia	Daylight hours	Solar radiation	ky Solar ra	solar radia	oltzmann	oing longwave	let radiation
2	MJ m-2 day-1	(hours/day)	Rs	Rso	Rns	σTK4	Rnl	Rn
3	Ra	N	MJ m-2 day-1	MJ m-2 day-	MJ m-2 d-1	MJ m-2 d-1	MJ m-2 day-1	MJ m-2 day-1
4	29.62	11.25	23.20	22.21	17.86	33.6	2.061	15.80
5	29.66	11.26	23.22	22.24	17.88	33.6	2.064	15.82
6	29.70	11.26	23.25	22.27	17.90	33.5	2.060	15.84
7	29.74	11.26	23.28	22.31	17.93	33.4	2.050	15.88
8	29.79	11.27	23.31	22.34	17.95	33.5	2.037	15.91
9	29.84	11.27	23.34	22.38	17.97	33.5	2.034	15.94
10	29.89	11.27	23.38	22.42	18.00	33.5	2.036	15.97
11	29.94	11.28	23.41	22.46	18.03	33.6	2.027	16.00
12	30.00	11.28	23.45	22.50	18.06	33.6	2.030	16.03
13	30.06	11.29	23.49	22.54	18.09	33.7	2.030	16.06
14	30.12	11.29	23.53	22.59	18.12	33.4	2.007	16.11
15	30.18	11.30	23.57	22.64	18.15	33.4	2.004	16.15
16	30.25	11.30	23.62	22.69	18.19	33.3	2.003	16.18
17	30.32	11.31	23.66	22.74	18.22	33.3	1.996	16.23
18	30.39	11.32	23.71	22.79	18.26	33.4	1.997	16.26

Fig. 23: Difference of R_{ns} and R_{nl}

Step 21: Reference evaporation is given by Penman-Monteith equation and is compared with the observed Pan evaporation.

$$ET_o = \frac{0.408\,\Delta(R_n - G) + \gamma \frac{900}{T+273} u_2 (e_s - e_a)}{\Delta + \gamma(1 + 0.34\,u_2)} \quad \text{……………….(12)}$$

	Y	Z	AA	AB	AC	AD	AE	AF	AG	AH
1	aterrestrial radia	Daylight hours	Solar radiation	ky Solar ra	solar radia	oltzmann	oing longwave	let radiatio	e evapotran	Pan evaporation
2	MJ m-2 day-1	(hours/day)	Rs	Rso	Rns	σTK4	Rnl	Rn	rence Evapora	Pan Evaporation
3	Ra	N	MJ m-2 day-1	IJ m-2 day-	MJ m-2 d-1	MJ m-2 d-1	MJ m-2 day-1	IJ m-2 day-	mm	mm
4	29.62	11.25	23.20	22.21	17.86	33.6	2.061	15.80	6.496	4.2775
5	29.66	11.26	23.22	22.24	17.88	33.6	2.064	15.82	6.499	4.38
6	29.70	11.26	23.25	22.27	17.90	33.5	2.060	15.84	6.512	4.4275
7	29.74	11.26	23.28	22.31	17.93	33.4	2.050	15.88	6.524	4.4675
8	29.79	11.27	23.31	22.34	17.95	33.5	2.037	15.91	6.546	4.4425
9	29.84	11.27	23.34	22.38	17.97	33.5	2.034	15.94	6.556	4.605
10	29.89	11.27	23.38	22.42	18.00	33.5	2.036	15.97	6.566	4.3975
11	29.94	11.28	23.41	22.46	18.03	33.6	2.027	16.00	6.581	4.58
12	30.00	11.28	23.45	22.50	18.06	33.6	2.030	16.03	6.591	4.6375
13	30.06	11.29	23.49	22.54	18.09	33.7	2.030	16.06	6.606	4.5775
14	30.12	11.29	23.53	22.59	18.12	33.4	2.007	16.11	6.622	4.78
15	30.18	11.30	23.57	22.64	18.15	33.4	2.004	16.15	6.640	4.695
16	30.25	11.30	23.62	22.69	18.19	33.3	2.003	16.18	6.647	4.6875
17	30.32	11.31	23.66	22.74	18.22	33.3	1.996	16.23	6.669	4.6525
18	30.39	11.32	23.71	22.79	18.26	33.4	1.997	16.26	6.686	4.61
19	30.47	11.32	23.76	22.85	18.30	33.4	1.985	16.31	6.706	4.615

Fig. 24: Penman-Monteith equation

Step 22: The difference between Reference evaporation and Actual evaporation is calculated as Error (E) and RMSE (root mean square error) is calculated as:

$$\text{RMSE} = \text{sqrt}(E^2/n) \text{ ………………...(13)}$$

Where n= number of readings

The average of all RMSE errors is found out to be 0.121

AJ369 =SQRT(AI369^2/COUNT($AJ$4:$AJ$369))

	Y	Z	AA	AB	AC	AD	AE	AF	AG	AH	AI	AJ
1	aterrestrial radia	Daylight hours	Solar radiation	ky Solar ra	solar radia	oltzmann	oing longwave	let radiatio	e evapotran	Pan evaporatio	Error	RMSE
359	30.87	11.36	24.02	23.15	18.50	33.6	2.082	16.42	6.748	4.27	-2.478	0.102
360	30.95	11.36	24.08	23.22	18.54	33.4	2.070	16.47	6.771	4.2675	-2.503	0.100
361	31.04	11.37	24.14	23.28	18.59	33.4	2.088	16.50	6.778	4.18	-2.598	0.097
362	31.13	11.38	24.20	23.35	18.63	33.4	2.088	16.54	6.794	4.2575	-2.536	0.100
363	31.22	11.39	24.26	23.42	18.68	33.7	2.040	16.64	6.832	4.405	-2.427	0.104
364	31.32	11.40	24.32	23.49	18.72	33.4	2.055	16.67	6.844	4.365	-2.479	0.103
365	31.41	11.40	24.38	23.56	18.77	33.4	2.044	16.73	6.872	4.4325	-2.439	0.107
366	31.51	11.41	24.44	23.63	18.82	33.6	2.029	16.79	6.897	4.4125	-2.485	0.104
367	31.61	11.42	24.51	23.71	18.87	33.7	2.054	16.82	6.909	4.4625	-2.446	0.110
368	31.70	11.43	24.57	23.78	18.92	33.6	2.052	16.87	6.930	4.335	-2.595	0.103
369	31.80	11.44	24.63	23.85	18.97	33.8	2.036	16.93	6.953	4.405	-2.548	0.105
370									6.8550567	5.309787358		0.121

Fig. 25: The difference between Reference evaporation and Actual evaporation is calculation

5.2 To calculate ET using Stefan's-Steward by MS office Excel.

Step 1: Daily Solar radiation R_s and Mean temperature Tmean is copied from the calculated ET^0 from the former method.

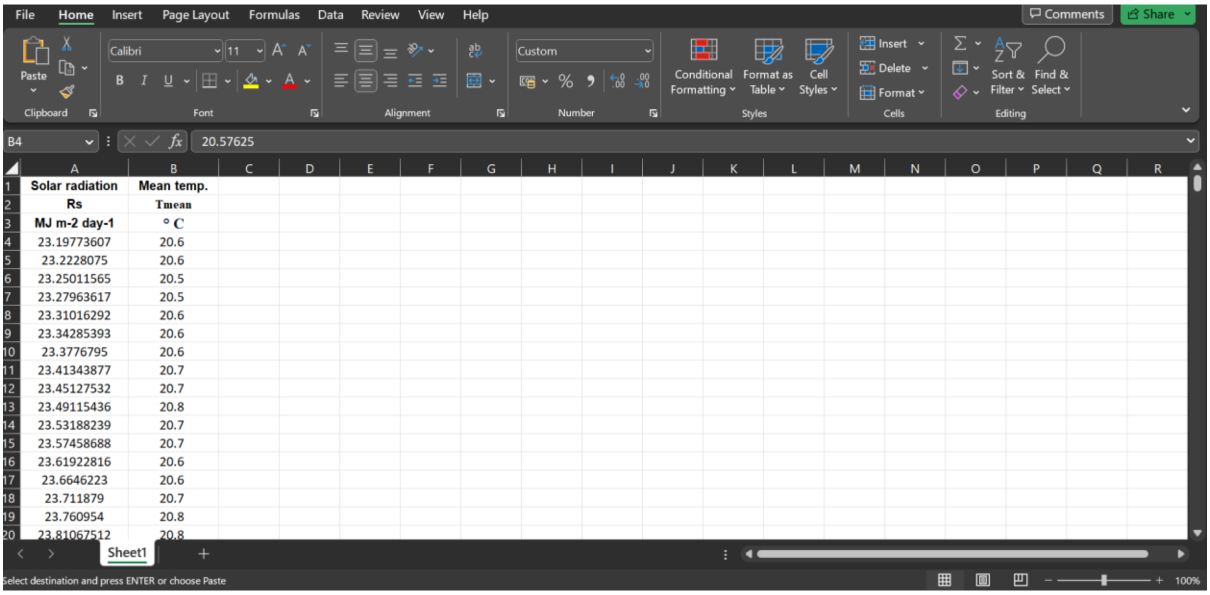

Solar radiation	Mean temp.
Rs	Tmean
MJ m-2 day-1	° C
23.19773607	20.6
23.2228075	20.6
23.25011565	20.5
23.27963617	20.5
23.31016292	20.6
23.34285393	20.6
23.3776795	20.6
23.41343877	20.7
23.45127532	20.7
23.49115436	20.8
23.53188239	20.7
23.57458688	20.7
23.61922816	20.6
23.6646223	20.6
23.711879	20.7
23.760954	20.8
23.81067512	20.8

Fig .26: Daily Solar radiation R_s and Mean temperature Tmean

Step 2: R_s and Tmean are multiplied in the next column

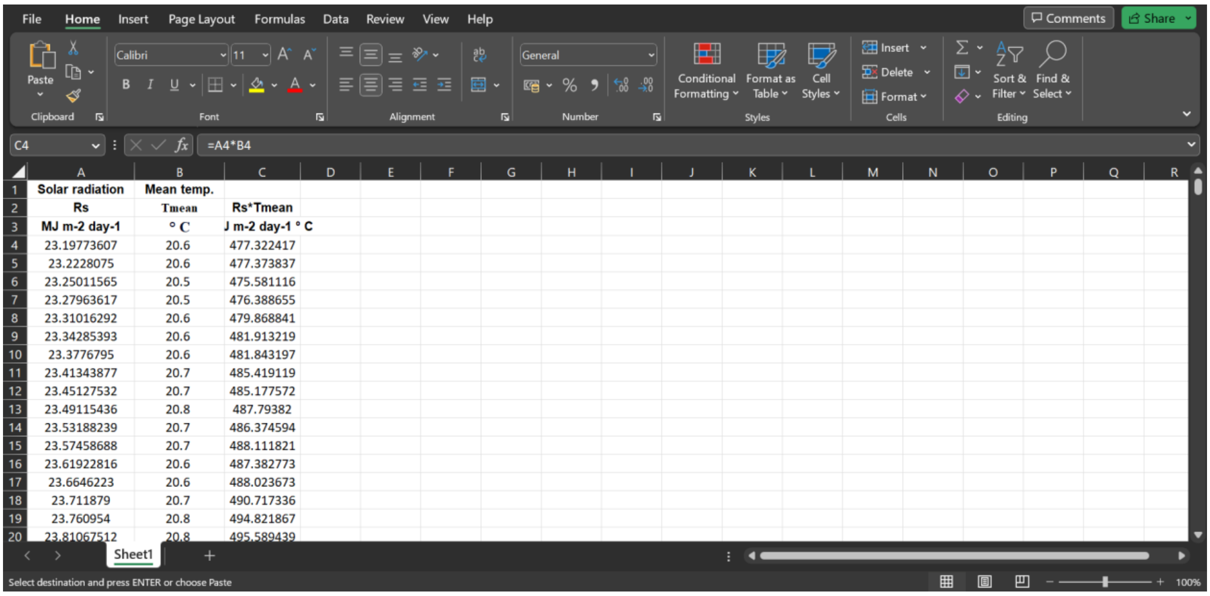

Solar radiation	Mean temp.	
Rs	Tmean	Rs*Tmean
MJ m-2 day-1	° C	J m-2 day-1 ° C
23.19773607	20.6	477.322417
23.2228075	20.6	477.373837
23.25011565	20.5	475.581116
23.27963617	20.5	476.388655
23.31016292	20.6	479.868841
23.34285393	20.6	481.913219
23.3776795	20.6	481.843197
23.41343877	20.7	485.419119
23.45127532	20.7	485.177572
23.49115436	20.8	487.79382
23.53188239	20.7	486.374594
23.57458688	20.7	488.111821
23.61922816	20.6	487.382773
23.6646223	20.6	488.023673
23.711879	20.7	490.717336
23.760954	20.8	494.821867
23.81067512	20.8	495.589439

Fig. 27: Rs and Tmean are multiplied

Step 3: Regression analysis is carried out to find out the values of the coefficients a and b using R_s and R_s*Tmean respectively.

The values of a and b are kept the same throughout the columns.

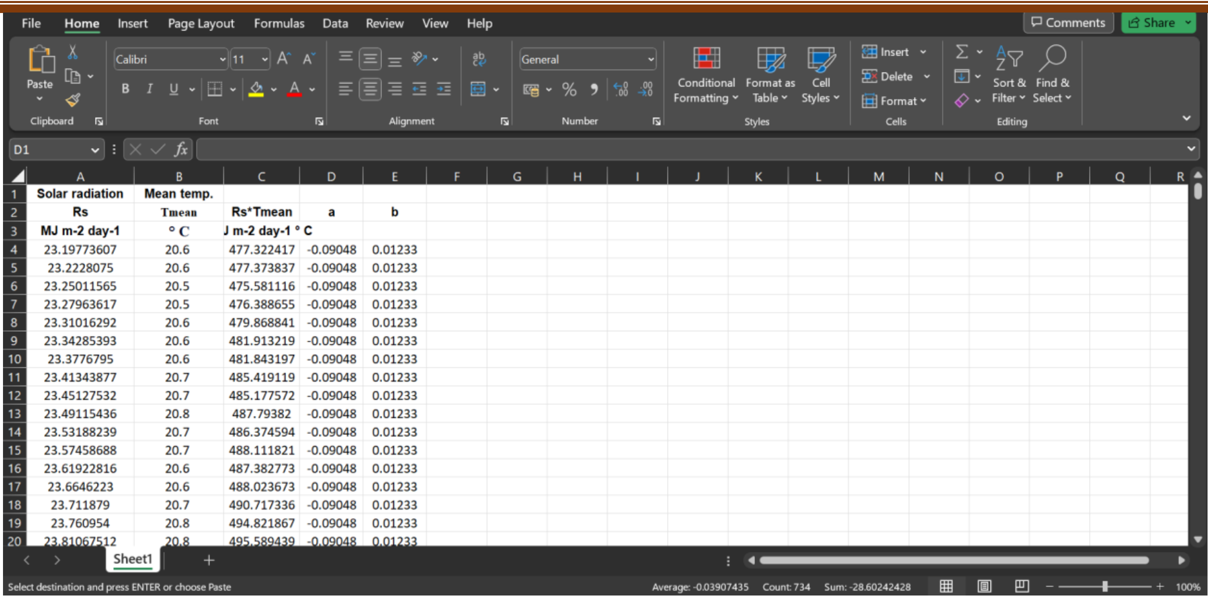

Solar radiation	Mean temp.			
Rs	Tmean	Rs*Tmean	a	b
MJ m-2 day-1	° C	J m-2 day-1 ° C		
23.19773607	20.6	477.322417	-0.09048	0.01233
23.2228075	20.6	477.373837	-0.09048	0.01233
23.25011565	20.5	475.581116	-0.09048	0.01233
23.27963617	20.5	476.388655	-0.09048	0.01233
23.31016292	20.6	479.868841	-0.09048	0.01233
23.34285393	20.6	481.913219	-0.09048	0.01233
23.3776795	20.6	481.843197	-0.09048	0.01233
23.41343877	20.7	485.419119	-0.09048	0.01233
23.45127532	20.7	485.177572	-0.09048	0.01233
23.49115436	20.8	487.79382	-0.09048	0.01233
23.53188239	20.7	486.374594	-0.09048	0.01233
23.57458688	20.7	488.111821	-0.09048	0.01233
23.61922816	20.6	487.382773	-0.09048	0.01233
23.6646223	20.6	488.023673	-0.09048	0.01233
23.711879	20.7	490.717336	-0.09048	0.01233
23.760954	20.8	494.821867	-0.09048	0.01233
23.81067512	20.8	495.589439	-0.09048	0.01233

Fig. 28: coefficients a and b using R_s and R_s*

Step 4: E_P is calculated using the formula and is compared with the observed Pan evaporation.

$$E_P = R_S(a + bT_m) \quad \text{……………….(2)}$$

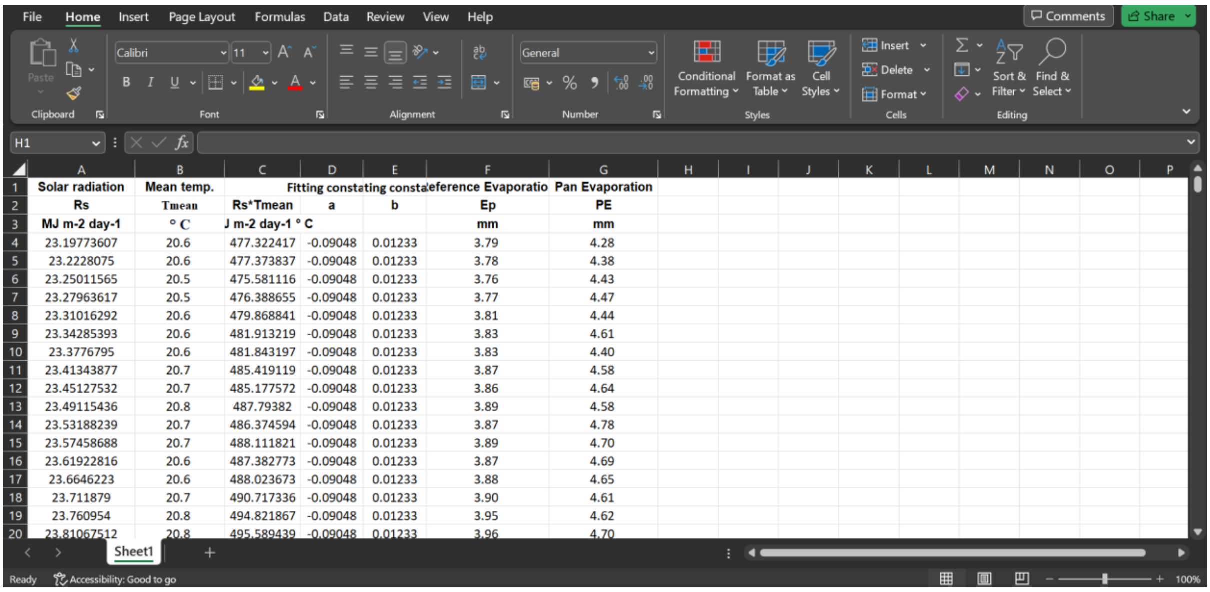

Solar radiation	Mean temp.		Fitting constating consta		eference Evaporatio	Pan Evaporation
Rs	Tmean	Rs*Tmean	a	b	Ep	PE
MJ m-2 day-1	° C	J m-2 day-1 ° C			mm	mm
23.19773607	20.6	477.322417	-0.09048	0.01233	3.79	4.28
23.2228075	20.6	477.373837	-0.09048	0.01233	3.78	4.38
23.25011565	20.5	475.581116	-0.09048	0.01233	3.76	4.43
23.27963617	20.5	476.388655	-0.09048	0.01233	3.77	4.47
23.31016292	20.6	479.868841	-0.09048	0.01233	3.81	4.44
23.34285393	20.6	481.913219	-0.09048	0.01233	3.83	4.61
23.3776795	20.6	481.843197	-0.09048	0.01233	3.83	4.40
23.41343877	20.7	485.419119	-0.09048	0.01233	3.87	4.58
23.45127532	20.7	485.177572	-0.09048	0.01233	3.86	4.64
23.49115436	20.8	487.79382	-0.09048	0.01233	3.89	4.58
23.53188239	20.7	486.374594	-0.09048	0.01233	3.87	4.78
23.57458688	20.7	488.111821	-0.09048	0.01233	3.89	4.70
23.61922816	20.6	487.382773	-0.09048	0.01233	3.87	4.69
23.6646223	20.6	488.023673	-0.09048	0.01233	3.88	4.65
23.711879	20.7	490.717336	-0.09048	0.01233	3.90	4.61
23.760954	20.8	494.821867	-0.09048	0.01233	3.95	4.62
23.81067512	20.8	495.589439	-0.09048	0.01233	3.96	4.70

Fig. 29: Calculation of Ep

Step 5: The difference between Reference evaporation and Actual evaporation is calculated as Error (E) and RMSE (root mean square error) is calculated as:

$$\text{RMSE} = \text{sqrt}(E^2/n) \quad \text{………… (3)}$$

Where n= number of readings.

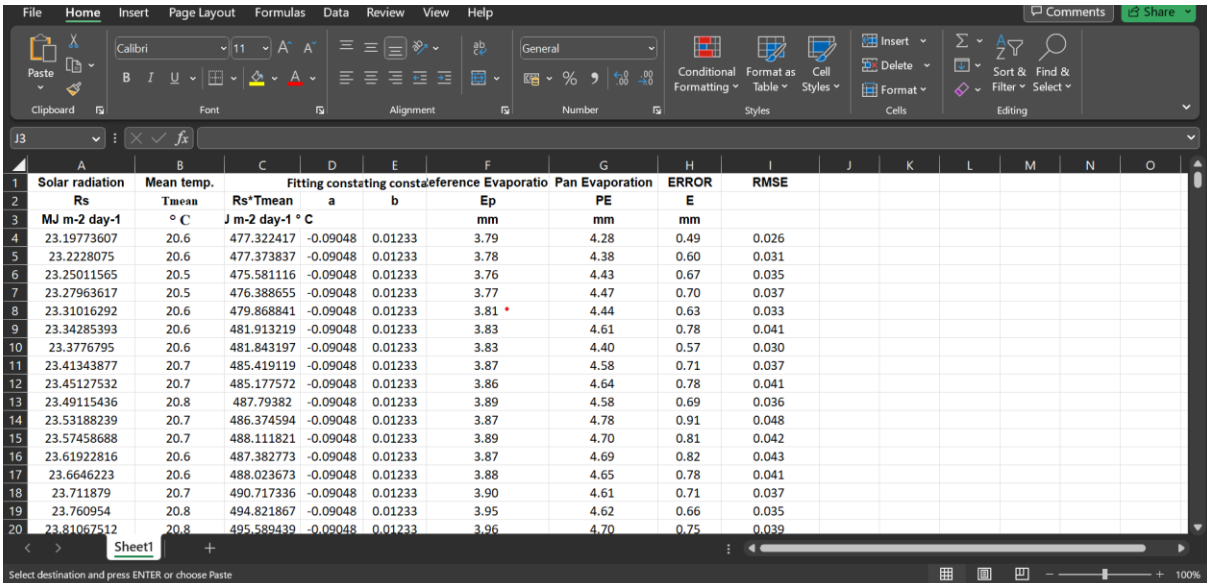

	A	B	C	D	E	F	G	H	I
1	Solar radiation	Mean temp.		Fitting constating consta		eference Evaporatio	Pan Evaporation	ERROR	RMSE
2	Rs	Tmean	Rs*Tmean	a	b	Ep	PE	E	
3	MJ m-2 day-1	° C	J m-2 day-1 ° C			mm	mm	mm	
4	23.19773607	20.6	477.322417	-0.09048	0.01233	3.79	4.28	0.49	0.026
5	23.2228075	20.6	477.373837	-0.09048	0.01233	3.78	4.38	0.60	0.031
6	23.25011565	20.5	475.581116	-0.09048	0.01233	3.76	4.43	0.67	0.035
7	23.27963617	20.5	476.388655	-0.09048	0.01233	3.77	4.47	0.70	0.037
8	23.31016292	20.6	479.868841	-0.09048	0.01233	3.81	4.44	0.63	0.033
9	23.34285393	20.6	481.913219	-0.09048	0.01233	3.83	4.61	0.78	0.041
10	23.3776795	20.6	481.843197	-0.09048	0.01233	3.83	4.40	0.57	0.030
11	23.41343877	20.7	485.419119	-0.09048	0.01233	3.87	4.58	0.71	0.037
12	23.45127532	20.7	485.177572	-0.09048	0.01233	3.86	4.64	0.78	0.041
13	23.49115436	20.8	487.79382	-0.09048	0.01233	3.89	4.58	0.69	0.036
14	23.53188239	20.7	486.374594	-0.09048	0.01233	3.87	4.78	0.91	0.048
15	23.57458688	20.7	488.111821	-0.09048	0.01233	3.89	4.70	0.81	0.042
16	23.61922816	20.6	487.382773	-0.09048	0.01233	3.87	4.69	0.82	0.043
17	23.6646223	20.6	488.023673	-0.09048	0.01233	3.88	4.65	0.78	0.041
18	23.711879	20.7	490.717336	-0.09048	0.01233	3.90	4.61	0.71	0.037
19	23.760954	20.8	494.821867	-0.09048	0.01233	3.95	4.62	0.66	0.035
20	23.81067512	20.8	495.589439	-0.09048	0.01233	3.96	4.70	0.75	0.039

Fig. 30: The difference between Reference evaporation and Actual evaporation

Step 6: The average of all RMSE errors is found out to be 0.035

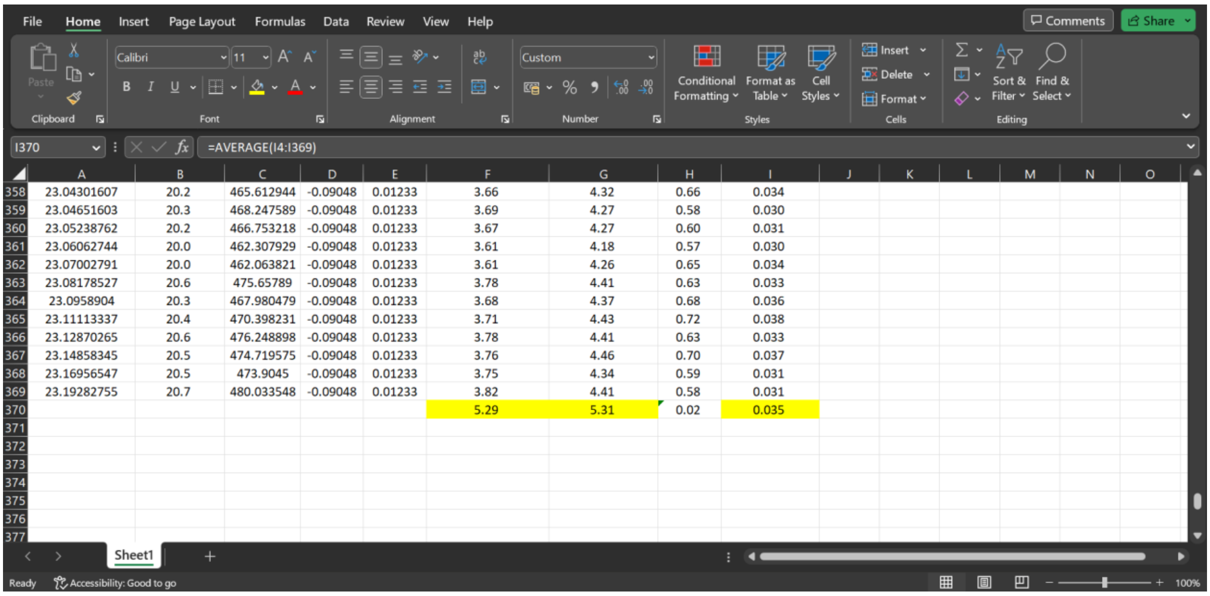

I370 =AVERAGE(I4:I369)

	A	B	C	D	E	F	G	H	I
358	23.04301607	20.2	465.612944	-0.09048	0.01233	3.66	4.32	0.66	0.034
359	23.04651603	20.3	468.247589	-0.09048	0.01233	3.69	4.27	0.58	0.030
360	23.05238762	20.2	466.753218	-0.09048	0.01233	3.67	4.27	0.60	0.031
361	23.06062744	20.0	462.307929	-0.09048	0.01233	3.61	4.18	0.57	0.030
362	23.07002791	20.0	462.063821	-0.09048	0.01233	3.61	4.26	0.65	0.034
363	23.08178527	20.6	475.65789	-0.09048	0.01233	3.78	4.41	0.63	0.033
364	23.0958904	20.3	467.980479	-0.09048	0.01233	3.68	4.37	0.68	0.036
365	23.11113337	20.4	470.398231	-0.09048	0.01233	3.71	4.43	0.72	0.038
366	23.12870265	20.6	476.248898	-0.09048	0.01233	3.78	4.41	0.63	0.033
367	23.14858345	20.5	474.719575	-0.09048	0.01233	3.76	4.46	0.70	0.037
368	23.16956547	20.5	473.9045	-0.09048	0.01233	3.75	4.34	0.59	0.031
369	23.19282755	20.7	480.033548	-0.09048	0.01233	3.82	4.41	0.58	0.031
370						5.29	5.31	0.02	0.035

Fig. 31: The average of all RMSE

5.3 To calculate Trend Analysis using Mann-Kendall by MS office Excel.

- The average of annual data.

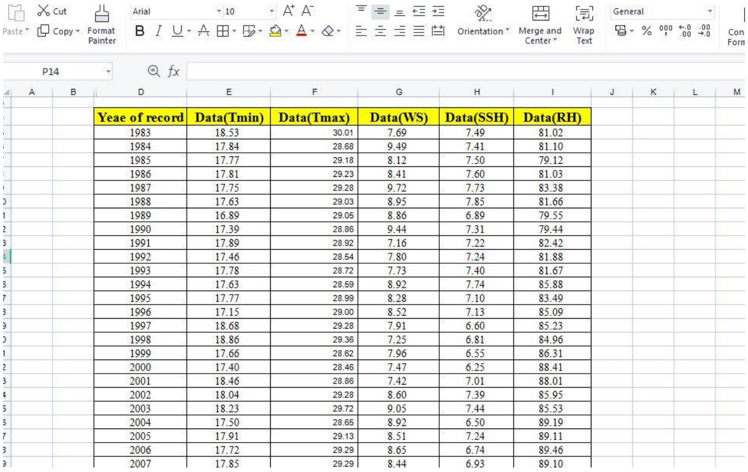

Yeae of record	Data(Tmin)	Data(Tmax)	Data(WS)	Data(SSH)	Data(RH)
1983	18.53	30.01	7.69	7.49	81.02
1984	17.84	28.68	9.49	7.41	81.10
1985	17.77	29.18	8.12	7.50	79.12
1986	17.81	29.23	8.41	7.60	81.03
1987	17.75	29.28	9.72	7.73	83.38
1988	17.63	29.03	8.95	7.85	81.66
1989	16.89	29.05	8.86	6.89	79.55
1990	17.39	28.86	9.44	7.31	79.44
1991	17.89	28.92	7.16	7.22	82.42
1992	17.46	28.54	7.80	7.24	81.88
1993	17.78	28.72	7.73	7.40	81.67
1994	17.63	28.59	8.92	7.74	85.88
1995	17.77	28.99	8.28	7.10	83.49
1996	17.15	29.00	8.52	7.13	85.09
1997	18.68	29.28	7.91	6.60	85.23
1998	18.86	29.36	7.25	6.81	84.96
1999	17.66	28.62	7.96	6.55	86.31
2000	17.40	28.46	7.47	6.25	88.41
2001	18.46	28.86	7.42	7.01	88.01
2002	18.04	29.28	8.60	7.39	85.95
2003	18.23	29.72	9.05	7.44	85.53
2004	17.50	28.65	8.92	6.50	89.19
2005	17.91	29.13	8.51	7.24	89.11
2006	17.72	29.29	8.65	6.74	89.46
2007	17.85	29.29	8.44	6.93	89.10

Fig .32: Average of annual data.

- Calculation of S Statistics.

Convert the ordered series (X, X) to a new one series (Y) with values 1, 0, -1, like this:

If $(Xj - Xk) > 0 \rightarrow 1$

If $(Xj - Xk) = 0 \rightarrow 0$

If $(Xj - Xk) < 0 \rightarrow -1$

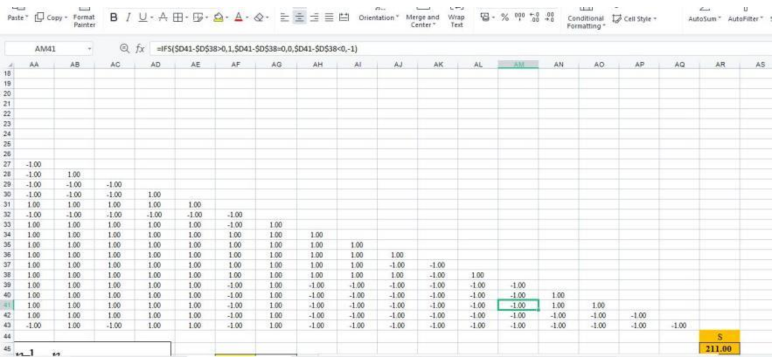

Fig. 33: Statistic, S calculation

- Calculation of (Var)S, Z_s

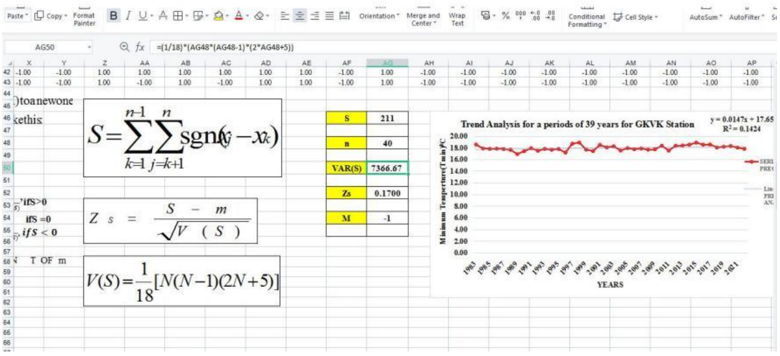

Fig. 34: Calculation of (Var)S

➢ Repeat the same procedure to all six parameters.

5.4 To calculate Trend Analysis using Sen's slope by MS office Excel.

➢ The average of annual data.

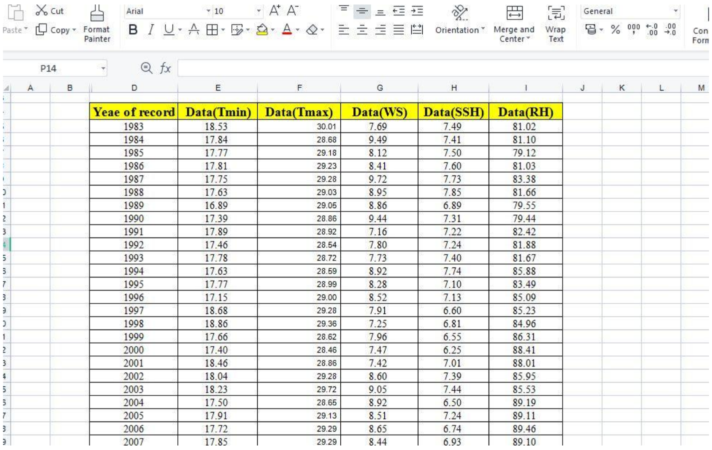

Yeae of record	Data(Tmin)	Data(Tmax)	Data(WS)	Data(SSH)	Data(RH)
1983	18.53	30.01	7.69	7.49	81.02
1984	17.84	28.68	9.49	7.41	81.10
1985	17.77	29.18	8.12	7.50	79.12
1986	17.81	29.23	8.41	7.60	81.03
1987	17.75	29.28	9.72	7.73	83.38
1988	17.63	29.03	8.95	7.85	81.66
1989	16.89	29.05	8.86	6.89	79.55
1990	17.39	28.86	9.44	7.31	79.44
1991	17.89	28.92	7.16	7.22	82.42
1992	17.46	28.54	7.80	7.24	81.88
1993	17.78	28.72	7.73	7.40	81.67
1994	17.63	28.59	8.92	7.74	85.88
1995	17.77	28.99	8.28	7.10	83.49
1996	17.15	29.00	8.52	7.13	85.09
1997	18.68	29.28	7.91	6.60	85.23
1998	18.86	29.36	7.25	6.81	84.96
1999	17.66	28.62	7.96	6.55	86.31
2000	17.40	28.46	7.47	6.25	88.41
2001	18.46	28.86	7.42	7.01	88.01
2002	18.04	29.28	8.60	7.39	85.95
2003	18.23	29.72	9.05	7.44	85.53
2004	17.50	28.65	8.92	6.50	89.19
2005	17.91	29.13	8.51	7.24	89.11
2006	17.72	29.29	8.65	6.74	89.46
2007	17.85	29.29	8.44	6.93	89.10

Fig. 35: Average of annual data.

➢ Calculation of $Q = Median(\frac{x_j - x_k}{j-k})\; j > k$

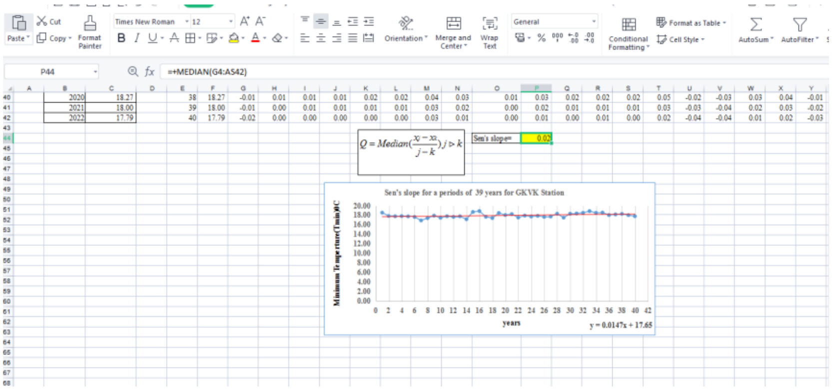

Fig. 36: calculation of slope

➢ Repeat the same procedure to all six parameters.

5.5 To determineTrend Analysis using Mann-Kendall and Sen's slope Method in XLSTAT

➢ Average of Monthly data.

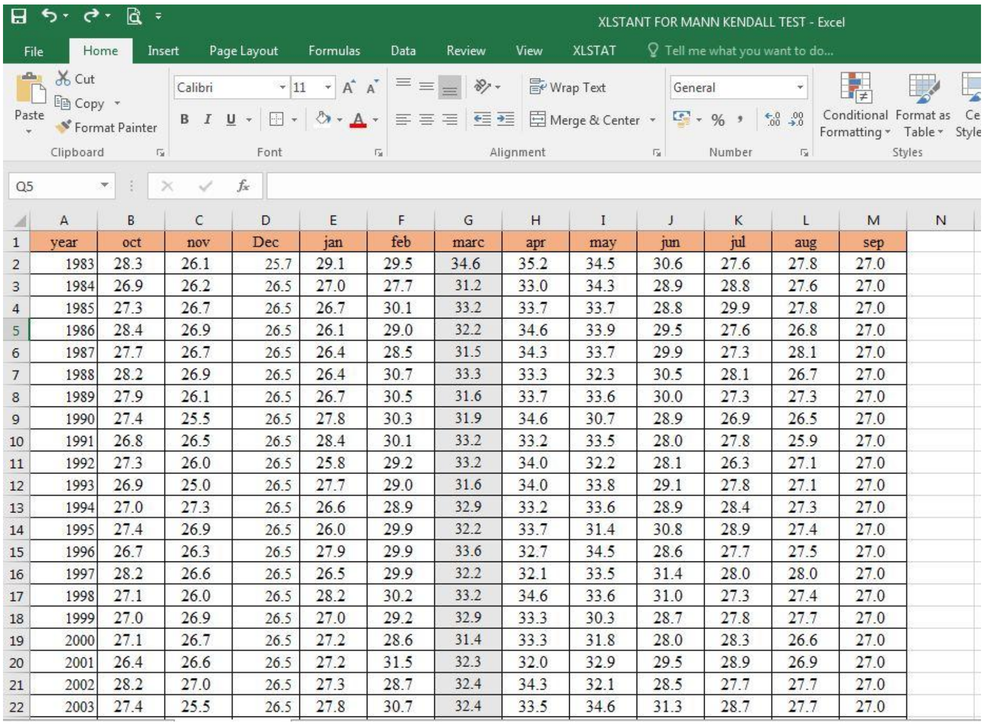

year	oct	nov	Dec	jan	feb	marc	apr	may	jun	jul	aug	sep
1983	28.3	26.1	25.7	29.1	29.5	34.6	35.2	34.5	30.6	27.6	27.8	27.0
1984	26.9	26.2	26.5	27.0	27.7	31.2	33.0	34.3	28.9	28.8	27.6	27.0
1985	27.3	26.7	26.5	26.7	30.1	33.2	33.7	33.7	28.8	29.9	27.8	27.0
1986	28.4	26.9	26.5	26.1	29.0	32.2	34.6	33.9	29.5	27.6	26.8	27.0
1987	27.7	26.7	26.5	26.4	28.5	31.5	34.3	33.7	29.9	27.3	28.1	27.0
1988	28.2	26.9	26.5	26.4	30.7	33.3	33.3	32.3	30.5	28.1	26.7	27.0
1989	27.9	26.1	26.5	26.7	30.5	31.6	33.7	33.6	30.0	27.3	27.3	27.0
1990	27.4	25.5	26.5	27.8	30.3	31.9	34.6	30.7	28.9	26.9	26.5	27.0
1991	26.8	26.5	26.5	28.4	30.1	33.2	33.2	33.5	28.0	27.8	25.9	27.0
1992	27.3	26.0	26.5	25.8	29.2	33.2	34.0	32.2	28.1	26.3	27.1	27.0
1993	26.9	25.0	26.5	27.7	29.0	31.6	34.0	33.8	29.1	27.8	27.1	27.0
1994	27.0	27.3	26.5	26.6	28.9	32.9	33.2	33.6	28.9	28.4	27.3	27.0
1995	27.4	26.9	26.5	26.0	29.9	32.2	33.7	31.4	30.8	28.9	27.4	27.0
1996	26.7	26.3	26.5	27.9	29.9	33.6	32.7	34.5	28.6	27.7	27.5	27.0
1997	28.2	26.6	26.5	26.5	29.9	32.2	32.1	33.5	31.4	28.0	28.0	27.0
1998	27.1	26.0	26.5	28.2	30.2	33.2	34.6	33.6	31.0	27.3	27.4	27.0
1999	27.0	26.9	26.5	27.0	29.2	32.9	33.3	30.3	28.7	27.8	27.7	27.0
2000	27.1	26.7	26.5	27.2	28.6	31.4	33.3	31.8	28.0	28.3	26.6	27.0
2001	26.4	26.6	26.5	27.2	31.5	32.3	32.0	32.9	29.5	28.9	26.9	27.0
2002	28.2	27.0	26.5	27.3	28.7	32.4	34.3	32.1	28.5	27.7	27.7	27.0
2003	27.4	25.5	26.5	27.8	30.7	32.4	33.5	34.6	31.3	28.7	27.7	27.0

Fig. 37: Monthly average

➢ Average of data year wise.

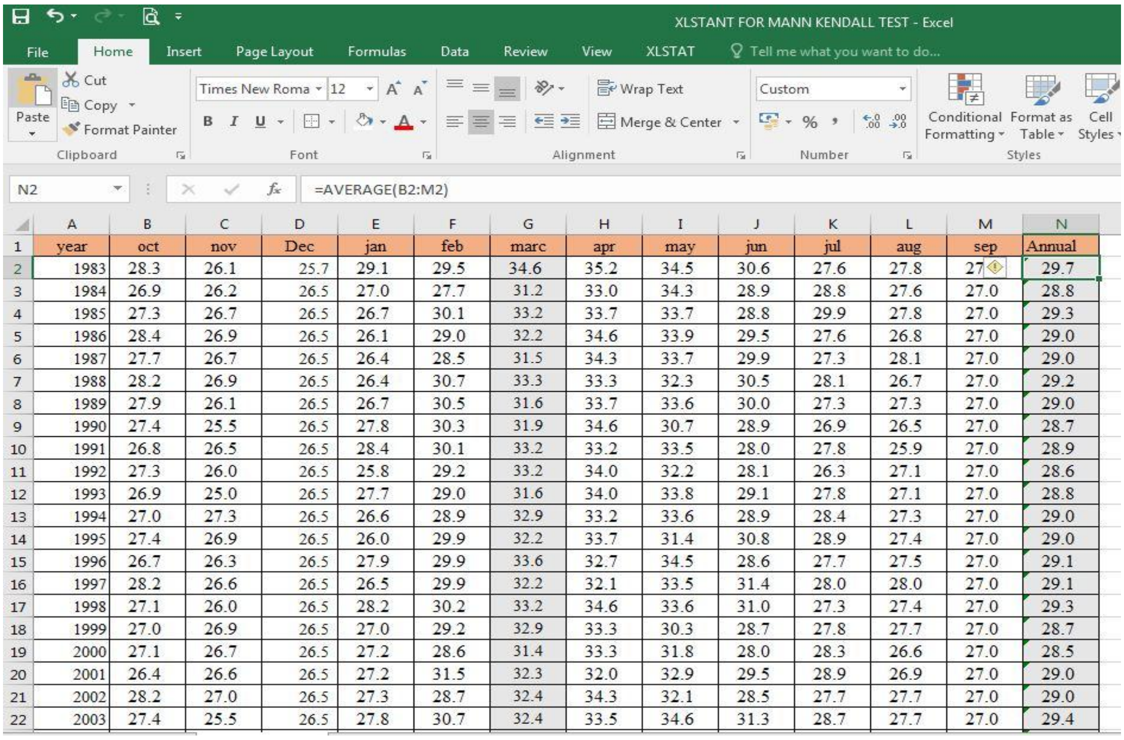

year	oct	nov	Dec	jan	feb	marc	apr	may	jun	jul	aug	sep	Annual
1983	28.3	26.1	25.7	29.1	29.5	34.6	35.2	34.5	30.6	27.6	27.8	27	29.7
1984	26.9	26.2	26.5	27.0	27.7	31.2	33.0	34.3	28.9	28.8	27.6	27.0	28.8
1985	27.3	26.7	26.5	26.7	30.1	33.2	33.7	33.7	28.8	29.9	27.8	27.0	29.3
1986	28.4	26.9	26.5	26.1	29.0	32.2	34.6	33.9	29.5	27.6	26.8	27.0	29.0
1987	27.7	26.7	26.5	26.4	28.5	31.5	34.3	33.7	29.9	27.3	28.1	27.0	29.0
1988	28.2	26.9	26.5	26.4	30.7	33.3	33.3	32.3	30.5	28.1	26.7	27.0	29.2
1989	27.9	26.1	26.5	26.7	30.5	31.6	33.7	33.6	30.0	27.3	27.3	27.0	29.0
1990	27.4	25.5	26.5	27.8	30.3	31.9	34.6	30.7	28.9	26.9	26.5	27.0	28.7
1991	26.8	26.5	26.5	28.4	30.1	33.2	33.2	33.5	28.0	27.8	25.9	27.0	28.9
1992	27.3	26.0	26.5	25.8	29.2	33.2	34.0	32.2	28.1	26.3	27.1	27.0	28.6
1993	26.9	25.0	26.5	27.7	29.0	31.6	34.0	33.8	29.1	27.8	27.1	27.0	28.8
1994	27.0	27.3	26.5	26.6	28.9	32.9	33.2	33.6	28.9	28.4	27.3	27.0	29.0
1995	27.4	26.9	26.5	26.0	29.9	32.2	33.7	31.4	30.8	28.9	27.4	27.0	29.0
1996	26.7	26.3	26.5	27.9	29.9	33.6	32.7	34.5	28.6	27.7	27.5	27.0	29.1
1997	28.2	26.6	26.5	26.5	29.9	32.2	32.1	33.5	31.4	28.0	28.0	27.0	29.1
1998	27.1	26.0	26.5	28.2	30.2	33.2	34.6	33.6	31.0	27.3	27.4	27.0	29.3
1999	27.0	26.9	26.5	27.0	29.2	32.9	33.3	30.3	28.7	27.8	27.7	27.0	28.7
2000	27.1	26.7	26.5	27.2	28.6	31.4	33.3	31.8	28.0	28.3	26.6	27.0	28.5
2001	26.4	26.6	26.5	27.2	31.5	32.3	32.0	32.9	29.5	28.9	26.9	27.0	29.0
2002	28.2	27.0	26.5	27.3	28.7	32.4	34.3	32.1	28.5	27.7	27.7	27.0	29.0
2003	27.4	25.5	26.5	27.8	30.7	32.4	33.5	34.6	31.3	28.7	27.7	27.0	29.4

Fig. 38: Annual data average

➢ Average the data Winter(D,J,f),Summer(M,A,M),Manson(J,J,A,S),Post Mansoon(O,N)

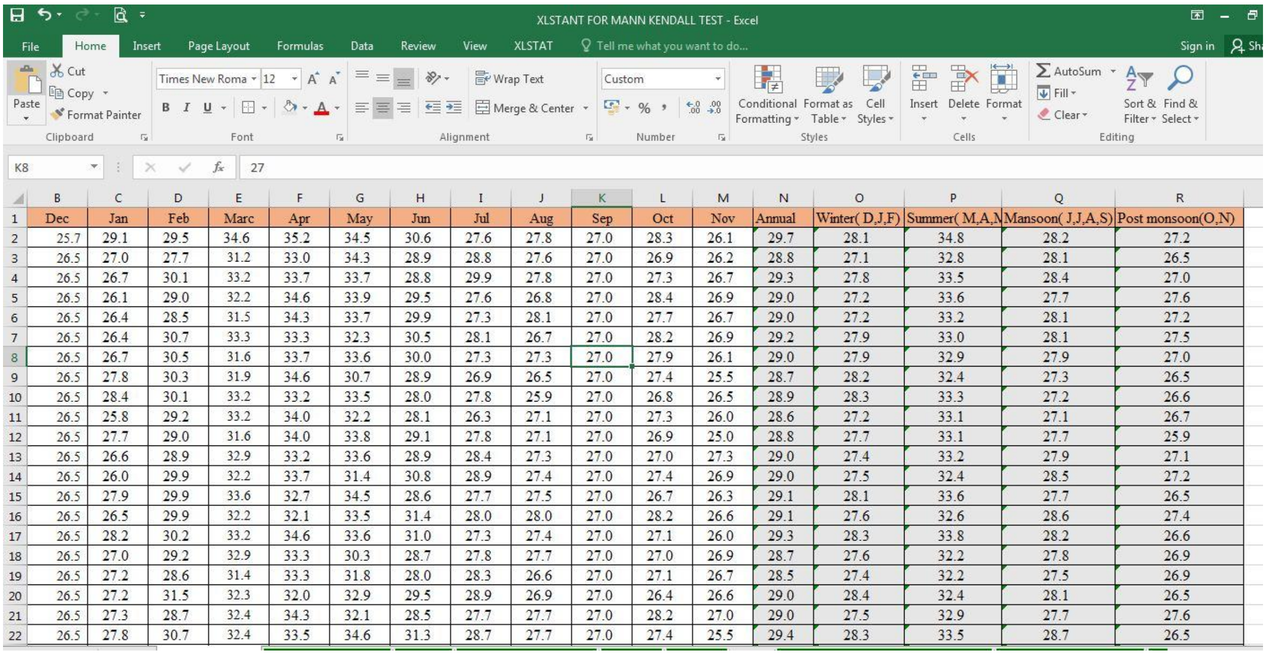

	Dec	Jan	Feb	Marc	Apr	May	Jun	Jul	Aug	Sep	Oct	Nov	Annual	Winter(D,J,F)	Summer(M,A,M	Mansoon(J,J,A,S)	Post monsoon(O,N)
2	25.7	29.1	29.5	34.6	35.2	34.5	30.6	27.6	27.8	27.0	28.3	26.1	29.7	28.1	34.8	28.2	27.2
3	26.5	27.0	27.7	31.2	33.0	34.3	28.9	28.8	27.6	27.0	26.9	26.2	28.8	27.1	32.8	28.1	26.5
4	26.5	26.7	30.1	33.2	33.7	33.7	28.8	29.9	27.8	27.0	27.3	26.7	29.3	27.8	33.5	28.4	27.0
5	26.5	26.1	29.0	32.2	34.6	33.9	29.5	27.6	26.8	27.0	28.4	26.9	29.0	27.2	33.6	27.7	27.6
6	26.5	26.4	28.5	31.5	34.3	33.7	29.9	27.3	28.1	27.0	27.7	26.7	29.0	27.2	33.2	28.1	27.2
7	26.5	26.4	30.7	33.3	33.3	32.3	30.5	28.1	26.7	27.0	28.2	26.9	29.2	27.9	33.0	28.1	27.5
8	26.5	26.7	30.5	31.6	33.7	33.6	30.0	27.3	27.3	27.0	27.9	26.1	29.0	27.9	32.9	27.9	27.0
9	26.5	27.8	30.3	31.9	34.6	30.7	28.9	26.9	26.5	27.0	27.4	25.5	28.7	28.2	32.4	27.3	26.5
10	26.5	28.4	30.1	33.2	33.2	33.5	28.0	27.8	25.9	27.0	26.8	26.5	28.9	28.3	33.3	27.2	26.6
11	26.5	25.8	29.2	33.2	34.0	32.2	28.1	26.3	27.1	27.0	27.3	26.0	28.6	27.2	33.1	27.1	26.7
12	26.5	27.7	29.0	31.6	34.0	33.8	29.1	27.8	27.1	27.0	26.9	25.0	28.8	27.7	33.1	27.7	25.9
13	26.5	26.6	28.9	32.9	33.2	33.6	28.9	28.4	27.3	27.0	27.0	27.3	29.0	27.4	33.2	27.9	27.1
14	26.5	26.0	29.9	32.2	33.7	31.4	30.8	28.9	27.4	27.0	27.4	26.9	29.0	27.5	32.4	28.5	27.2
15	26.5	27.9	29.9	33.6	32.7	34.5	28.6	27.7	27.5	27.0	26.7	26.3	29.1	28.1	33.6	27.7	26.5
16	26.5	26.5	29.9	32.2	32.1	33.5	31.4	28.0	28.0	27.0	28.2	26.6	29.1	27.6	32.6	28.6	27.4
17	26.5	28.2	30.2	33.2	34.6	33.6	31.0	27.3	27.4	27.0	27.1	26.0	29.3	28.3	33.8	28.2	26.6
18	26.5	27.0	29.2	32.9	33.3	30.3	28.7	27.8	27.7	27.0	27.0	26.9	28.7	27.6	32.2	27.8	26.9
19	26.5	27.2	28.6	31.4	33.3	31.8	28.0	28.3	26.6	27.0	27.1	26.7	28.5	27.4	32.2	27.5	26.9
20	26.5	27.2	31.5	32.3	32.0	32.9	29.5	28.9	26.9	27.0	26.4	26.6	29.0	28.4	32.4	28.1	26.5
21	26.5	27.3	28.7	32.4	34.3	32.1	28.5	27.7	27.7	27.0	28.2	27.0	29.0	27.5	32.9	27.7	27.6
22	26.5	27.8	30.7	32.4	33.5	34.6	31.3	28.7	27.7	27.0	27.4	25.5	29.4	28.3	33.5	28.7	26.5

Fig. 39: Average data Winter(D,J,f), Summer(M,A,M) ,Mansoon(J,J,A,S), Post Mansoon(O,N)

➢ Analyzing data and performing statistical test as mann-kendall.

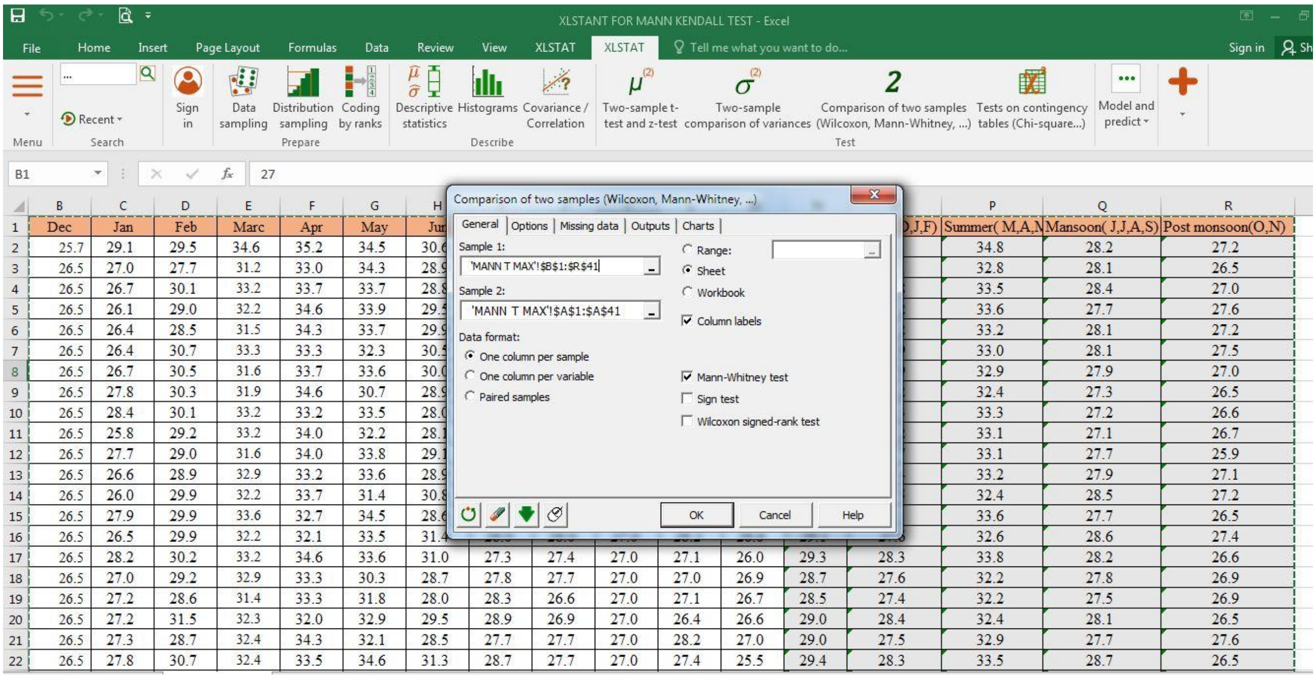

Fig. 40: Analyzing data

➢ We can obtain the final findings along a graph by choosing the data from a specific sheet and comparing the samples.

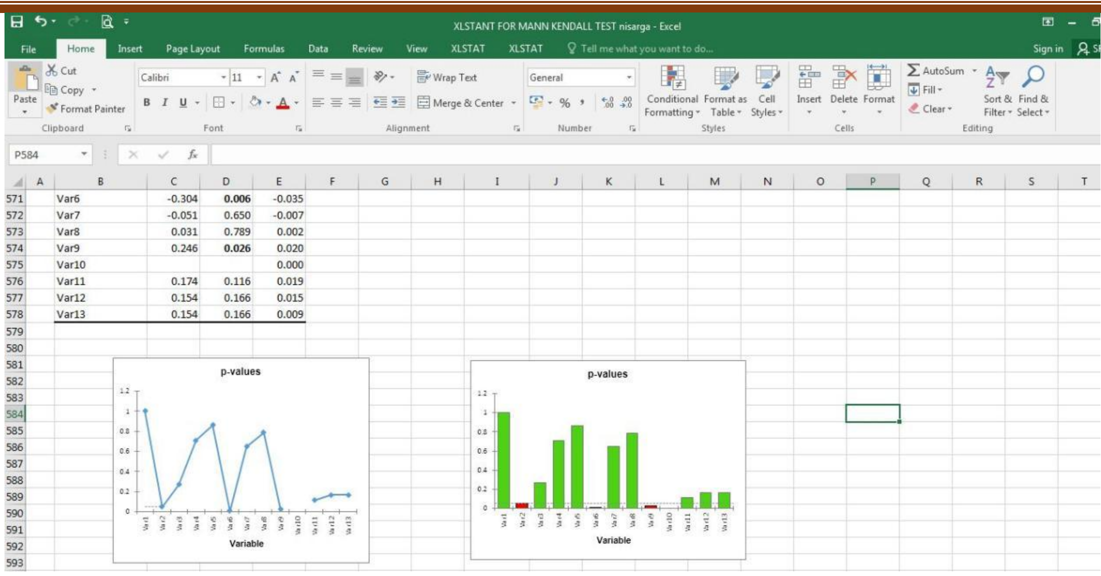

Fig. 41: Final outcome Tmax

- Repeat the same procedure to all six parameters.

5.6 TO CALCULATE TREND ANALYSIS USING MANN-KENDALL BY AND SEN'S SLOPE BY R STUDIO

R is an open-source programming language and environment used for statistical analysis, data visualization, and data science. Being open-source, R has a massive community that continuously works to improve the environment as well as helps members worldwide to improve and innovate.

R can be used for data analytics, statistical analysis, as well as machine learning purposes. R is compatible with a number of different technologies and is highly flexible. R is an extension of the S-programming language, which was created by John Chambers at Bell Laboratories (formerly AT&T, now Lucent Technologies) in 1976. S was a premiere tool for statistical research, but it wasn't very feasible outside scholarly research. Why one should learn a specific technology is a good question to ask. Is it worth my time and effort? R is among the most demanded scripting languages when it comes to data science.

Fig. 42: Benefits of R Studio

Why one should learn a specific technology is a good question to ask. Is it worth my time and effort? R is among the **most demanded** scripting languages when it comes to **data science**.

- R can be used for data analysis, statistical analysis, as well as machine learning.
- Several industries like health, finance, banking, e-commerce, manufacturing, and much more use R as their primary tool for data modeling.
- It integrates seamlessly with other technologies like Hadoop, which makes an ideal combination for large scale data processing.
- Academic research, healthcare industry, government surveys, finance industry, banking industry, retail and manufacturing sectors, e-commerce companies as well as tech giants like Facebook, Google, and Amazon all use R for some purpose or the other and, therefore, need R programmers.

5.3.1 How to Install R

Install the **R-base package** using the following code

After running the command, a confirmation prompt will appear. Answer it with a '**Y**' for yes.

Step –2 Next comes installing RStudio. To install RStudio, go to download R Studio, click on the download button for RStudio desktop, click the link for the latest R version for your OS and save the .deb file.

Step – 2 Answer with a '**Y**' for yes to confirm when prompted.

Installing R and RStudio on Windows

To install R and RStudio on windows, go through the following steps:

Install R on windows

Step – 1 Go to CRAN R project website.

Step – 2: Click on the **Download R for Windows** link.

Step – 3: Click on the **base** subdirectory link or **install R for the first time link**.

Step – 4: Click **Download RX.X.X for Windows** and save the executable .exe file.

Step – 5: Run the **.exe** file and follow the installation instructions.

5.a. Select the desired language and then click **Next**.

Read the license agreement and click **Next**.

Select the components you wish to install (it is recommended to install all the components). Click **Next**.

Enter/browse the folder/path you wish to install R into and then confirm by clicking **Next**.

Wait for the installation process to complete.

Click on **Finish** to complete the installation.

5.3.2 Install RStudio on Windows

Step – 1: With R-base installed, let's move on to installing RStudio. To begin, go to downloadRStudio and click on the download button for RStudio desktop.

Step – 2: Click on the link for the windows version of RStudio and save the .exe file.

Step – 3**:** Run the .exe and follow the installation instructions.

3.a. Click **Next** on the welcome window.

Enter/browse the path to the installation folder and click **Next** to proceed.

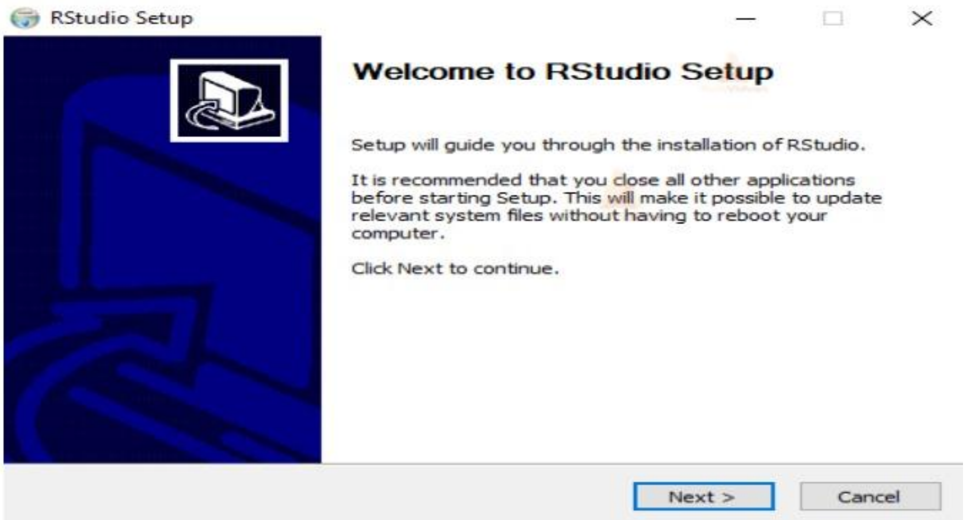

Fig. 43: Rstudio setup

3.b. Enter/browse the path to the installation folder and click **Next** to proceed.

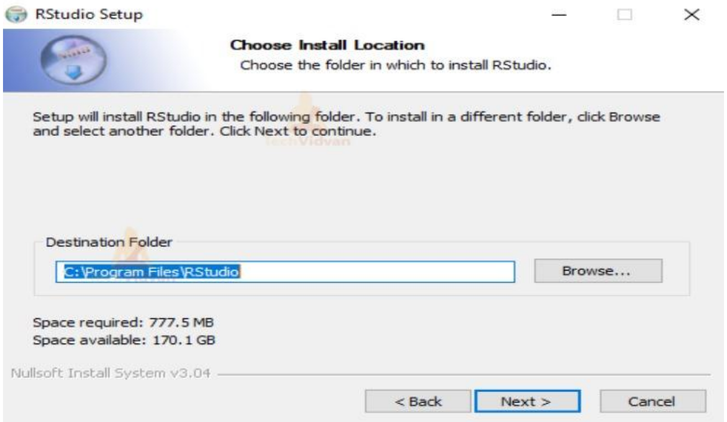

Fig. 44: Selection of location to Install R Studio

3.c. Select the folder for the start menu shortcut or click on do not create shortcuts and then click **Next**.

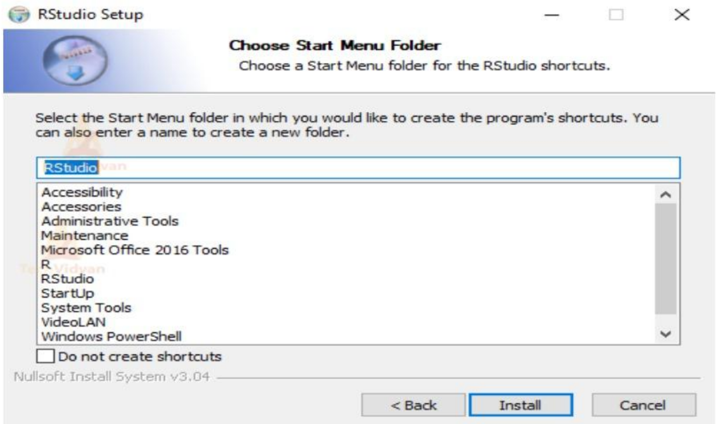

Fig. 45: Creating shortcut

3.d. Wait for the installation process to complete

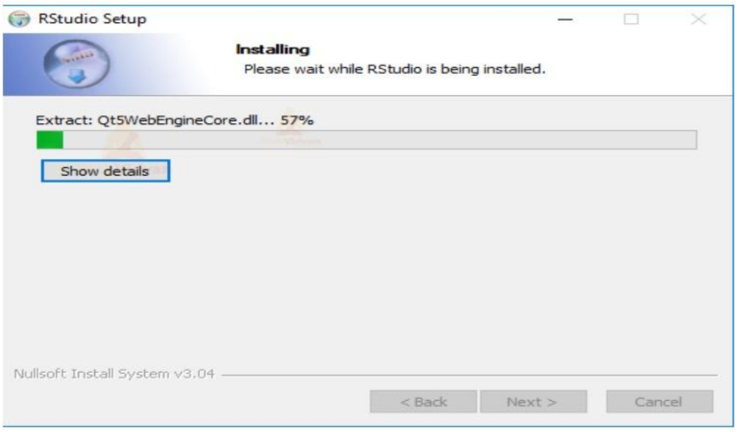

Fig. 46: Installation of R Studio

3.e. Click **Finish** to end the installation.

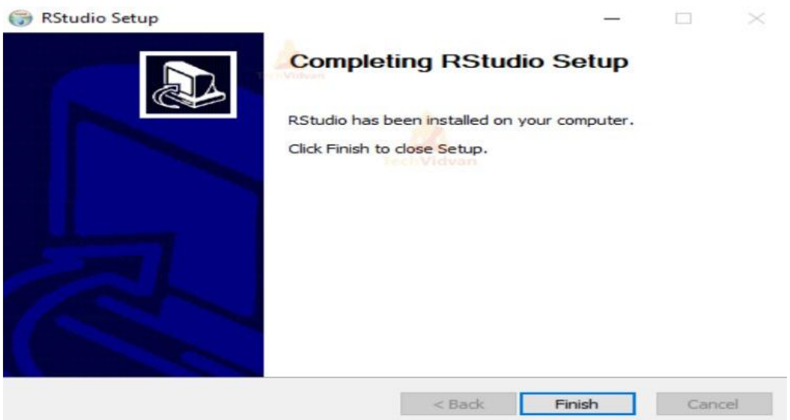

Fig. 47: Completion of Installation

Screen Layout of R Studio

- When you open R Studio for the first time you will see a screen something like this:

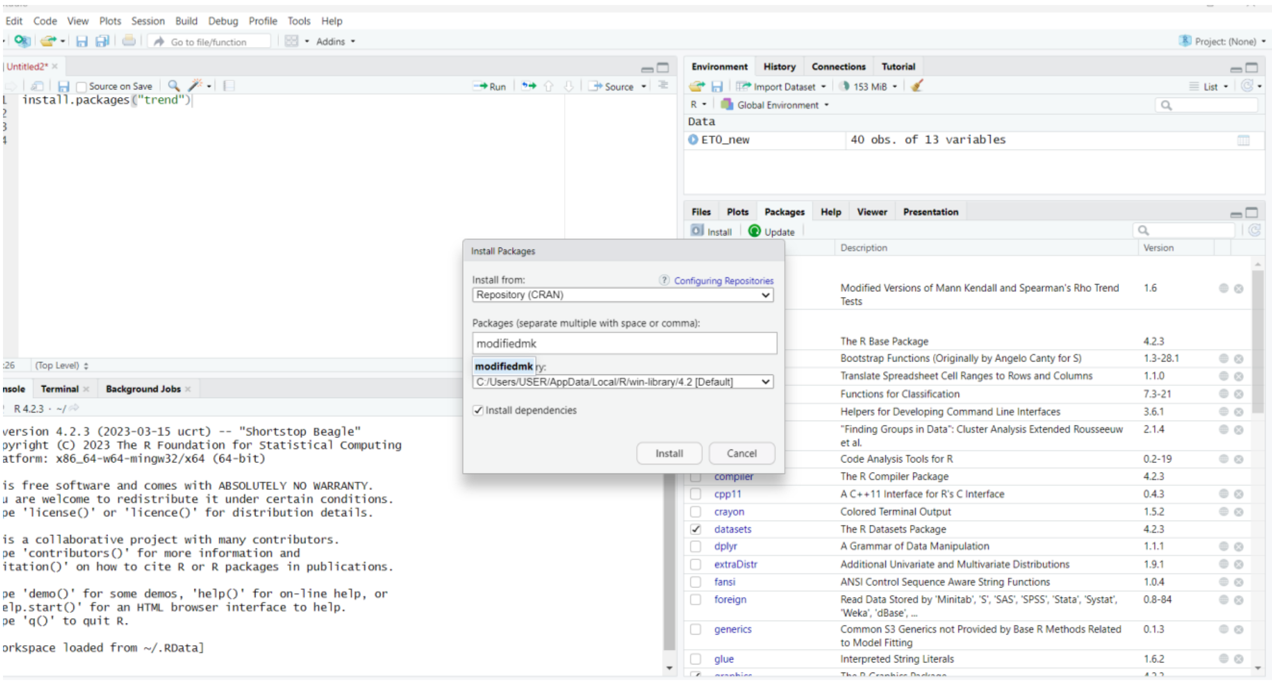

Fig. 48: Installation of modifiedmk tool

- In packages we need to install the "modifiedmk".

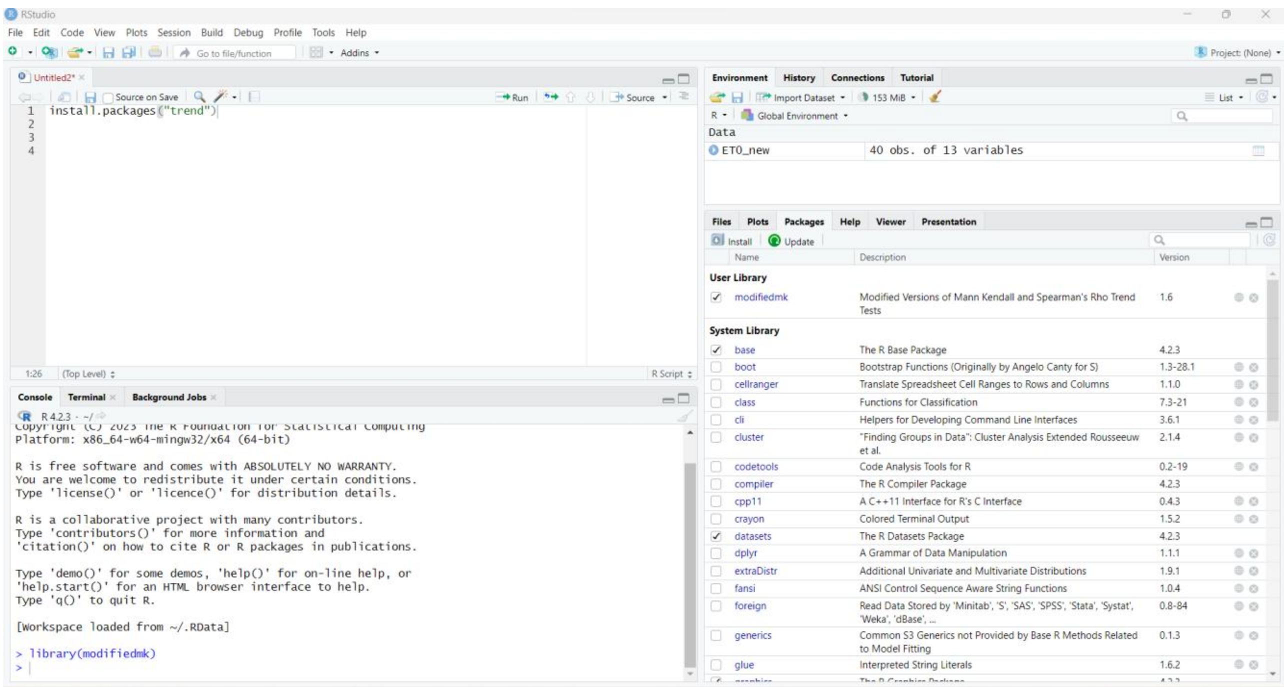

Fig. 49: Enabling modifiedmk tool

- Activate the modifiedmk tool from the user library.
- Through the dataset import, open the excel folder.

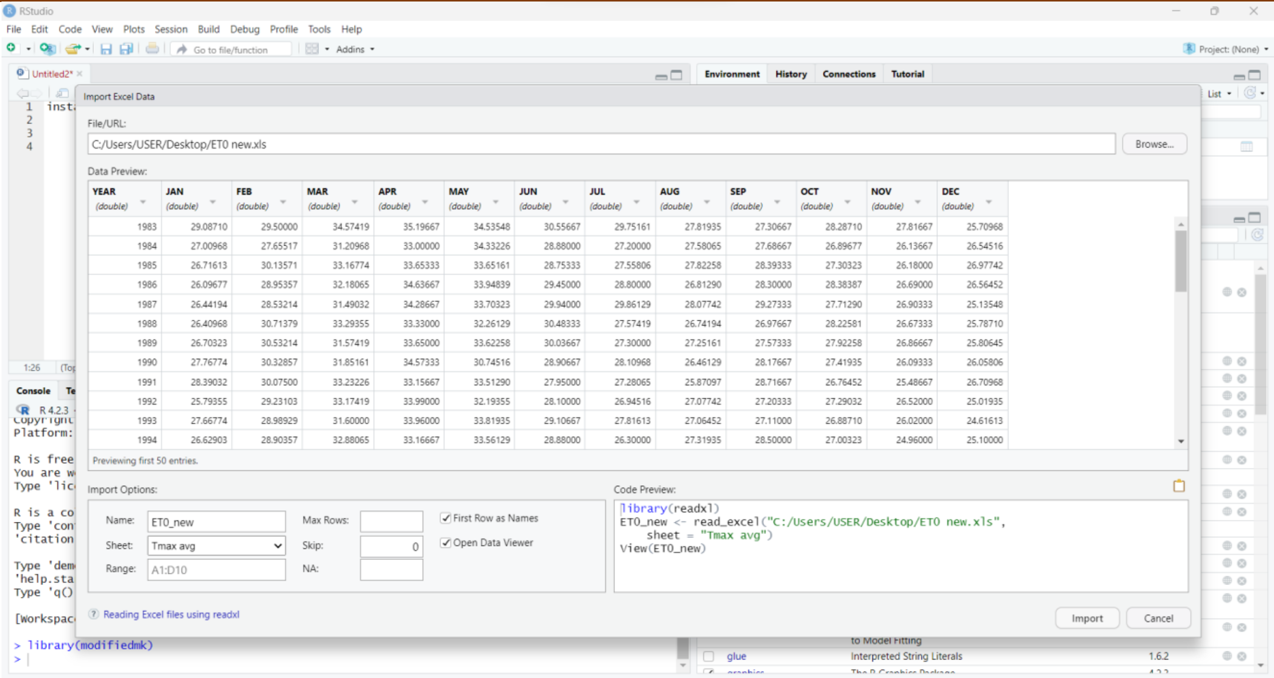

Fig. 50: Importing data using an excel file

➤ Now select the particular spreadsheet in the selected excel folder.

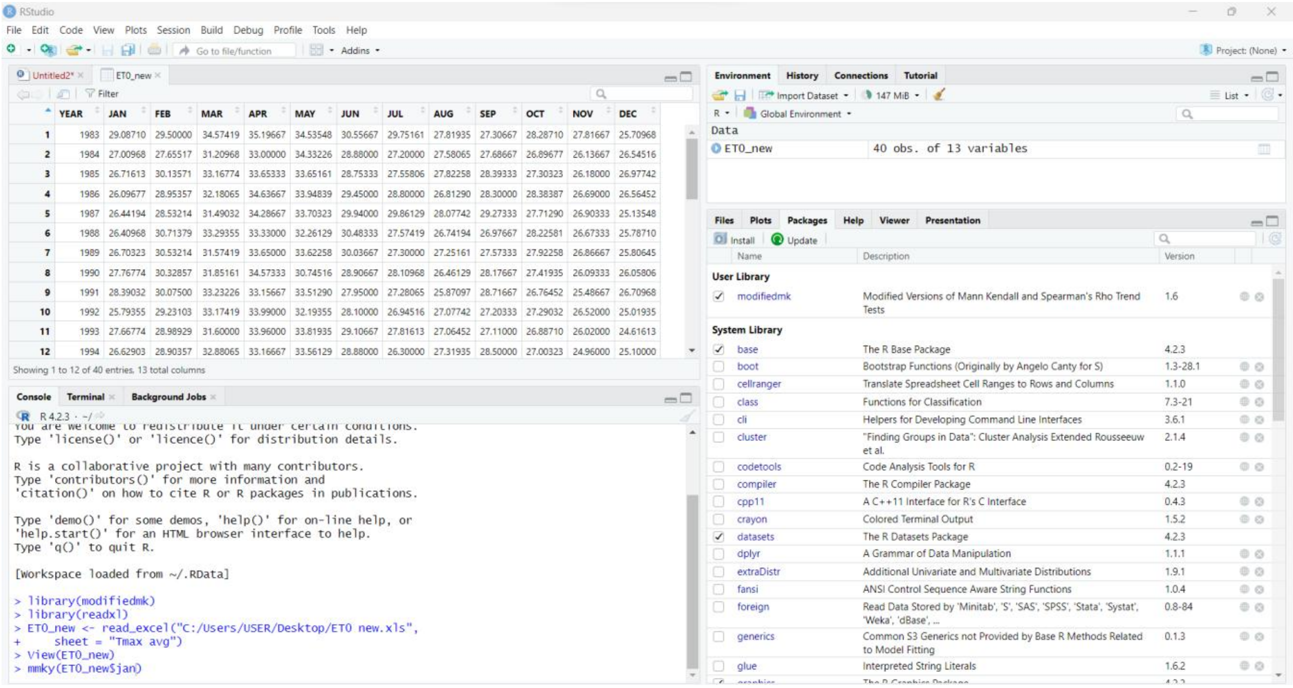

Fig. 51: Selection of particular sheet

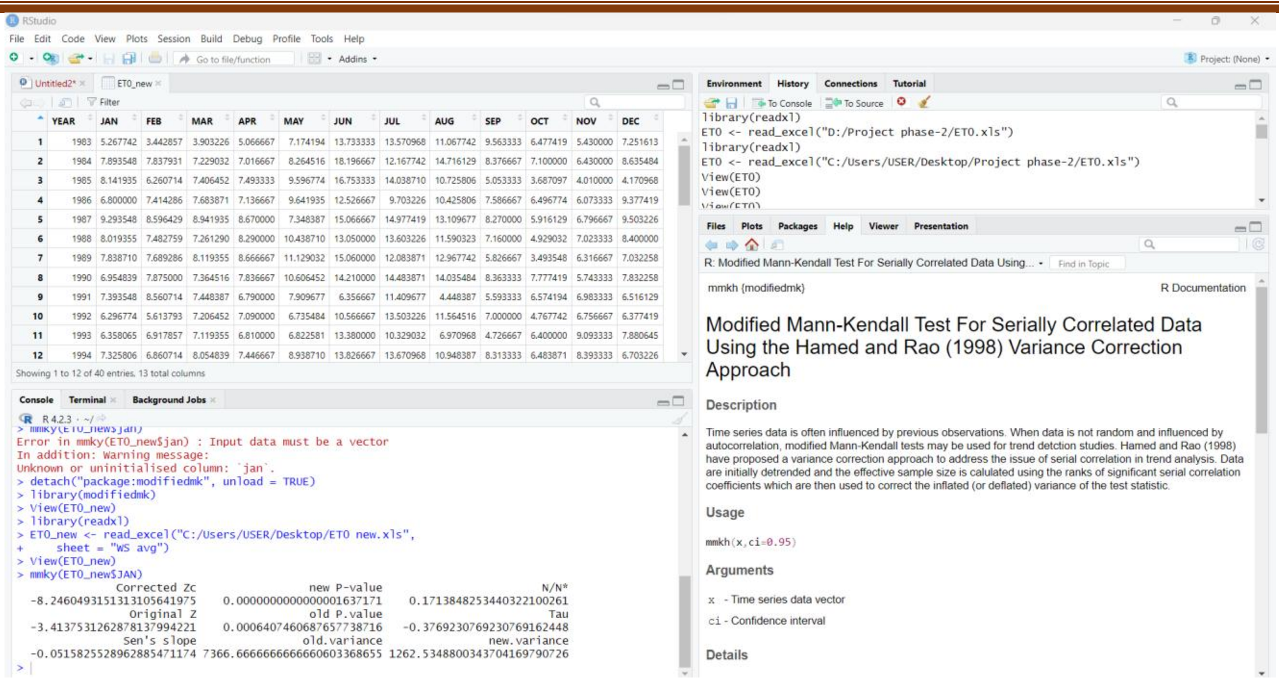

Fig. 52: Detailed procedure

5.7 SENSITIVITY ANALYSIS OF CLIMATE VARIABLES

Step 1: The reference evaporation is copied from the previous method and the difference between every two values is computed in the next column.

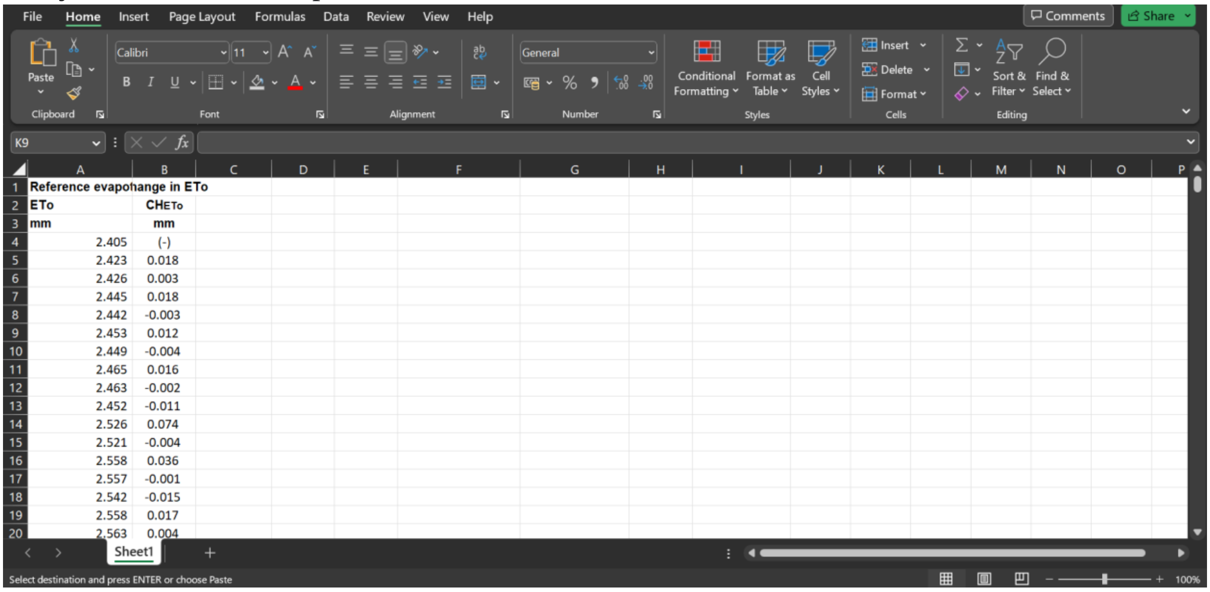

Fig. 53: ETo and change in ETo

Step 2: Maximum temperature and change in maximum temperature is copied and computed in the same way as Step 1.

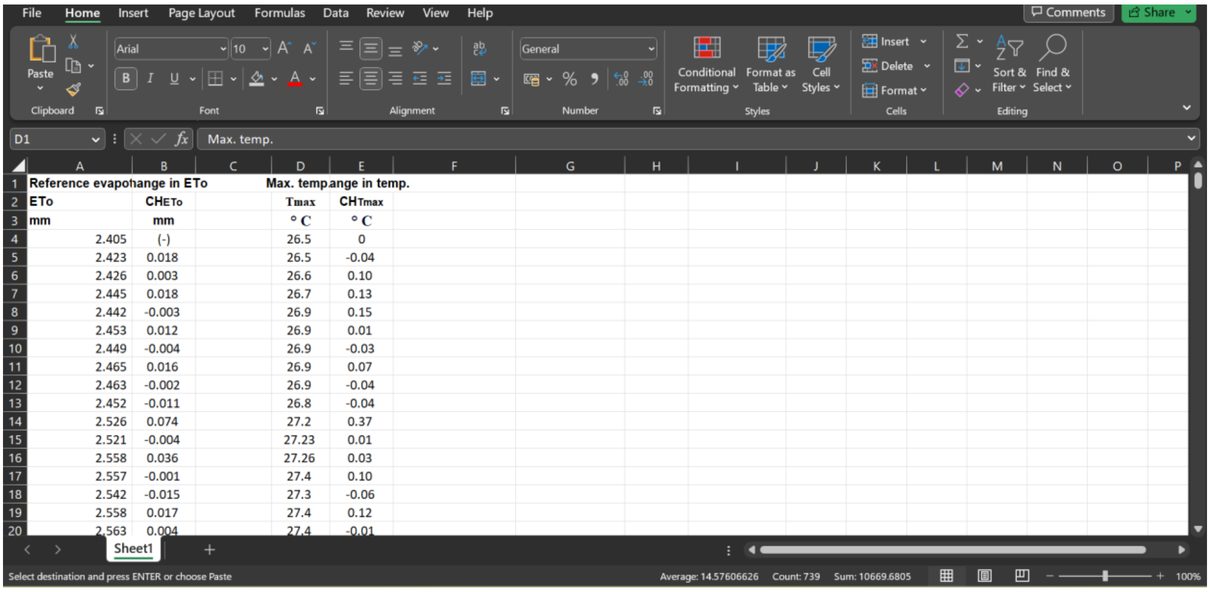

	A	B	C	D	E
1	Reference evapo	hange in ETo		Max. temp.	ange in temp.
2	ETo	CHETo		Tmax	CHTmax
3	mm	mm		° C	° C
4	2.405	(-)		26.5	0
5	2.423	0.018		26.5	-0.04
6	2.426	0.003		26.6	0.10
7	2.445	0.018		26.7	0.13
8	2.442	-0.003		26.9	0.15
9	2.453	0.012		26.9	0.01
10	2.449	-0.004		26.9	-0.03
11	2.465	0.016		26.9	0.07
12	2.463	-0.002		26.9	-0.04
13	2.452	-0.011		26.8	-0.04
14	2.526	0.074		27.2	0.37
15	2.521	-0.004		27.23	0.01
16	2.558	0.036		27.26	0.03
17	2.557	-0.001		27.4	0.10
18	2.542	-0.015		27.3	-0.06
19	2.558	0.017		27.4	0.12
20	2.563	0.004		27.4	-0.01

Fig. 54: Maximum temperature and change in maximum temperature

Step 3: Sensitivity coefficient is calculated by dividing the change in evaporation by change in maximum temperature.

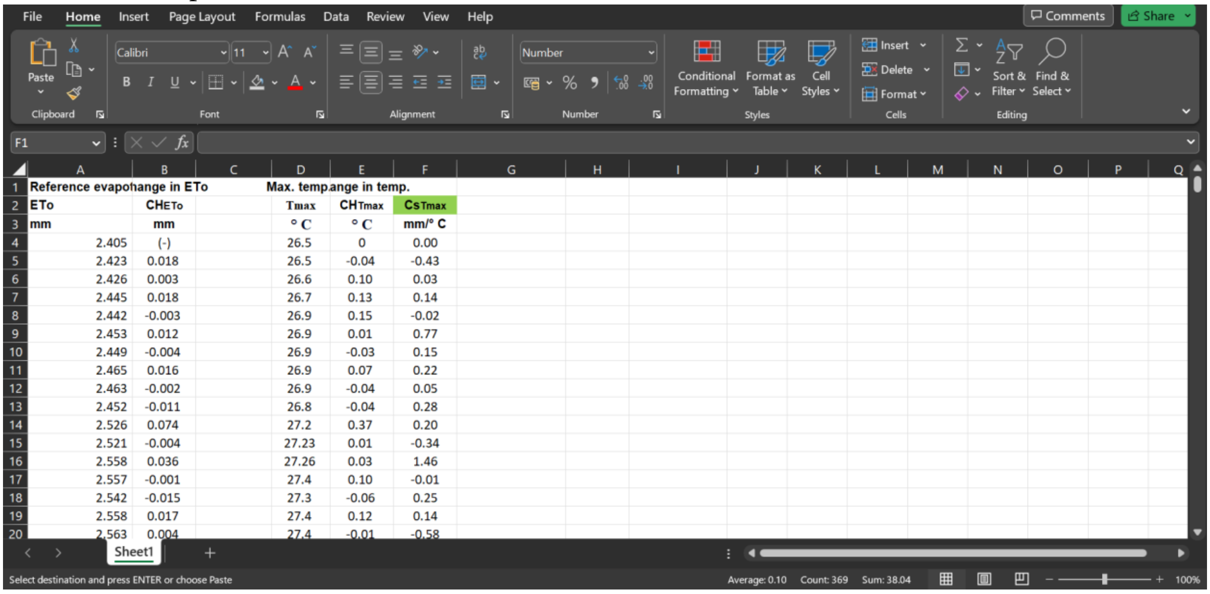

	A	B	C	D	E	F
1	Reference evapo	hange in ETo		Max. temp.	ange in temp.	
2	ETo	CHETo		Tmax	CHTmax	CsTmax
3	mm	mm		° C	° C	mm/° C
4	2.405	(-)		26.5	0	0.00
5	2.423	0.018		26.5	-0.04	-0.43
6	2.426	0.003		26.6	0.10	0.03
7	2.445	0.018		26.7	0.13	0.14
8	2.442	-0.003		26.9	0.15	-0.02
9	2.453	0.012		26.9	0.01	0.77
10	2.449	-0.004		26.9	-0.03	0.15
11	2.465	0.016		26.9	0.07	0.22
12	2.463	-0.002		26.9	-0.04	0.05
13	2.452	-0.011		26.8	-0.04	0.28
14	2.526	0.074		27.2	0.37	0.20
15	2.521	-0.004		27.23	0.01	-0.34
16	2.558	0.036		27.26	0.03	1.46
17	2.557	-0.001		27.4	0.10	-0.01
18	2.542	-0.015		27.3	-0.06	0.25
19	2.558	0.017		27.4	0.12	0.14
20	2.563	0.004		27.4	-0.01	-0.58

Fig. 55: Sensitivity coefficient

Step 4: Sensitivity coefficients of all other variables are computed in a similar manner.

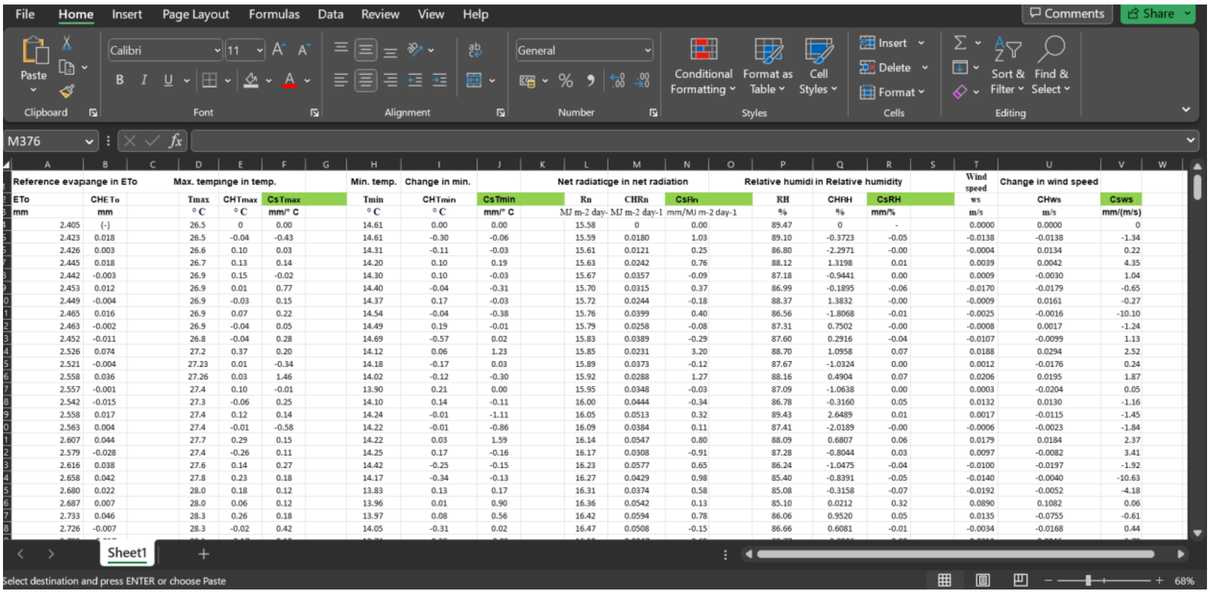

Fig. 56: Sensitivity coefficients of all variables

Step 5: The average of all the sensitivity coefficients is calculated and compared.

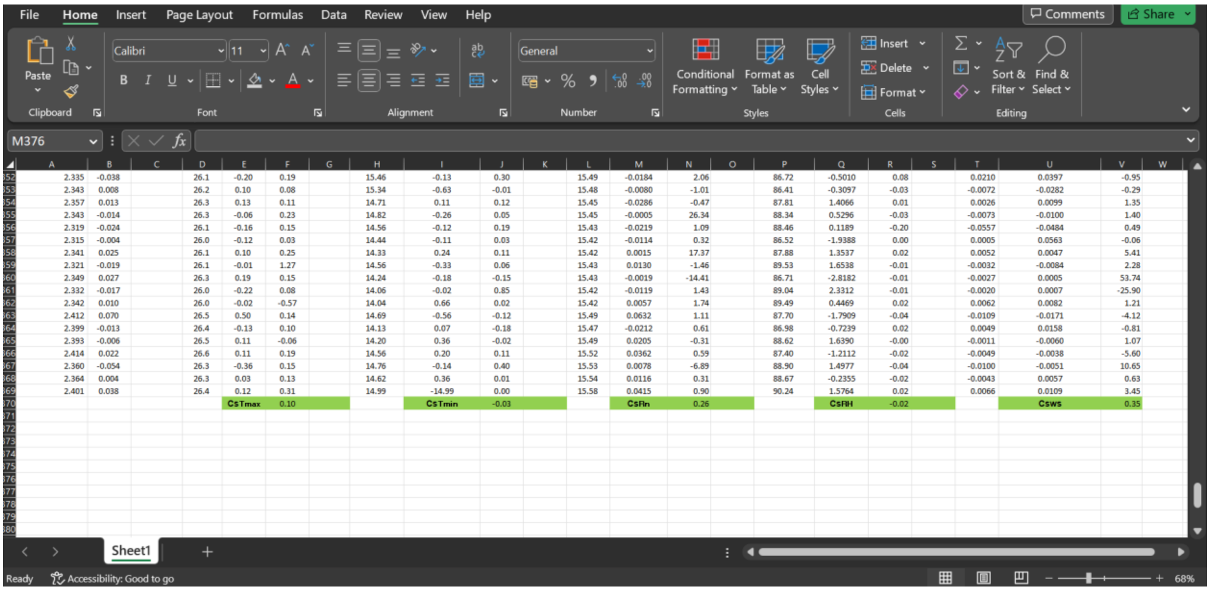

Fig. 57: Average of all sensitivity coefficients

Among all the climate variables (i.e., maximum temperature, minimum temperature, net radiation, relative humidity and wind speed), the following conclusions were derived:

- Coefficients of Minimum temperature (C_sTmin) and relative humidity (CsRH) have negative values, which means that an increase in these variables will result in decrease in the evaporation i.e., they are inversely proportional.
- The predominant factor affecting evaporation is wind speed (Csws), followed by net radiation ($C_s R_n$) having the coefficient values of 0.35 and 0.26 respectively.

CHAPTER-6

RESULTS AND DISCUSSION

Conventional method to find out reference evapotranspiration.

1) To calculate ET using Penman-Monteith

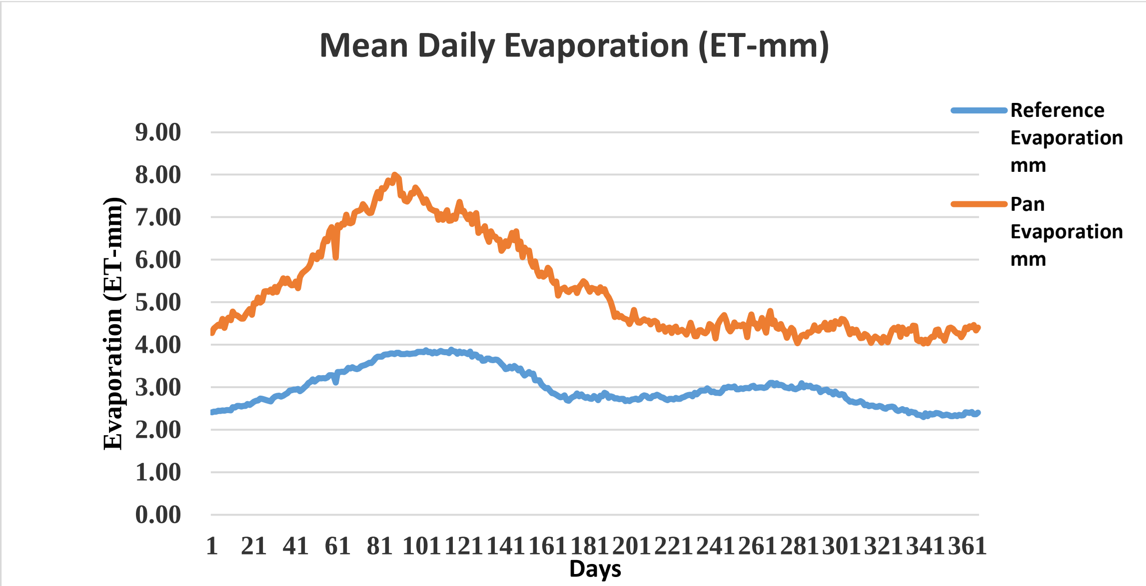

Fig. 58: Plot of reference evaporation of Penman model and actual evaporation

The blue line represents the reference evaporation calculated using Penman-Montecito equation and the orange line is the observed pan evaporation. It is observed that the reference evaporation varies in a considerable amount than the actual value. The RMSE error is 0.121.

2) To calculate ET using Stefan's-Steward

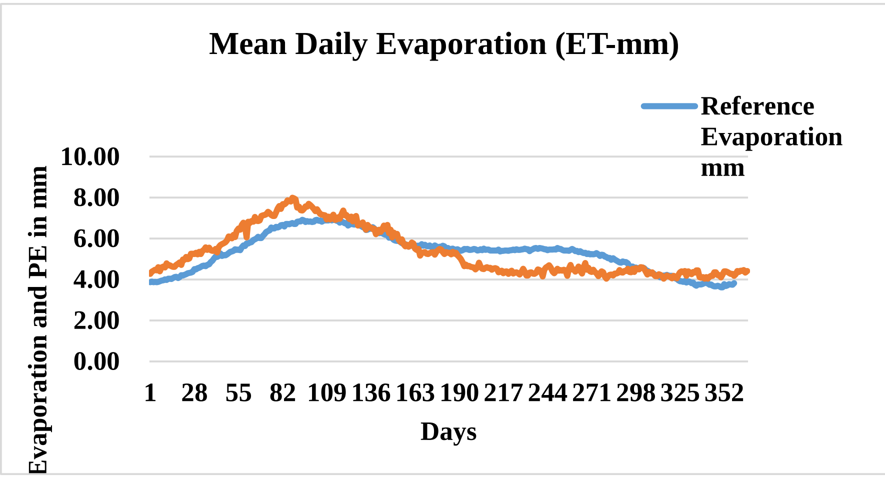

Fig. 59: Plot of reference evaporation of Stefan's-Stewart model and actual evaporation

The blue line represents the reference evaporation computed using Stephans-Stewart method and the orange line is the observed pan evaporation. It is observed that the computed values are comparatively close to the actual values than the former method, which means that there is more closeness to the calculated as well as the observed values with an error of 0.035.

3) To calculate Trend Analysis using Mann-Kendall.

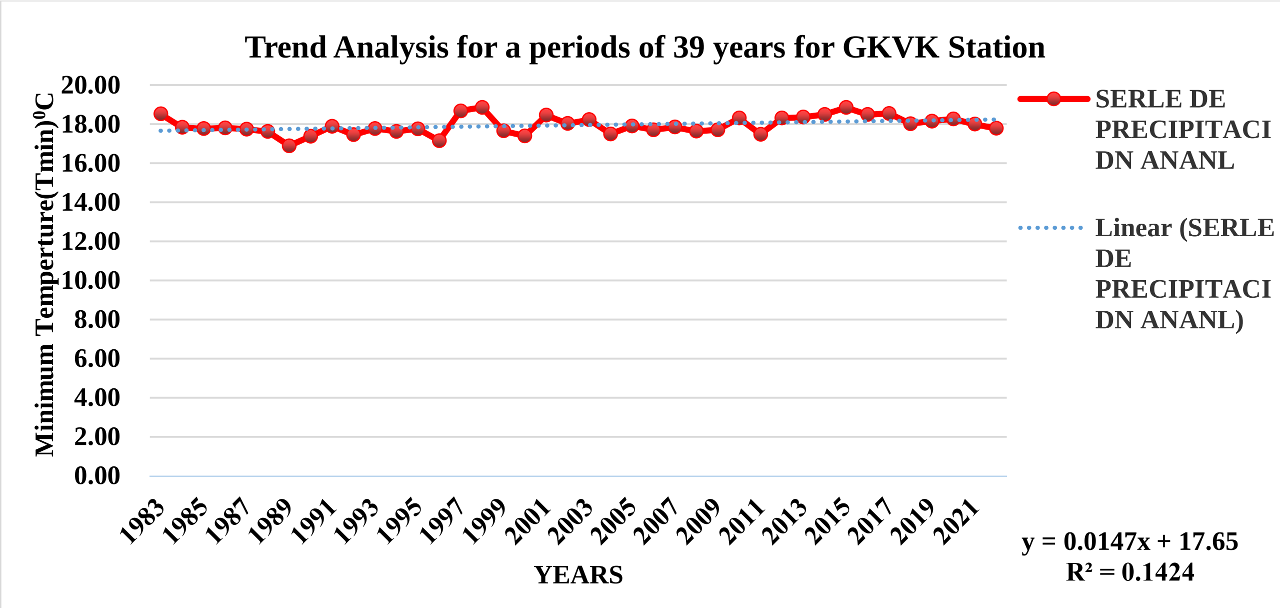

Fig. 56: Minimum temperature trend (Tmin) °C

The above graph shows the years various of the Minimum Temperature(Tmin)^{o}C result for the GKVK station. From this figure, it is apparent that the year (1983-2021) indicated a decrease in trend for the Minimum Temperature values during these years. the coefficient of determination, is a statistical measure that indicate R^2=0.1424.the relationship between the variables x and y is y=0.00147x+17.65.

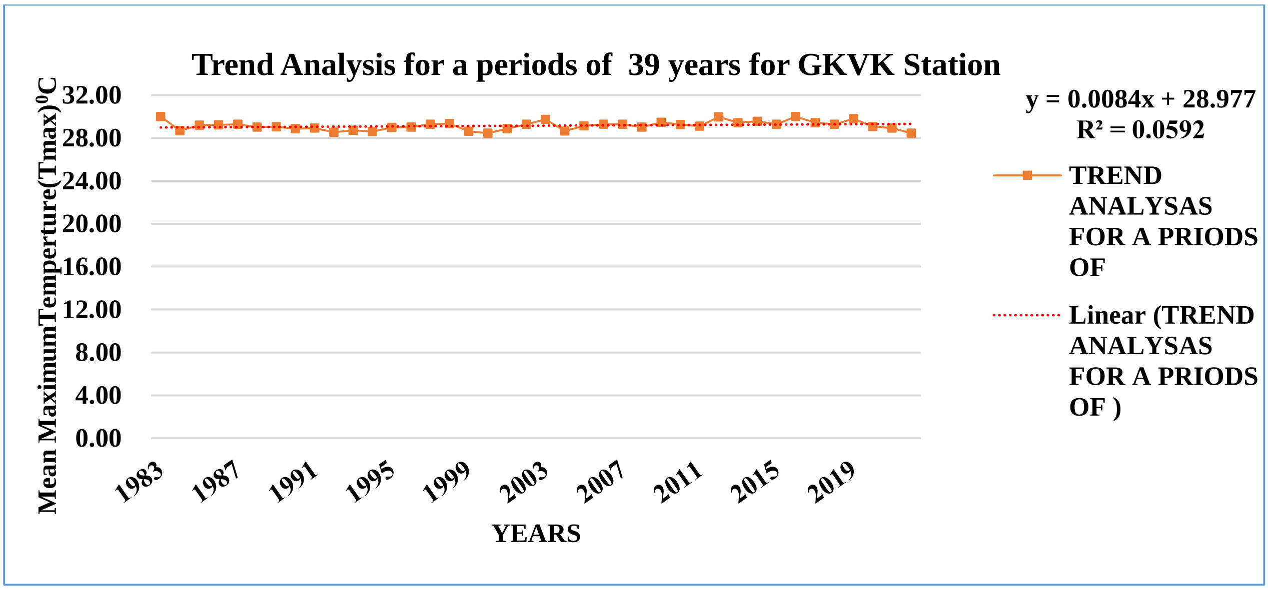

Fig. 61: Maximum temperature trend (Tmax) °C

The above graph shows the years various of the Maximum Temperature trend (Tmax)°C result for the GKVK station. From this figure, it is apparent that the year (1983-2021) indicated a decrease in trend for the Maximum Temperature values during these years. the coefficient of determination, is a statistical measure that indicate R^2=0.0592. the relationship between the variables x and y is y=0.0084x+28.977.

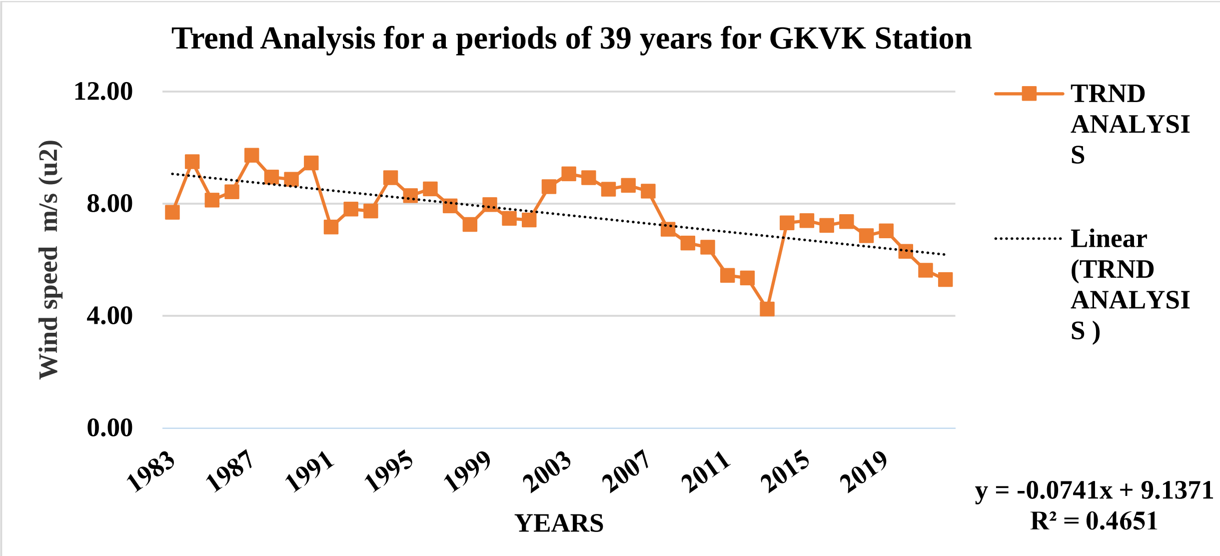

Fig. 62: Wind speed trend (u_2) m/s

The above graph shows the years various of the Wind speed trend(u_2) m/s result for the GKVK station. From this figure, it is apparent that the year (1983-2021) indicated a decrease in trend for the Wind speed values during these years. the coefficient of determination, is a statistical measure that indicate R^2=0.4651. The relationship between the variables x and y is y=-0.0741x+9.1371.

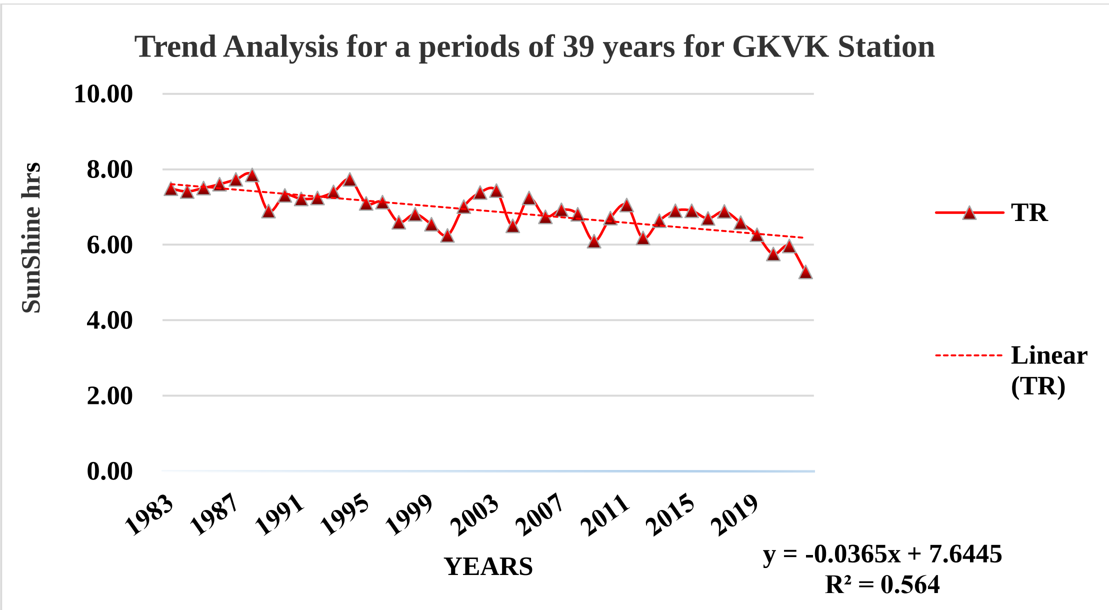

Fig. 63: Sunshine hours trend (ws) kmph

The above graph shows the years various of the Sunshine hours trend(ws) kmph result for the GKVK station. From this figure, it is apparent that the year (1983-2021) indicated a decrease in trend for the Sunshine hours trend(ws) kmph values during these years. the coefficient of determination, is a statistical measure that indicate R^2=0.564. the relationship between the variables x and y is y=-0.0365x+7.6445.

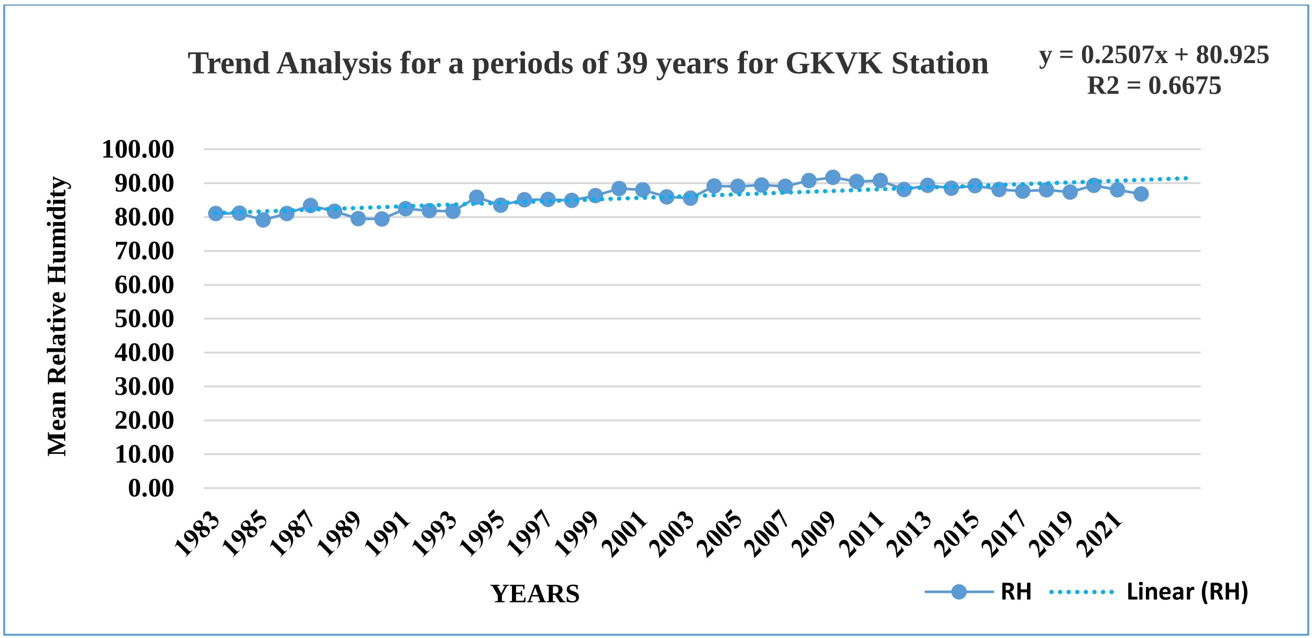

Fig. 64: Relative humidity trend (RH)%

The above graph shows the years various of the Relative humidity trend(RH)% result for the GKVK station. From this figure, it is apparent that the year (1983-2021) indicated a decrease in trend for the Relative humidity trend(RH)% values during these years. The coefficient of determination, is a statistical measure that indicate R^2=0.0.6675. the relationship between the variables x and y is y=0.2507x+80.925.

4) To calculate Trend Analysis using Sen's Slope.

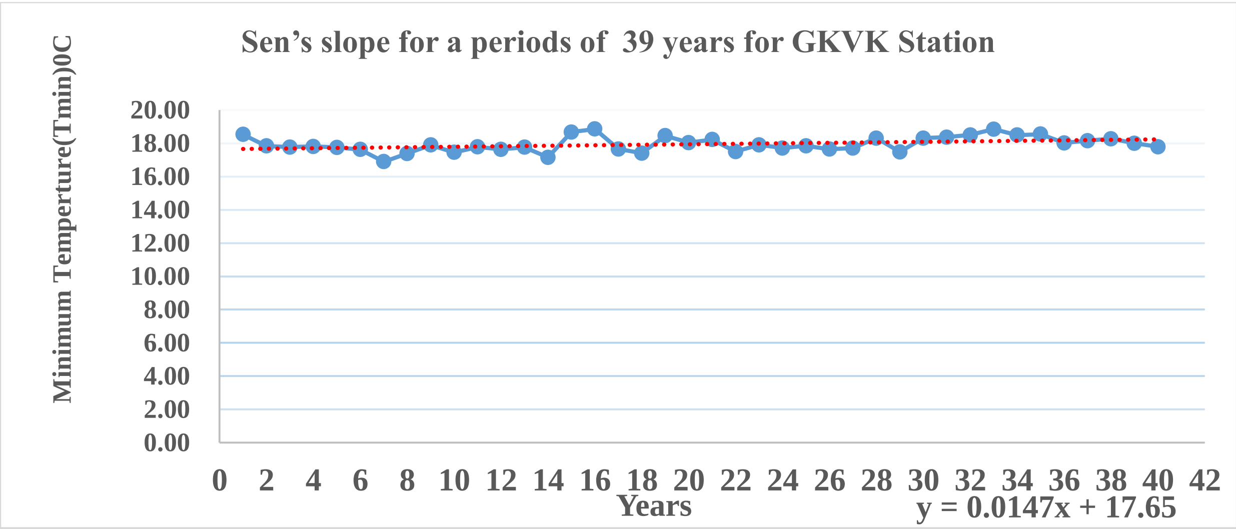

Fig. 65: Minimum temperature trend (Tmin)°C

The Sen's slope of the Minimum Temperature values to the various input variables for GKVK station are shown in above Figure. From this figure, it is apparent that the year (1983-2021) indicated a decrease in trend for the Minimum Temperature values during these years. the Sen's slope value of 0.01.the relationship between the variables x and y is y=0.0147x+17.65.

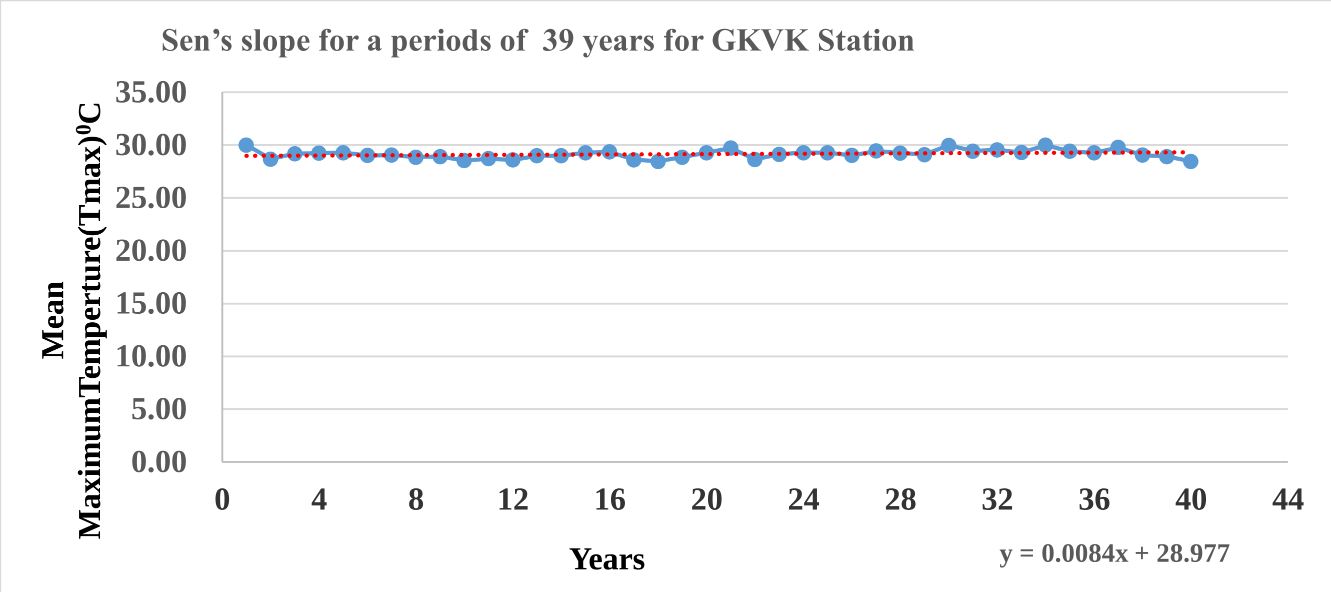

Fig. 66: Maximum temperature trend (Tmax)°C

The Sen's slope of the Maximum Temperature values to the various input variables for GKVK station are shown in above Figure. From this figure, it is apparent that the year (1983-2021) indicated a decrease in trend for the Maximum Temperature values during these years. the Sen's slope value of 0.02.the relationship between the variables x and y. y=0.0084x+28.977.

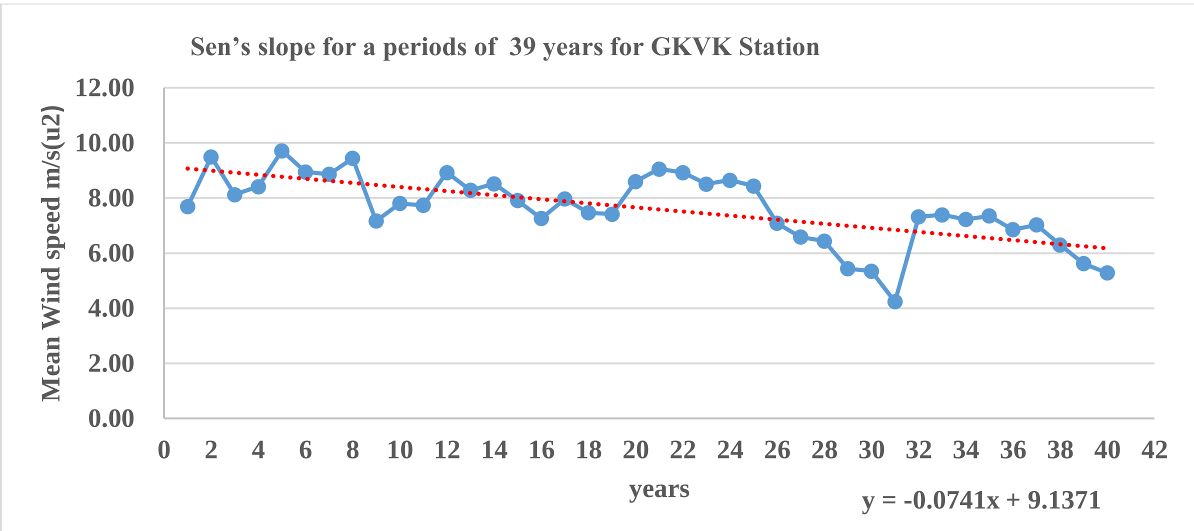

Fig. 67: Wind speed trend (u_2) m/s

The Sen's slope of the Wind speed trend values to the various input variables for GKVK station are shown in above Figure. From this figure, it is apparent that the year (1983-2021) indicated a decrease in trend for the Wind speed values during these years. the Sen's slope value of -0.07.the relationship between the variables x and y. y=-0.0741x+9.1371.

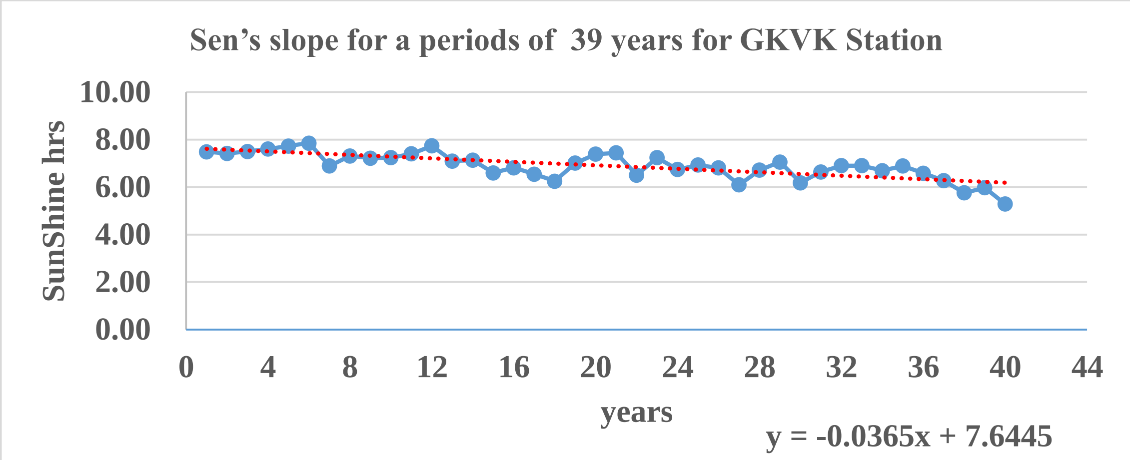

Fig. 68: Sunshine hours' trend (ws) kmph

The Sen's slope of the Sunshine hours' trend values to the various input variables for GKVK station are shown in above Figure. From this figure, it is apparent that the year (1983-2021) indicated a decrease in trend for the Sunshine hours'values during these years. the Sen's slope value of -0.03.the relationship between the variables x and y. y=-0.0365x+7.6445.

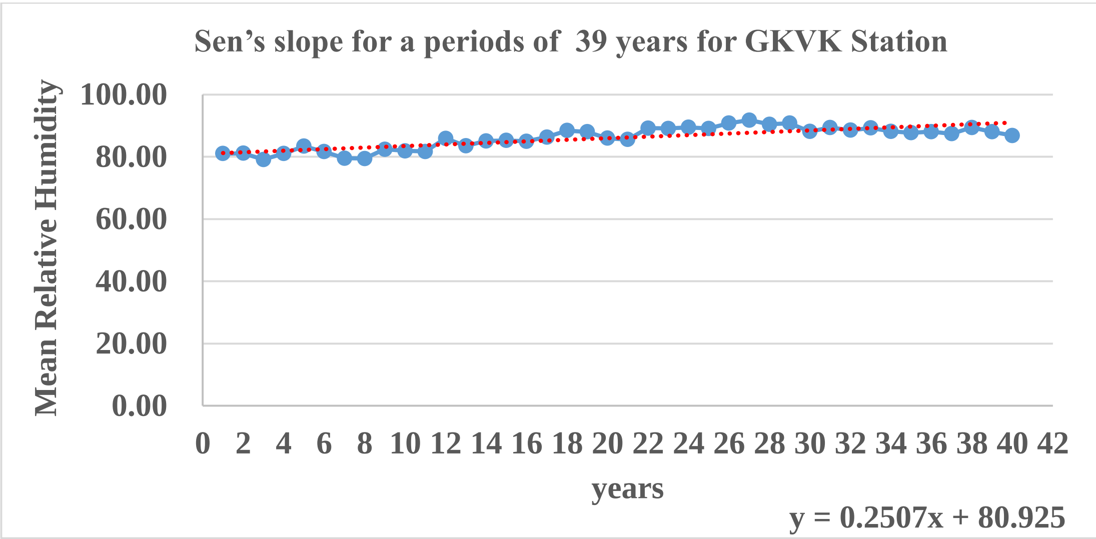

Fig. 69: Relative humidity trend (RH)%

The Sen's slope of the Relative humidity trend values to the various input variables for GKVK station are shown in above Figure. From this figure, it is apparent that the year (1983-2021) indicated a decrease in trend for the Relative humidity values during these years. the Sen's slope value of 0.25.the relationship between the variables x and y. y= 0.2507x+80.925.

5) To determine Trend Analysis using Mann-Kendall by and Sen's slope in XLSTST

Table 2: Summary of Maximum temperature (Tmax)ºC

Series\Test	Kendall's tau	p-value	Sen's slope
Dec	0.004	1.99	0.025
Jan	0.218	1.97	0.026
Feb	0.123	1.11	0.014
Marc	0.042	0.37	0.007
Apr	0.021	0.17	0.002
May	-0.304	-2.75	-0.035
Jun	-0.051	-0.43	-0.007
Jul	0.031	1.01	0.011
Aug	0.246	2.23	0.02
Sep	0.174	0.44	0.004
Oct	0.154	1.57	0.019
Nov	0.154	1.29	0.014

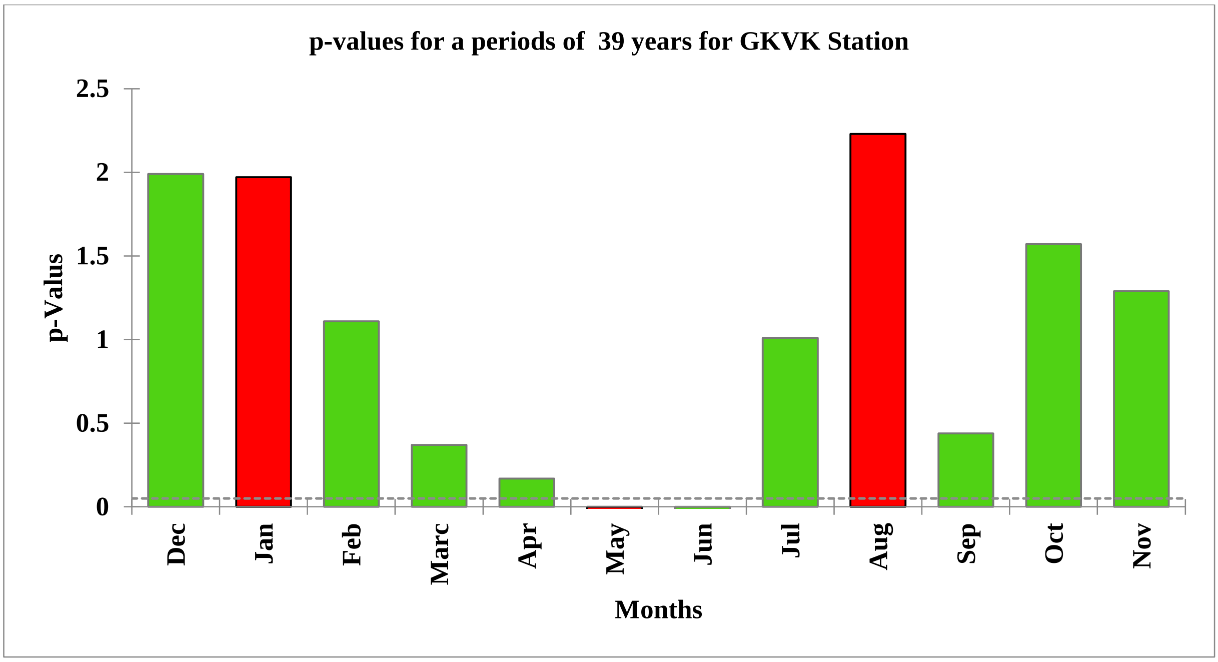

Fig. 70: Maximum temperature trend (Tmax)ºC

The above graph shows the monthly variation of the Maximum Temperature trend (Tmax)ºC result for the GKVK station. Tmax shows a negative trend in the months of May till June. Hottest months are January and August.

Table 3: Summary of Minimum temperature (Tmin)°C

Series\Test	Kendall's tau	p-value	Sen's slope
Dec	0.005	1.000	0.000
Jan	0.318	0.049	0.026
Feb	0.223	0.268	0.014
Marc	0.052	0.709	0.007
Apr	0.031	0.861	0.002
May	-0.404	0.006	-0.035
Jun	-0.041	0.650	-0.007
Jul	0.021	0.789	0.002
Aug	0.346	0.026	0.020
Sep	0.184	0.116	0.019
Oct	0.194	0.166	0.015
Nov	0.254	0.166	0.009

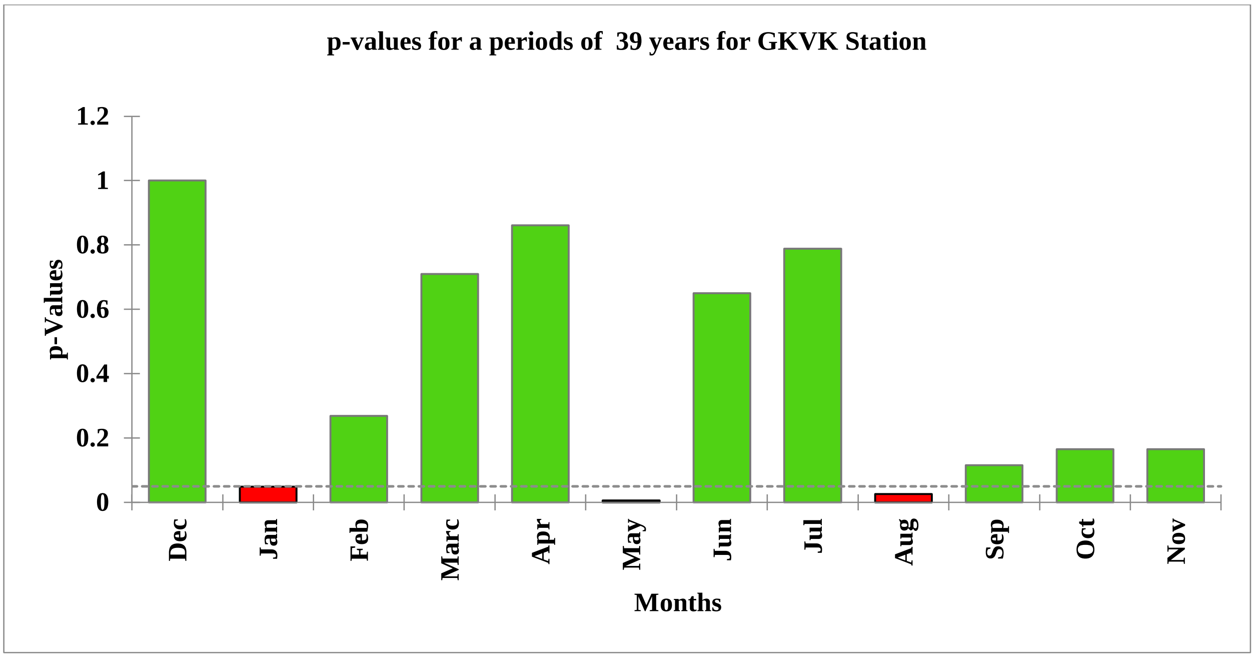

Fig. 71: Minimum temperature trend (Tmin)°C

The above graph shows the monthly variation of the Minimum temperature trend (Tmin)°C result for the GKVK station. Tmin shows a negative trend in the month of May. Hottest months are January and August.

Table 4: Summary of Wind speed trend (u_2) m/s

Series\Test	Kendall's tau	p-value	Sen's slope
Dec	-0.204	0.078	-0.064
Jan	-0.123	0.300	-0.052
Feb	-0.241	**0.023**	-0.025
Marc	-0.479	< **0.0001**	-0.04
Apr	-0.507	< **0.0001**	-0.068
May	-0.523	< **0.0001**	-0.094
Jun	-0.072	0.600	-0.191
Jul	-0.174	0.118	-0.148
Aug	-0.219	**0.050**	-0.137
Sep	-0.338	**0.003**	-0.046
Oct	-0.149	0.190	-0.054
Nov	-0.546	< **0.0001**	-0.019

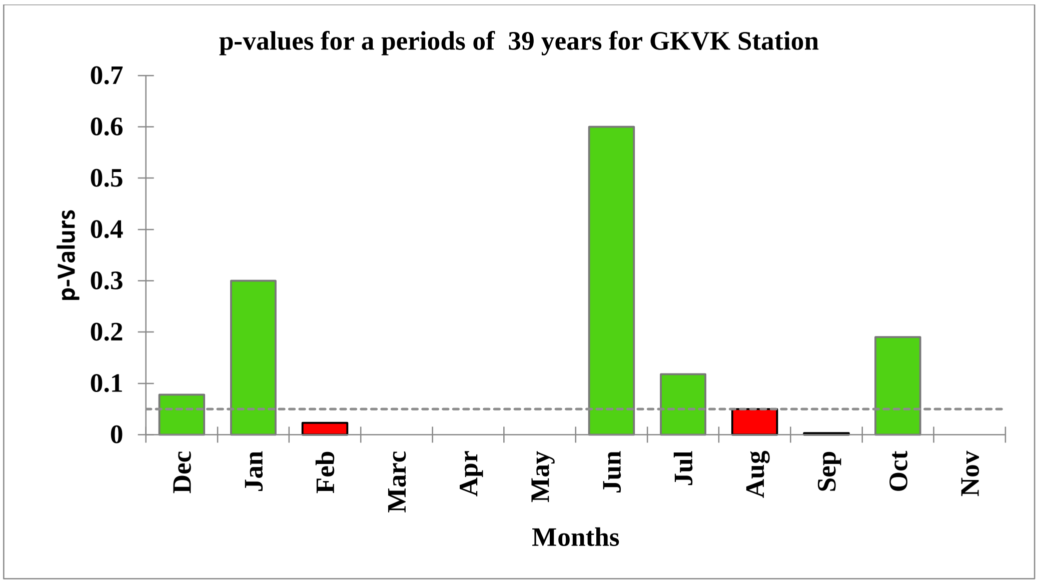

Fig. 72: Wind speed trend (u_2) m/s

The above graph shows the monthly variation of the Wind speed trend (u_2) m/s result for the GKVK station. Wind speed shows a negative trend in the months of March till May. Hottest months are February and August.

Table 4: Summary of Sunshine hours' trend (ws) kmph

Series\Test	Kendall's tau	p-value	Sen's slope
Dec	-0.204	0.066	-0.040
Jan	-0.123	0.268	-0.012
Feb	-0.241	**0.029**	-0.023
Marc	-0.479	< **0.0001**	-0.043
Apr	-0.507	< **0.0001**	-0.040
May	-0.523	< **0.0001**	-0.055
Jun	-0.072	0.522	-0.006
Jul	-0.174	0.116	-0.016
Aug	-0.219	**0.048**	-0.028
Sep	-0.338	**0.002**	-0.052
Oct	-0.149	0.180	-0.019
Nov	-0.546	< **0.0001**	-0.027

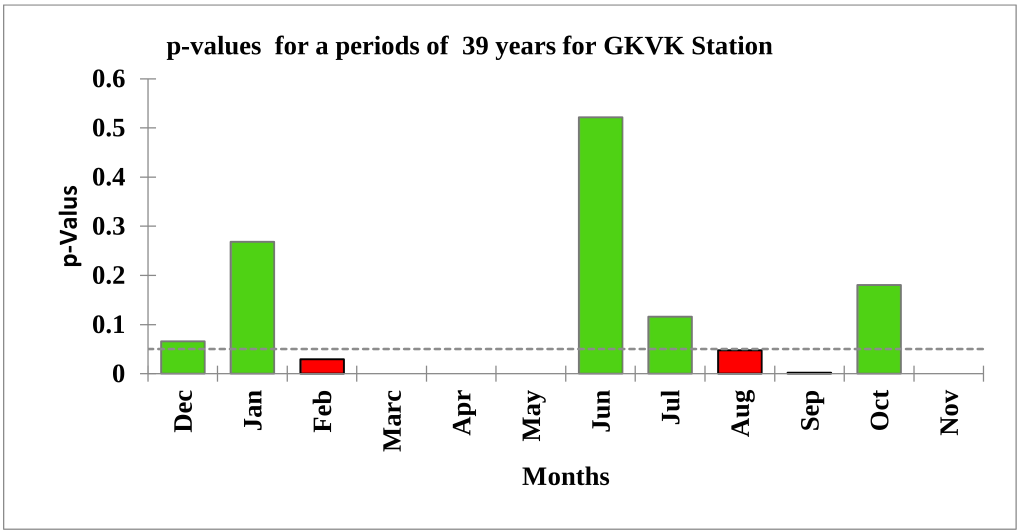

Fig. 73: Sunshine hours' trend (ws) kmph

The above graph shows the monthly variation of the Sunshine hours' trend (ws) kmph result for the GKVK station. Sunshine hours' shows a negative trend in the months of March till May. Hottest months are February and August.

Table 2: Summary of Relative humidity trend (RH)%

Series\Test	Kendall's tau	p-value	Sen's slope
Dec	-0.204	3.92	-0.040
Jan	-0.123	4.25	-0.012
Feb	-0.241	0.37	-0.023
Marc	-0.479	5.63	-0.043
Apr	-0.507	4.24	-0.040
May	-0.523	4.11	-0.055
Jun	-0.072	2.95	-0.006
Jul	-0.174	4.79	-0.016
Aug	-0.219	4.57	-0.028
Sep	-0.338	4.32	-0.052
Oct	-0.149	4.09	-0.019
Nov	-0.546	4.11	-0.027

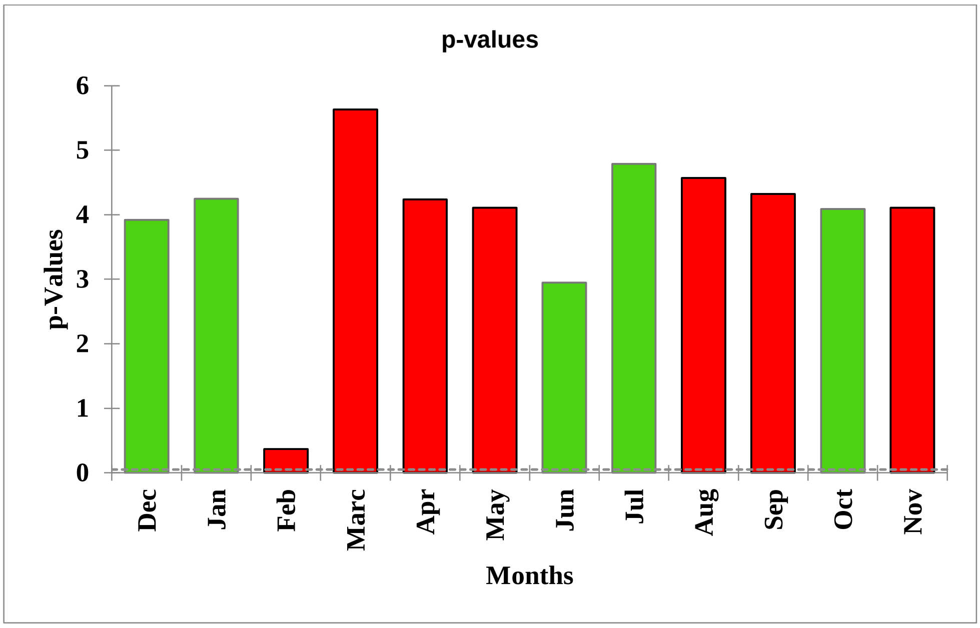

Fig. 74: Relative humidity trend (RH)%

The above graph shows the monthly variation of the Sunshine hours' trend (ws) kmph result for the GKVK station. Relative humidity shows a only positive trend.

6) To calculate Trend Analysis using Mann-Kendall by and Sen's slope by R studio.

Table No 7: Results of Mann-Kendall by R studio.

MANNKENDALL	JAN	FEB	MAR	APR	MAY	JUN	JUL	AUG	SEP	OCT	NOV	DEC
Tmax	1.97	1.11	0.37	0.17	-2.75	-0.43	1.01	2.23	0.44	1.57	1.29	1.99
Tmin	1.22	-0.31	1.40	0.36	-0.43	1.78	1.61	1.61	1.26	1.03	1.90	2.20
WS	-3.41	-1.20	-2.48	-4.17	-3.53	-5.00	-4.39	-3.88	-2.11	-2.99	-1.22	-3.32
RS	4.25	0.37	5.63	4.24	4.11	2.95	4.79	4.57	4.32	4.09	4.11	3.92
EPan	-4.80	-3.41	-1.08	-2.04	-4.33	-4.81	-5.91	-6.37	-5.67	-4.44	-4.60	-3.37
SSH	-1.48	-1.48	-4.70	-4.89	-5.16	-0.52	-2.04	-2.47	-3.41	-1.88	-1.53	-2.26

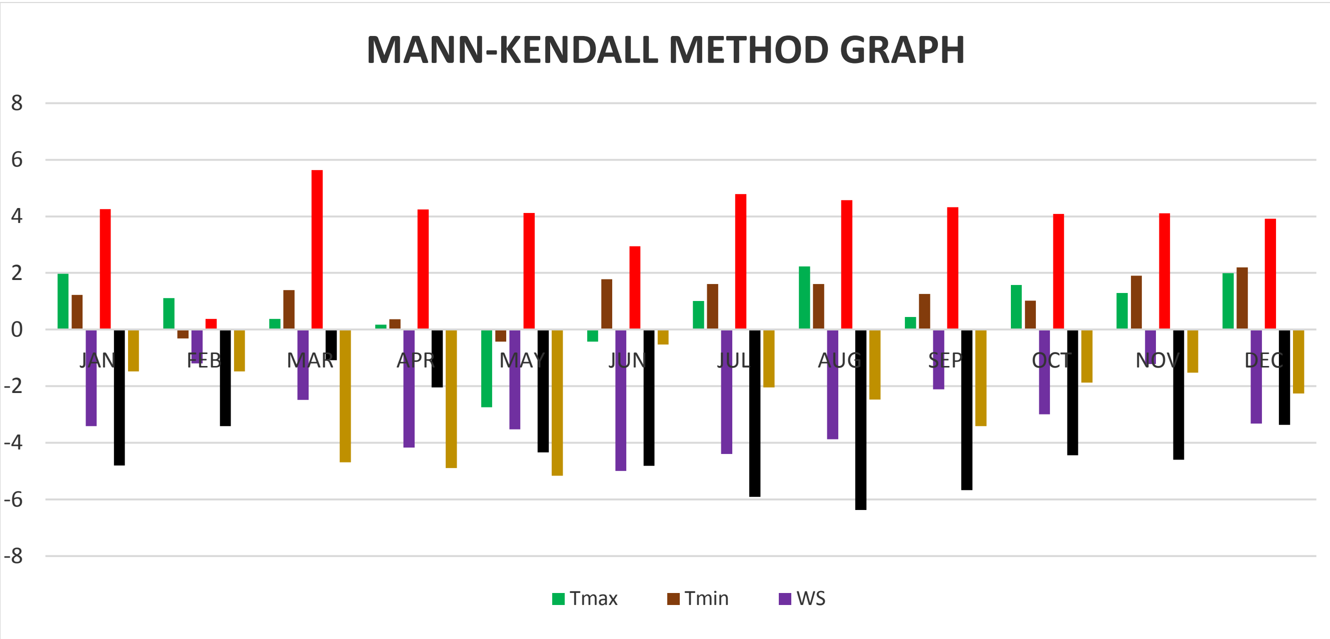

Table No 8: Results of Sen's slope by R studio.

SENSLOPE	JAN	FEB	MAR	APR	MAY	JUN	JUL	AUG	SEP	OCT	NOV	DEC
Tmax	0.026	0.014	0.007	0.002	-0.035	-0.007	0.011	0.020	0.004	0.019	0.014	0.025
Tmin	0.024	-0.006	0.026	0.005	-0.005	0.013	0.014	0.013	0.007	0.011	0.024	0.040
WS	-0.052	-0.025	-0.040	-0.068	-0.094	-0.191	-0.148	-0.137	-0.046	-0.054	-0.019	-0.064
RS	0.218	0.374	0.444	0.237	0.244	0.174	0.206	0.202	0.196	0.170	0.263	0.231
EPan	-0.044	-0.039	-0.010	-0.031	-0.068	-0.073	-0.075	-0.081	-0.071	-0.049	-0.047	-0.039
SSH	-0.015	-0.015	-0.047	-0.041	-0.064	-0.005	-0.022	-0.036	-0.059	-0.032	-0.023	-0.050

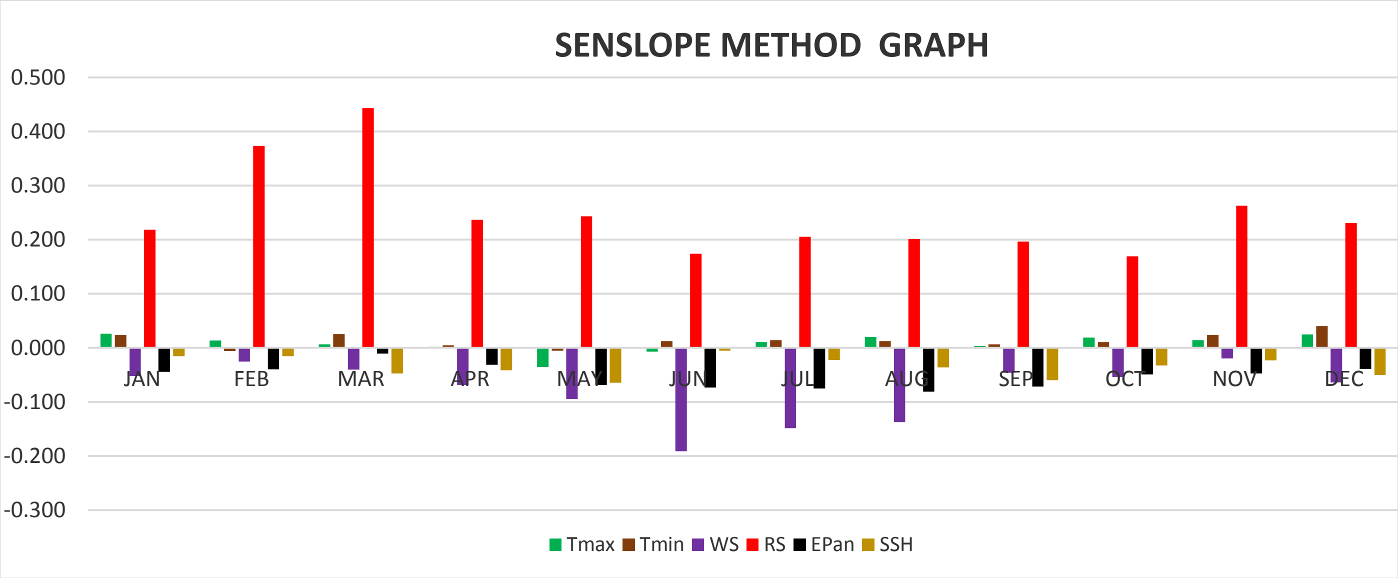

Tmax shows a negative trend in the months of January till May, graduatory rises till drops August and during fall ie. September (0.44) then rises again till December. Tmin shows a negative trend from March till May due to summer season it varies substantially from June to February. Wind speed shows an overall negative trend with the maximum value being in the month of May, June and July. Solar radiation shows a net positive Trends over the months except of February where it is 0.37. SSH is maximum in the month of March, April and May with an overall negative trend otherwise.

REFERENCE

1. *Snyder, Morteza*, Scott and Mark. (2005), "Simplified Estimation of Reference Evapotranspiration from Pan Evaporation Data in California", Journal of Irrigation DrainEngineering 2005.131:249-253.
2. *Terzi, Keskin,* (2006)"Estimating Evaporation Using ANFIS",Journal of Irrigation and drainage engineering (ASCE) 2006.132:503-507.
3. *Cahoon, Thomas*A.(1990),"Estimating pan evaporation using limited meteorological observations", Agricultural and Forest Meteorology (Elsevier)0168-1923.
4. *I. J. Verma,* "Recent variations and trends in pan evaporation over India", Journal of Irrigation and drainge engineering (ASCE) 3 (July 2008), 347-356.
5. *Hossein Tabari,* "Changes of Pan Evaporation in the West of Iran", Water Retour Manage (2011) 25:97–111.
6. *Mostafa Ali Benzaghta, Thamer A. Mohammed, Abdul Halim Ghazali and Mohd Amin MohdSoom,* "Prediction of evaporation in tropical climate using artificial neural network and climate based models", Scientific research and essays 2012, 7(36) ,3133-3148.
7. *Pankaj Kumar and Ajai Kumar Tiwari,* "Evaporation Estimation using artificial neural network", International Journal of Computer Theory and Engineering 2012, 4(1), 51-53.
8. *SurinderDeswal and Mahesh Pal,* "Artificial Neural Network based modeling of Evaporation losses in reservoirs", World academy of Science, Engineering and Technology 2008, 39, 279-283.
9. *Anurag Malik, Anil Kumar and Ozgur Kisi* (2018), "Daily Pan Evaporation Estimation Using Heuristic Methods with Gamma Test", Journal of Irrigation Drain Engineering, 2018, 144(9)
10. *SubhankarDebnath, SirishaAdamala and N. S. Raghuwanshi* (2015), "Sensitivity Analysis of FAO-56 Penman-Monteith Method for Different Agro-ecological Regions of India", Springer International Publishing Switzerland 2:689–704
11. *Milan Gocic and SlavisaTrajkovic*(2013), "Analysis of changes in meteorological variables using Mann-Kendall and Sen's slope estimator statistical tests in Serbia", Global and Planetary change 100, 172-182
12. *Gicy M. Kovoor and LakshmanNandagiri* (2018), "Sensitivity Analysis of FAO-56 Penman– Monteith Reference Evapotranspiration Estimates Using Monte Carlo Simulations", Springer Nature Singapore Pte Ltd. 73 V.